The Adsorption of Gold on Carbons

A thesis submitted for the degree of Doctor of Philosophy of the University of London and Diploma of Imperial College.

Raymond Cook B.Sc.(Eng.), ARSM

Department of Metallurgy and Materials Science, Royal School of Mines, Imperial College, University of London.

1986

Abstract

An investigation has been carried out into the nature of gold adsorption from cyanide solutions by activated carbons and carbon blacks.

The maximum gold loading capacity of the carbons as determined by the Langmuir adsorption model was shown to be dependent on the BET surface area of the adsorbent, with a gold concentration of 0.0847 $mg.m^{-2}$ on adsorption by carbon blacks from carbonate buffered solution. Reduced gold adsorption was shown to occur in unbuffered solutions and using acid washed carbons. The surface area correlation was still obtained however, with a gold concentration of 0.0398 $mg.m^{-2}$ on the carbon blacks.

Addition of 'spectator' cations to adsorption systems was shown to increase gold loading in the order $H^+ > Ca^{2+} > Mg^{2+} > Na^+$. These cations also lowered the molar gold:cation adsorption ratios, from values as high as 17.25:1 for activated carbons from pure $KAu(CN)_2$ solution to 1:1 from $HAu(CN)_2$ solution. Deoxygenation of solutions was also shown to reduce the gold:cation adsorption ratio to 1:1, but also reduced gold loading. The loading was restored if oxygen was added afterwards, but cation desorption also occurred.

XPS analysis of loaded carbons showed the adsorbed gold to be in the +1 oxidation state. Nitrogen was shown

to be adsorbed in two states, a cyanide species adsorbed evenly over the total surface and a decomposition product of cyanide only adsorbed on the external surface. From nitrogen contents determined by XPS and microanalysis it was shown that the gold was probably adsorbed as a mixture of $KAu(CN)_2$ and AuCN from pure $KAu(CN)_2$ solution.

Acknowledgements

The author wishes to express his appreciation to several individuals and organizations who have helped in the production of this thesis.

Dr. A.J. Monhemius of Imperial College and Mrs. E. Crathorne of B.P. Research for their supervision and guidance throughout the duration of this project.

Dr. D.L. Perry and Mr. R.C.W. Goodman for the XPS analysis of the carbons. Mr. D. Mealor for the analysis of the eluate in Chapter 5.3.2. Mr. D.M. Thornley and the analytical department at the B.P. Research Centre at Sunbury for the pore size distributions and surface areas of the carbons.

Mr. K.I. Jones for the microanalytical data. Mr. J.E.A. Burgess for his assistance in obtaining the necessary equipment for the experimental work.

Dr. H.L. Shergold, Mr. R.D. Hancock, Dr. S.R. Tennison and the many other people from B.P. Research and Imperial College who have given help or encouragement during the course of the project.

Finally I would like to thank the Science and Engineering Research Council and B.P. Research for financing this project by the provision of a CASE award.

To my parents.

Contents

List of Figures

List of Tables

1 Gold and Adsorbent Carbons

1.1 Gold

Gold has occupied a unique position in history due to its remarkable physical and chemical properties. Gold is one of only two pure metals exhibiting colours other than grey/white. It is one of only four metals commonly found in the elemental state in nature. A high density of 19.32 $g.cm^{-3}$ means that gravity concentration operations can lead to simple methods of recovery from natural streams after weathering of deposits. Gold is not corroded by any naturally occurring chemicals in the atmosphere or in water, and can thus retain its brilliant yellow gleam indefinitely. Its malleability and ductility allow it to be beaten into very thin sheets or fine wire.

The combination of colour and nobility has led to golds major use in ornamentation throughout the ages. Its scarcity and uniqueness led to the development of currency by bartering gold for goods or services. In modern times gold has found many more uses in the fields of medicine, dentistry and electronics.

The quest for gold has led to the rise and fall of many great empires. It is because of the wealth to be obtained from mining gold that mining methods have had to be developed in order to recover the more inaccessible ores. Attempts to manufacture gold from other substances

eventually led to the development of the art and then science of chemistry. Ultimately it is plain to see that the lust for gold has been instrumental in developing our modern day civilization.

1.1.1 History of Gold Extraction

As one of the four naturally occurring pure metals found in any significant quantity (copper, meteoric iron and silver being the others), it was naturally among the first metals used by man. Almost always found alloyed with silver, it was used extensively for ornamentation and currency [1].

The nobility of metallic gold led to physical methods of concentration/extraction such as winnowing, sifting and panning which rely on the high density of metallic gold. Riffling was also used, often coating the base of the riffle with fat or animal skins to aid in the retention of the nuggets. There is a possibility that the use of sheep skins in this kind of operation led to the legend of the Golden Fleece [2]. Gold ore mined from quartz veins could also treated in this way after crushing.

Early methods of separating gold from base metals included cupellation and amalgamation, removal of silver by the salt and sulphur processes or much later with nitric or boiling sulphuric acid, chlorination, or

electrolytic processes [1,3]. Amalgamation was also used as a method of extracting gold from ores [4]. The ore or concentrate was ground with mercury to dissolve the gold and silver and form the amalgam. Distillation of the amalgam allowed the mercury to be recovered for re-use, leaving gold and silver bullion.

An alternative method was the formation of soluble Auric Chloride ($AuCl_3$) by the action of chlorine gas, in the presence of moisture, on the ore [5]. This process was superseded by the dissolution of gold in cyanide solution, with recovery by precipitation using zinc.

The cyanide process has remained the major gold extraction route to the present day, though environmental pressures may see a change in the future to systems using acid chlorine, acid thiourea or ammoniacal thiosulphate leaching processes [6].

1.2 Chemistry of Gold

Gold is the most noble of the metals, being the only one not attacked by either oxygen or sulphur at any temperature, and not easily affected by water or most acids [7]. Gold does react with tellurium at high temperatures, and with all the halogens. In aqueous solutions the presence of an oxidizing agent and a good ligand for gold is needed for dissolution. Thus gold dissolves in aqua regia to give $HAu(Cl)_4$, and in cyanide

solutions with oxygen or hydrogen peroxide to give $Au(CN)_2^-$. Gold has the electronic configuration (Xe) $4f^{14}$ $5d^{10}$ $6s^1$, and has been shown to form complexes with single gold atoms in the I, II, III, and V oxidation states. Of these the I and III states are the more important. The Au(I) complexes generally form linear structures, whereas the Au(III) complexes are usually planar. The Au(III) complexes are generally more stable than Au(I) in aqueous solution, with the exception of the very stable cyanide species.

1.3 Activated Carbon

Since their first practical use as a decolourant in the French sugar-beet industry , activated carbons have been used extensively for their properties in selectively adsorbing low concentrations of impurities from gases and liquids [8]. They have been produced from a wide variety of carbonaceous materials, for example coal, peat, olive stones, coconut shells and bone, which along with the method and conditions of activation determines the physical and chemical structure and properties of the activated carbon produced [9].

1.3.1 Manufacture of Activated Carbon

Activated carbons are manufactured by a two stage process of carbonization and activation.

1.3.1.1 Carbonization

Carbonization consists of heating the original carbonaceous material in the absence of air up to 400-600°C. Considering the carbonization of wood [10], drying occurs up to approximately 170°C, then the evolution of carbon monoxide, carbon dioxide and acetic acid. At around 270-280°C the wood starts to decompose exothermally with the production of tar, methanol, etc. The carbon content of this carbonized product is typically about 80 %, depending on the final temperature and original material. Structurally this product is composed of a random arrangement of graphitic crystallites, separated by amorphous carbon produced by the decomposition of tar. At the lower carbonization temperatures tar may also be left in the pores without decomposition. The presence of amorphous carbon and other products of carbonization blocking the pores results in a carbonized material with a low surface area and limited activity.

1.3.1.2 Activation

Partial activation can be achieved by removal of the tar by heating in an inert gas. To produce a high surface area adsorbent with a large adsorption capacity the carbonized product must also be oxidized. Activation is thus achieved by heating the carbonized material in an

oxidizing atmosphere, usually steam, air or carbon dioxide, resulting initially in the oxidation of the amorphous carbon. This opens up the crystallites which burn preferentially in a direction parallel to the basal plane [11]. This results in a microporous activated carbon. If oxidation is continued the number of crystallites orientated for preferential oxidation decreases, further burning being of the pore walls resulting in the formation of a more macroporous activated carbon.

A different way of producing activated carbon is by addition of chemical agents to the starting material before carbonization [10]. These agents, such as zinc chloride, minimise the production of tar and thus the formation of areas of amorphous carbon. After carbonization the product is cooled and the agent recovered for re-use by acid washing [8]. The porosity of the activated carbon produced in this way is dependent on the amount of activating agent added. If relatively small amounts are added a microporous structure is produced, correspondingly larger pores being formed with larger additions.

1.3.2 Physical Structure of Activated Carbon

The skeletal structure of activated carbon is essentially a highly disordered form of graphite.

Graphite (figure 1.1), with a density of 2.26 $g.cm^{-3}$, has a layer structure of the ABAB type, the layer spacing being 0.335 nm. The layer planes are held together by weak Van der Waals forces. Each layer consists of carbon bonded in a planar hexagonal lattice, with a carbon-carbon bond length of 0.124 nm [12,13].

Activated carbon (figure 1.2), with an apparent density of between 0.5 and 1.0 $g.cm^{-3}$ [14], consists of many small crystallites or platelets [15], of an essentially graphitic structure. The crystallites, from 2-10 nm wide and around 1 nm thick, are more ordered in graphitizing than non-graphitizing activated carbons (figure 1.3). Each crystallite thus has a number of parallel graphite layers. It has been shown that the number of these layers, and thus the thickness of the crystallite, is a function of the crystallite width [16]. The planar carbon-carbon bond length is the same as in graphite [17], but the layer spacing is larger, up to 0.344 nm for a completely disordered activated carbon [12,18].

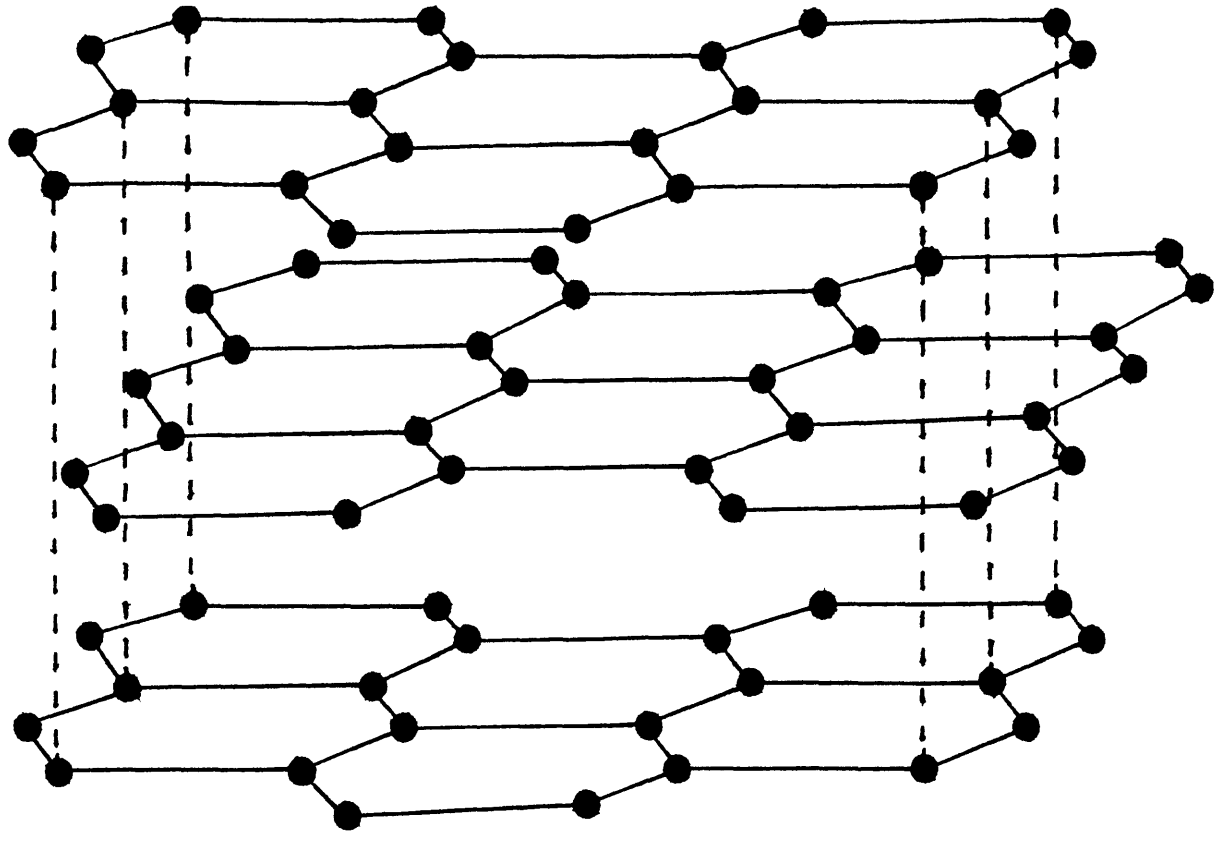

Figure 1.1 Schematic representation of the crystalline structure of graphite.

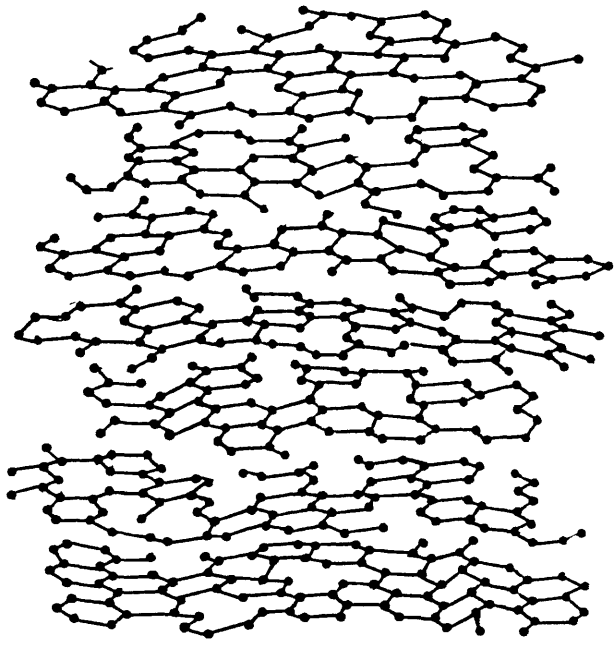

Figure 1.2 Schematic representation of the proposed turbostratic structure of activated carbon [18].

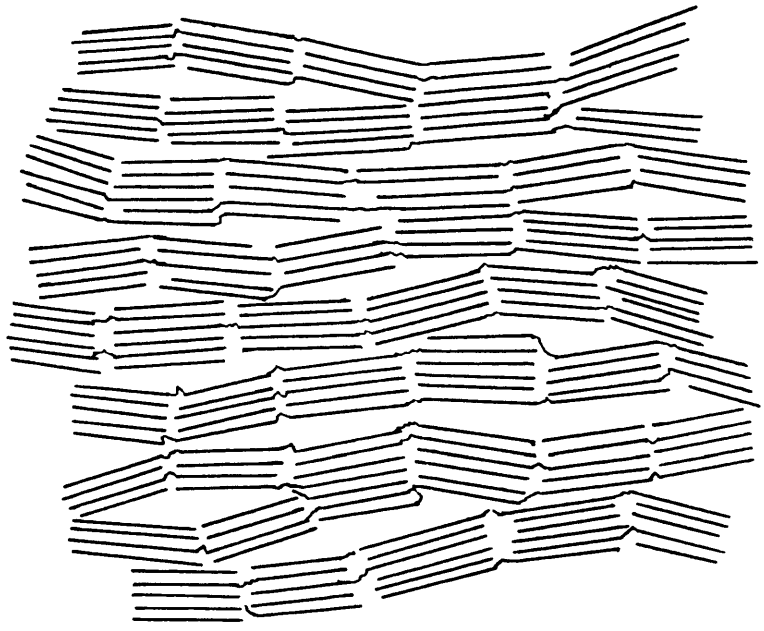

(a) Graphitizing.

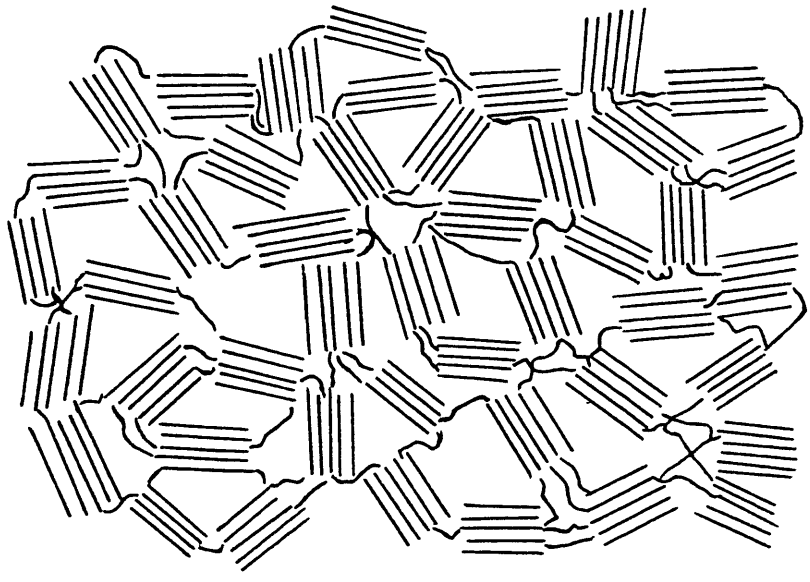

(b) Non-graphitizing.

Figure 1.3 Schematic representations of the crystallite structure of graphitizing and non-graphitizing activated carbons [16].

The density difference between graphite and activated carbon is due to the presence of an extensive system of pores of differing shapes and sizes [19,20]. The complex nature of these pores makes any classification difficult. By convention pores are categorized according to an assumed characteristic dimension (r) such as radius or half slit width [14,21,22]:-

Micropores	$r < 2$ nm
Mesopores	$2 < r < 2500$ nm
Macropores	$r > 2500$ nm

Because of the highly porous nature of activated carbons, they have very high surface areas, 500 - 2000 $m^2.g^{-1}$ [23,24], and large pore volumes, 0.4 - 2 $cm^3.g^{-1}$ [25]. Thus when studying activated carbons the pore size distribution can be very informative because it gives an indication of the size of molecule that can be adsorbed.

1.3.3 Surface Chemical Structure of Activated Carbon

The surface chemical structure of activated carbon will be dependent on the method and conditions of activation, and is usually categorized according to the activation temperature. 'H' type activated carbons are

activated above 500-600°C, adsorb acid from solution and contain mainly basic surface oxide functional groups [26]. 'L' type activated carbons are activated at lower temperatures, adsorb alkali from solution and contain mainly acidic surface oxide functional groups. The precise nature of the surface chemical structure of activated carbon is not fully understood. Many functional groups have been identified by different researchers [12,26-29]. Acidic surface oxide groups reported are usually carboxylic, phenolic hydroxide and quinone type carbonyl in character. Normal and fluorescein type lactones, cyclic peroxides and carboxylic acid anhydrides have also been reported (figure 1.4A). Much less is known about basic oxide groups, though Garten and Weiss [30] proposed the presence of chromene type structures to explain acid adsorption (figure 1.4B).

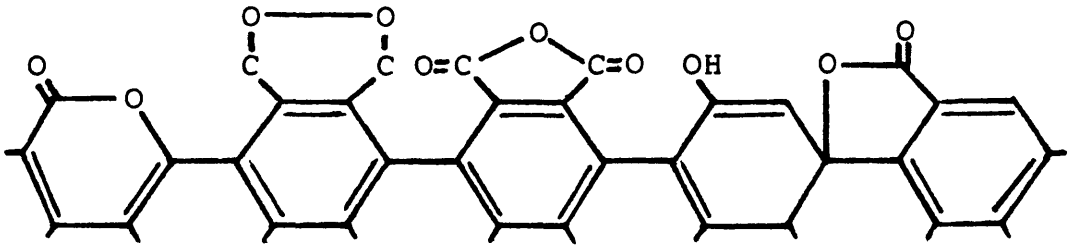

Normal lactone | Cyclic peroxide | Carboxylic acid anhydride | Fluorescein type lactone

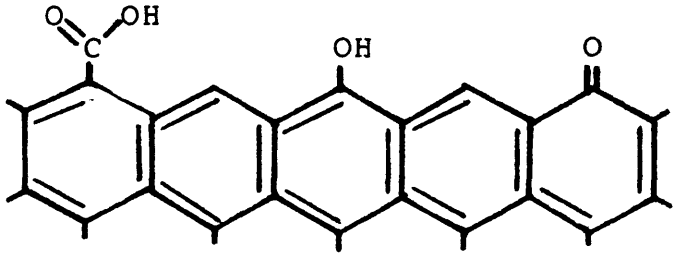

Carboxyl | Phenolic hydroxyl | Quinone type carbonyl

(A) Acidic oxide groups [12,26-29].

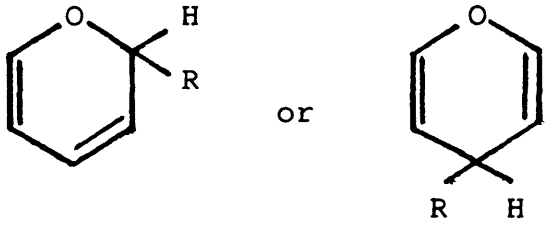

Chromene

(B) Basic oxide group [30].

Figure 1.4 Suggested oxide groups on the surface of activated carbon.

1.4 Carbon Black

Initially produced as black pigments for inks, the major use of carbon blacks today is as reinforcing agents in the rubber industry [31]. Other uses include pigments in paints, plastics and paper; carbon electrodes, dry cells, and thermal insulation.

1.4.1 Manufacture of Carbon Black

Carbon blacks are made by either decomposition or partial combustion of liquid and gaseous hydrocarbons to form elemental carbon and hydrogen [31]. This produces a carbon with a much lower impurity content than activated carbons made from peat, coconut shells, etc.

The structure and properties of a carbon black will be determined by the method and conditions of manufacture.

1.4.1.1 Types of Carbon Black

Lampblack was the first carbon black produced. Originally made from resin, fat, or oil, today the raw materials are usually petroleum residues. These materials are burned in shallow, open pans with a restricted air supply. The airborne reaction products pass through a series of settling chambers and bag filters where the carbon black is collected.

Channel blacks were produced after the discovery of oil, because of the abundance of cheap natural gas. The gas is burned by a series of small flames which impinge on steel channels. Carbon is deposited on the channels, and is then periodically scraped off.

Furnace blacks are produced by burning a gas or gas/oil mixture in a single flame furnace. The carbon black is removed from the flue gases, after water spray quenching and floculation, by cyclones and bag filters.

Thermal blacks are produced by decomposition rather than partial combustion of gaseous hydrocarbons. The gas is passed through one of a pair of furnaces packed with preheated silica bricks. The carbon black is recovered as in the furnace black process, and the waste gas, which has a high hydrogen content, is used as fuel to heat the second furnace. Cycling the furnaces between heating and carbon black production ensures a continuous process.

1.4.1.2 Mechanism of Carbon Black Formation

The mechanism of carbon black formation by decomposition or partial combustion is far from certain [32]. Current theories propose the initial production of polyaromatic macromolecules that nucleate into small droplets. Growth of these particles occurs by adsorption of further macromolecules from the gaseous phase, or coalescence of several droplets. Pyrolysis of

these particles results in the formation of carbon black.

1.4.2 Physical Structure of Carbon Blacks

Carbon blacks are produced in the form of aggregates of spherical particles during the combustion process [33]. These particles are composed of randomly orientated stacks of parallel basal layer planes about 1.2 nm thick and 1.5 - 2.0 nm wide [34]. These layer stacks are ordered on the outside of the particle to give a surface composed mainly of basal planes (figure 1.5). For particles with a single nucleation site the degree of order decreases towards the centre of the particle with randomly ordered stacked layer planes, single layer planes and amorphous carbon in the centre [34,35]. For particles with several nucleation sites order decreases towards the centre of each site with intermediate orientation between the sites [36].

Due to the greater degree of order of the stacked layer planes, surface areas are lower than in activated carbons, generally less than 200 $m^2.g^{-1}$ [37].

1.4.3 Surface Chemical Structure of Carbon Blacks

As with activated carbons, many different oxide groups have been detected on the surface of carbon black. The nature of these oxides is dependent on the temperature at which freshly manufactured carbon black is

first brought into contact with gaseous oxygen [38].

1.5 Structural Modifications of Carbons by Heat-Treatment

It is possible to change the pore and surface chemical structures of activated carbons and carbon blacks by heat-treatment in inert atmospheres. Surface oxide groups are removed between 200 and 1500°C as carbon monoxide, carbon dioxide and hydrogen [31]. Heat-treating above 1300°C results in crystallite structure modification. The crystallites grow and turbostratic regions are rearranged into preferred orientations. In carbon blacks peripheral crystallites are formed with basal planes tangential to the particle surface [34]. Oxidative heat-treatments up to about 500°C result in preferential oxidation of the less organized areas of carbon black particles to leave a shell of orientated crystallites [39].

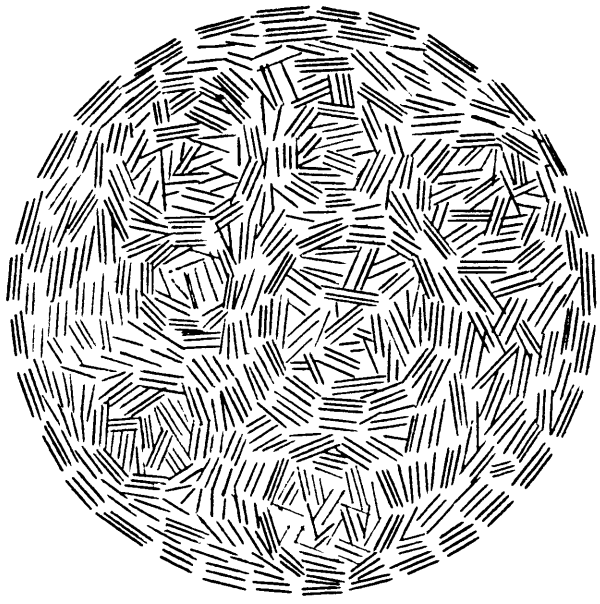

(a) Several nucleation sites.

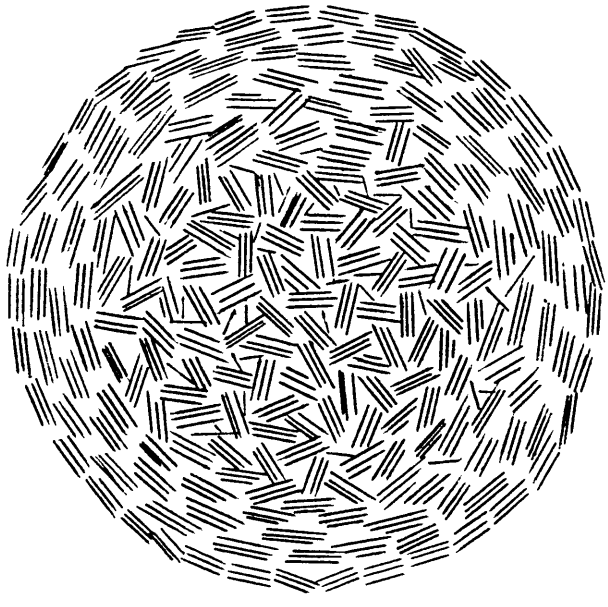

(b) Single nucleation site.

Figure 1.5 Schematic representation of the crystallite structure of carbon blacks with one or more nucleation sites.

2 Adsorption of Gold by Activated Carbon

The lust for gold, either because of its beauty or value, has led to the investigation of numerous non-standard methods of production. Among these the most well known is that of alchemy, to produce gold from base metal. Although Arthur C. Clarke's view in his novel 'Imperial Earth' of genetically engineered coral extracting gold to make reefs with is fiction at the present, it is known that certain plants concentrate gold in their system [40], and that marine sponges can adsorb gold from seawater [41].

Research into techniques of getting gold from seawater is increasing as the more readily mineable deposits are being worked out [42]. The extraction of gold from seawater may well be achieved using selective micro-organisms or adsorbents, as the alchemists dream has been realized in todays atomic age. Whether or not such a process can be done successfully will depend on its cost and the demand for gold.

2.1 Process History

It has been known since at least the start of the nineteenth century that charcoal will adsorb gold from chloride solutions in the metallic state [43].

The first recorded use of activated carbon to

extract gold was in a patent by Davis [44] in 1880. He described a method of recovering gold from aqueous chloride solutions. In 1887 MacArthur and the Forrest brothers patented a process for dissolving gold in weak cyanide solution, and later a method of precipitating gold using zinc [45,46]. In 1894 Johnston patented a process for the extraction of gold using activated carbon in place of zinc [47], the gold being recovered from the activated carbon by burning, followed by smelting of the ash. The main disadvantage of this process was the lack of an efficient method of stripping the gold that did not result in the destruction of the activated carbon. Thus it was only used when zinc cementation was inefficient [48,49]. Interest in the process was then rekindled in 1950 when Zadra [50] reported using a caustic sodium sulphide solution to recover the gold from the activated carbon, the gold then being recovered from solution by electrolysis. In 1952 he improved the method by using a hot caustic cyanide solution, which recovered both gold and silver [51]. Extraction of gold using activated carbon thus became more economic and could be used to a far greater extent.

At the present time, of the ten largest free world gold producing mines, all in South Africa, four utilize activated carbon adsorption in their recovery circuits, though they all still use zinc precipitation [52]. In the United States six of the ten largest gold mines use activated carbon adsorption in their main gold recovery

operation.

2.2 Chemical Effects

2.2.1 pH

The pH of the adsorption medium has been shown by many researchers to have a significant effect on both the rate of gold adsorption and the equilibrium capacity. It is usually shown that increasing the acidity of the solution causes an increase in the rate and capacity of gold loading (figure 2.1). In neutral and alkaline solutions there is little or no effect [53-55].

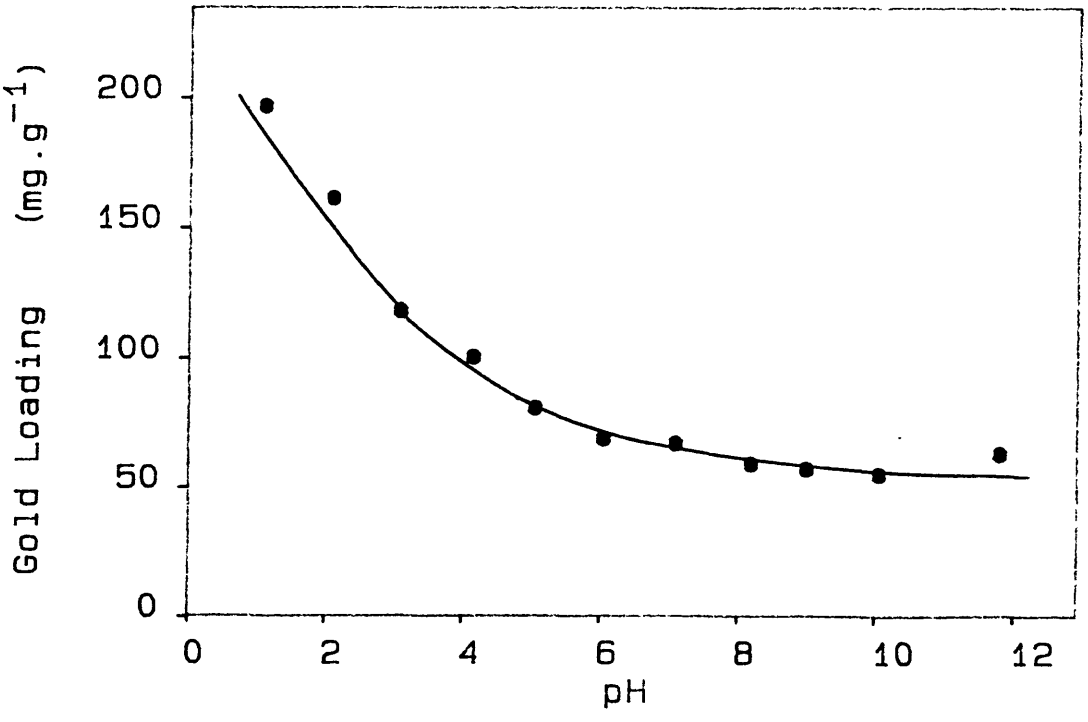

Figure 2.1 Effect of pH on the adsorption capacity of activated carbon (from McDougall et al. [53]).

Davidson et al. [56] presented similar results for the gold capacity, but showed that for the gold adsorption rate the optimum pH is about 4.

2.2.2 Foreign Cations

The presence of foreign or 'spectator' cations in the adsorption medium has been shown to lead to faster rates and increased loading capacity [53,54,57]. The effectiveness of the different cations studied has been given as [54]

$$Ca^{2+} > Mg^{2+} > H^{+} > Li^{+} > Na^{+} > K^{+}$$

and [57]

$$Ba^{2+} > Ca^{2+} > Mg^{2+} > Cs^{+} > K^{+} > Li^{+}$$

The reason for these effects is usually given as adsorption of a $M^{n+}(Au(CN)_2^-)_n$ complex where M^{n+} is the cation added. Considering the addition of H^+ ions to the solution, a possible explanation for the difference in relationships between pH and gold loading reported is apparent. McDougall et al. [53] in determining pH effects maintained the required pH by addition of acid or alkali during adsorption, Tsuchida [57] did not. Experiments have shown that in acid solution $HAu(CN)_2$ is adsorbed [58], this would result in an increase in pH. If the pH is maintained by further addition of acid we would expect

acid solutions to lead to adsorption of significantly greater amounts of gold than neutral ones. This is because the relevant cation concentration is constant. In alkaline solutions this pH change would not occur as another cation is adsorbed, and the concentration of this cation would be reduced by a similar amount as the gold. Thus by maintaining a set acid pH gold adsorption will be increased significantly due to the relatively increased cation concentration. An interesting experiment would be continuous monitoring of Ca^{2+} concentrations (for example), with addition of calcium salts to keep it constant.

2.2.3 Temperature

The adsorption of gold is an exothermic process, with an activation energy of 10.9 $kJ.mole^{-1}$ [55,59]. Higher gold loadings occur at lower temperatures, but the effect on adsorption rates is small with only a slight increase at higher temperatures.

2.2.4 Free Cyanide

The presence of free cyanide in solution leads to a reduction in both the rate and amount of gold adsorption that is unaffected by the pH [55,57]. Low concentrations have a greater effect due to the presence of significant quantities of cations from the cyanide salt at higher concentrations.

2.2.5 Oxygen and Nitrogen

When nitrogen is bubbled through solutions during adsorption there is a reduction in the expected amount of gold adsorbed but no change in the initial rate [57,59]. With air or oxygen there is no change in either the rate or amount of gold adsorbed.

2.2.6 Particle Size

Using smaller particle size activated carbons results in an increase in the rate of adsorption, but the capacity for gold is unaltered [55].

2.3 Physical Effects

Due to the complex structure of activated carbon, little research appears to have been undertaken to relate liquid phase adsorption to pore size distribution or surface chemical structure. Davidson [24] measured the Freundlich K value, pH, ash content, methylene blue number, iodine number and surface area of twenty four commercially available activated carbons. A statistically significant linear correlation between K and pH suggested that gold adsorption was favoured by activated carbons containing basic oxide functional groups. No significant correlations between K and surface areas, methylene blue number (a measure of the ability to adsorb large molecules) or the iodine number (another measure of

surface area) were indicated. Thus the pore size distribution appeared to have little effect on gold adsorption. It must be stressed that the activated carbons chosen were produced from several starting materials and were activated under different conditions, thus any comparison between them may be subject to a large degree of error.

2.4 Selection of Activated Carbon

The selection of an activated carbon for a gold extraction operation must take into account many factors. As well as being an efficient adsorbent for gold, the activated carbon must be readily stripped (of gold) without seriously impairing its adsorption ability. A high attrition resistance is also necessary to reduce gold losses in fines. The kinetics of adsorption are also very important. The optimum conditions being high gold loadings in short times leaving very dilute gold solutions. In general each extraction plant must test a selection of activated carbons to choose the one most suited for its needs.

2.5 Extraction Processes

There are numerous possible flow sheets currently available to produce an efficient gold extraction plant utilizing adsorption onto activated carbon. However some

unit operations are common to all flowsheet options.

2.5.1 Adsorption of Gold

Adsorption normally takes place in either a column or tank containing activated carbon particles.

In carbon-in-column adsorption the upward flow of liquor causes a bed expansion of around 35 %, providing sufficient mixing for efficient adsorption [60-62]. The liquor must be clear to prevent blocking or carry-over of loaded activated carbon, and is thus often used in heap-leaching circuits. It is possible to use a single column or a series of several. Loaded activated carbon is removed at regular intervals, or when the barren solution reaches a predetermined gold concentration. Fresh activated carbon is loaded into the end of the adsorption circuit, and thus advances through the system.

The carbon-in-pulp process utilizes adsorption tanks where the activated carbon and the pulp after gold leaching are agitated together during adsorption [63-67]. The size of the activated carbon particles used is larger than the particle size of the solids contained in the pulp to allow interstage screening. A series of tanks are used, the flow of activated carbon and liquor is countercurrent, with interstage screening to retain the loaded activated carbon, which is periodically moved by airlifting pulp from one tank to another. Fresh activated

carbon is added to the final tank.

It is also possible to combine the leaching and adsorption steps using carbon-in-leach operations. Thus instead of initially leaching the ore to produce a pulp containing dissolved gold, the activated carbon and ore are added simultaneously to the leach solution. This results in a capital saving in leaching equipment over the carbon-in-pulp process as the number of agitation tanks can be reduced [67].

2.5.2 Elution of Gold

Up to 1950 the only efficient method of recovering gold from loaded activated carbon involved burning the activated carbon and smelting the ash. This process was costly due to the destruction of the activated carbon. Then Zadra [50,51] developed an efficient method of eluting the gold to allow re-use of the activated carbon. At present there are several methods available.

2.5.2.1 Zadra Procedure

This method consists of treating the loaded activated carbon, at atmospheric pressure, with a boiling solution of 1 % sodium hydroxide and 0.1 % sodium cyanide. Used in closed circuit with electrolytic cells it has been shown to be possible to strip gold from 8400 to 140 $g.tonne^{-1}$ activated carbon in 50 hours [63].

2.5.2.2 AARL Procedure

Developed by the Anglo-American Research Laboratories, this method can be considered as an improved Zadra process. The loaded activated carbon is pretreated with a solution of 1 % sodium hydroxide, 10 % sodium cyanide. Elution then follows using hot, deionized water [68,69]. The process gives 99 % gold and 98 % silver recovery in 14 hours at 90°C from an activated carbon loaded with 2900 $g.tonne^{-1}$ gold and 64 $g.tonne^{-1}$ silver. Shorter elution times of about 3 hours can be achieved using pressurized elution at 125°C.

2.5.2.3 Organic Procedures

The addition of 20 % ethanol or methanol to Zadra's solution of 1 % sodium hydroxide, 0.1 % sodium cyanide, results in 99 % gold and silver recovery, from an activated carbon assaying 6600 $g.tonne^{-1}$ gold and 1000 $g.tonne^{-1}$ silver, in 6 hours. Elution is at 80°C under atmospheric pressure [70].

The Murdoch desorption procedure comprises an initial wash with 80 % acetonitrile in water. Elution, with 40 % acetonitrile, 1 % sodium cyanide and 0.2 % sodium hydroxide, at 70°C gives > 90 % gold recovery in 8-10 hours [71]. A major advantage of this process is that about 80 % of the gold can be recovered in the first

bed volume of eluant, thus giving highly concentrated gold solutions for electrolysis.

2.5.3 Activated Carbon Regeneration

During the adsorption stage the activated carbon adsorbs small quantities of organic and inorganic impurities. These must be removed if the gold adsorption capacity is to be maintained. After elution the activated carbon is fed, with an approximately 50 % moisture content, into a horizontal rotary kiln at 650°C. Steam generation creates a positive pressure, excluding air from the kiln. The discharged regenerated activated carbon is either water quenched or allowed to cool in air before return to the adsorption circuit [62,72,73].

2.5.4 Electrowinning

The eluate from the desorption stage is circulated to electrolytic cells containing stainless steel screen anodes and stainless steel wool cathodes [63]. Electrolysis can be continuous or batch, the barren solution being recycled to the desorption stage. The gold and silver values are recovered from the cathode by smelting, usually after an initial acid wash.

Cation exchange membranes have been used in an attempt to improve current efficiency by separating the anodic and cathodic reactions [49].

Anode reaction,

$$4\ OH^- = O_2 + 2\ H_2O + 4\ e^- \qquad (2.1)$$

Cathode reactions,

$$2\ e^- + 2\ H_2O = H_2 + 2\ OH^- \qquad (2.2)$$

$$e^- + Au(CN)_2^- = Au + 2\ CN^- \qquad (2.3)$$

The improvement in current efficiency is small and is usually negated by the cost of the membranes.

2.6 Mechanism of Gold Adsorption

In the first detailed study of gold adsorption in 1913, Green believed $KAu(CN)_2$ was reduced by wood charcoal and gold precipitated in the metallic state [74]. Only 5.6 % of the adsorbed gold could be recovered by equilibration of the loaded charcoal with a solution of KCN. Vacuum degassing experiments suggested the presence of adsorbed gases in the wood charcoal, predominantly oxygen, carbon monoxide, carbon dioxide, hydrogen and nitrogen. These gases appeared to be held in two states. Loosely held gases were evolved either slowly after manufacture of the charcoal during exposure to air, or by vacuum degassing at up to 200°C. Removal of these gases had no effect on the adsorption efficiency of the charcoal. The more firmly bound gases were evolved after

prolonged exposure to air, or by vacuum degassing at up to 500°C. The removal of the firmly bound gases resulted in a large drop in adsorption efficiency, and it was thus thought that these gases were responsible for the reduction process. Of the two reducing gases found carbon monoxide was removed in greater abundance than hydrogen. Thus the mechanism proposed was the reduction of $KAu(CN)_2$ by strongly adsorbed carbon monoxide (possibly hydrogen also), and precipitation of metallic gold in the pores of the charcoal.

In an attempt to understand why carbonaceous deposits in gold ores were leading to reduced extraction efficiencies by cyanidation, Feldtmann [75] in 1914 found that significant, but not total recovery of adsorbed gold could be achieved with alkaline sulphide solutions. The resultant wash solution was also shown to contain significant quantities of cyanogen. Adsorption of metallic gold was discounted due to low gold recovery by cyanide washing of loaded charcoals, and no visible metallic precipitate seen on microscopic examination. Noting also the effect of adsorbed carbon monoxide on gold adsorption, Feldtmann proposed that the adsorbed species was a combination of aurocyanide, cyanogen and carbon monoxide termed 'carbonyl aurocyanide', with a possible formula of $AuCN.CO.(CN)_2$. In the discussion which followed the presentation of the report Picard proposed that $NaAu(CN)_2$ could react with oxygen produced from adsorbed species to form insoluble aurocyanide and

sodium cyanate:

$$NaAu(CN)_2 + (O) = AuCN + NaCNO \qquad (2.4)$$

This would also account for the formation of cyanate, and the deleterious effect of free cyanide on gold adsorption noted by Feldtmann, aurocyanide being soluble in cyanide. To explain partial dissolution of the adsorbed gold in alkaline sulphide solutions, Picard proposed the following reaction:

$$3\ AuCN + Na_2S = NaCNS + NaAu(CN)_2 + Au_2 \qquad (2.5)$$

With no free cyanide present this would give one third gold recovery, but Feldtmann had reported two thirds recovered with just sodium sulphide solution.

Also in the discussion Trewartha-James pointed out that if, as Feldtmann reported, carbonaceous deposits adsorbed gold up to a maximum loading, this may be due to a physical process. Adsorption occurring onto the particle surfaces until they are completely coated. Restoration of adsorption capacity occurring when the species was desorbed.

In 1917 Edmands [48] doubted Feldtmann's idea of gold being precipitated as $AuCN.CO.(CN)_2$, since formation of this compound would require 1 mole of free cyanide per mole of gold precipitated. Although free cyanide was

shown to be adsorbed by charcoal, the amount was much less than predicted, and was seen to be unrelated to gold adsorption.

Noting the formation of addition products of $KAu(CN)_2$ ($KCN.AuCN.X_2$ where X=Cl, Br, I.), Edmands proposed the formation of KCN.AuCN.CO on the carbon surface, with HCN.AuCN.CO in acidic solutions.

In the discussion which followed, Rose thought that the active agent in charcoal was liquefied carbon monoxide. Allen doubted Green's [74] theory of adsorbed carbon monoxide being responsible for gold adsorption. It was noted that Rhead [76] concluded, after studying the combustion of charcoal, that initially a complex C_xO_y decomposes on heating and evacuation to liberate carbon monoxide and carbon dioxide. Since this carbon monoxide was only formed at high temperature and reduced pressure, it seemed unlikely that it could be held responsible for gold adsorption. Commenting on Feldtmann's [75] assumption that washing gold loaded charcoal removed the adsorbed gold, leaving precipitated gold, it was known that adsorbed species could only be washed off with 'extreme difficulty', so the gold recovered was more likely simply held in solution in the pores of the charcoal. Further proof of this could be found if the adsorbed and precipitated values were correlated with the equilibrium gold concentration in solution using the empirical Freundlich adsorption isotherm. The correlation

with precipitated gold is significant, but not with adsorbed gold. Allen thus proposed that gold was adsorbed without chemical change, by an equilibrium process which agrees with the Freundlich adsorption isotherm. The equilibrium was said to be dependent on the surface tension. Thus by altering the surface tension of the solution, the equilibrium could be affected. This was thought to be why gold could be recovered from charcoal by sulphide solutions.

In 1923 Williams [77] analysed the ashes of burnt, gold loaded charcoal and discovered large quantities of calcium salts, but very small amounts of sodium. The adsorbed species was thus thought to be $Au(CN)_2^-$ but no mention was made of the corresponding cation adsorbed.

McKee and Horton [78], in 1925 also noted the change in colour of charcoal, seen by Green [74], on loading gold from dilute aurocyanide solution, indicating the adsorption of metallic gold. In more concentrated solutions they also proposed that some gold was adsorbed as an ion or molecule.

In 1927 Gross and Scott [79] showed that surface tension does not affect gold adsorption. In acidic solutions the efficiency of pine charcoal to adsorb gold was increased, and this adsorbed gold was more readily recovered by KCN. This suggests that from acidic solution the adsorbed species is wholly or partly AuCN.

It was noted that on gradual heating, alkaline aurocyanides pass through a range of colours - pink, red, deep brown/purplish red, to leave metallic gold. Aurocyanide turns green on heating, then brown, and finally metallic gold is left. Heating gold loaded pine charcoal gave colours indicating alkaline aurocyanide, as did the residues produced by evaporation of solutions obtained after hot water washing of the loaded charcoal. This suggests that in neutral solution AuCN is not adsorbed. Unfortunately they did not repeat these tests using charcoal loaded from acidic solution.

Using pure solutions of $KAu(CN)_2$, they showed that potassium and bicarbonate were left in solution after gold adsorption. The solutions obtained by hot water washing of the loaded charcoal did not contain enough potassium to account for $KAu(CN)_2$, but there was sufficient calcium. Thus they proposed that for pine charcoal the adsorption equation was:

$$2\ KAu(CN)_2 + Ca(OH)_2 + 2\ CO_2 = Ca(Au(CN)_2)_2 + 2\ KHCO_3 \qquad (2.6)$$

The calcium oxide was contained as an impurity in the charcoal, and carbon dioxide had been shown by Green [74] to be important.

For sugar charcoals that contain little or no calcium impurities, they showed that the colour change

obtained on heating loaded charcoal did not occur unless it was treated with calcium oxide. Thus if calcium is not present they proposed adsorption of $HAu(CN)_2$:

$$KAu(CN)_2 + H_2O + CO_2 = HAu(CN)_2 + KHCO_3 \qquad (2.7)$$

Garten and Weiss [80] were the first to suggest a reaction with a specific surface functional group. In 1957 they proposed that in alkaline solution, any chromene sites will be oxidized to chromenols. Exchange of hydroxyl with aurocyanide ions at the carbonium ion site then occurs (equation 2.8). However they offered no explanation for increased adsorption obtained from acidic solutions.

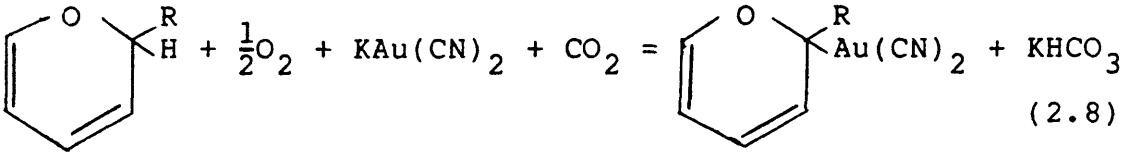

(2.8)

In 1968 Kuz'minykh and Tyurin [58] studied the change in concentration of ions, in solution, when de-calcified birch charcoal was added to solutions of $KAu(CN)_2$ acidified with HCl. They concluded that the form of the adsorbed complex was dependent on the pH of solution. $HAu(CN)_2$ being adsorbed from acid solution, $KAu(CN)_2$ from neutral or alkaline solution.

Davidson [54] reported on the effects of 'spectator' cations in solution on gold adsorption in 1974. It was

shown that an increase in the rate and capacity of gold adsorption occurs in acidic solutions, and by the addition of sodium or calcium ions. The differing effects of the several cations was thought to be due to the stability of the aurocyanide complex formed, and was given to be in the order:

$$Ca^{2+} > Mg^{2+} > H^{+} > Li^{+} > Na^{+} > K^{+}$$

The decrease in adsorption in alkaline solution was considered as being due to competition between aurocyanide and hydroxide anions for adsorption sites.

Recovery of adsorbed gold by elution with deionized water was shown to be improved greatly after a sodium or potassium carbonate pretreatment. Acid washing the loaded activated carbon greatly reduced this effect, but it was shown that the addition of potassium hydroxide to the pretreatment restored it. For loadings from potassium aurocyanide solution, a calcium chloride treatment resulted in little gold recovery being obtained by elution without carbonate pretreatment.

These elution results suggested to Davidson that if calcium is not present in solution then $HAu(CN)_2$ was adsorbed in acidic or alkaline solution, $Ca(Au(CN)_2)_2$ being adsorbed if calcium is present in neutral or alkaline solution. However, if adsorption of $HAu(CN)_2$ from neutral or alkaline solutions of $KAu(CN)_2$ occurs

then, as in the case of acid washing, potassium hydroxide would be needed with the carbonate pretreatment to obtain the recovery reported by elution.

The effect of the carbonate pretreatment was thought to be exchange of the cation adsorbed with gold with potassium:

$$2\ HAu(CN)_2 + K_2CO_3 = 2\ KAu(CN)_2 + H_2CO_3 \qquad (2.9)$$

$$Ca(Au(CN)_2)_2 + K_2CO_3 = 2\ KAu(CN)_2 + CaCO_3 \qquad (2.10)$$

In 1978, Dixon et al. [59] noted that if nitrogen is bubbled through the solutions during adsorption, there is a significant drop in equilibrium gold loading, but little change in the initial rate. Oxygen was shown to have no effect. Increased adsorption at low pH was thought to be due to the formation of positive sites, thus:

$$C_xO + H_2O = C_x^{2+} + 2\ OH^- \qquad (2.11)$$

Evidence for this theory was the release of hydroxide by activated carbon in aqueous solution.

Cho and Pitt [81] studied the adsorption of gold and silver cyanides, and in 1979 noted that three times as much gold as silver is adsorbed. From this they concluded that adsorption was electrostatic in nature, since the

larger aurocyanide ion will be more easily stabilized in the electrical double layer.

In 1980 McDougall, et al. [53] used X-ray photoelectron spectroscopy to determine the binding energies of electrons in the adsorbed gold species. They found that the binding energy was between those expected for metallic gold or $KAu(CN)_2$, and was not significantly affected by 'spectator' cations or cyanide in solution. Thus they calculated that the adsorbed species had a mean oxidation state of 0.3. Another possible species adsorbed was AuCN without reduction. However, they were unable to determine the Au(I) binding energy for AuCN and thus could not show whether or not this species was adsorbed.

Measurement of nitrogen contents of loaded activated carbons, by microanalysis, indicated insufficient nitrogen is adsorbed to account for $Au(CN)_2^-$, and at high loadings the molar Au:N ratio approaches 1:1. As it was reported that no free cyanide could be detected in solution after the adsorption tests, it was thought that the activated carbon was acting as a catalyst for the oxidation of CN^- to NH_3, and that the NH_3 was being lost.

The mechanism of adsorption was proposed to consist of 2 steps.

(1) Initial adsorption of $M^{n+}(Au(CN)_2^-)_n$, (where M^{n+} is K^+, Na^+, H^+, or Ca^{2+}) the cation adsorbed being the

one which forms a complex with the lowest solubility.

(2) Reduction of the adsorbed species to form either a cluster compound containing gold in the 0 and +1 oxidation states, or a sub-stoichiometric aurocyanide polymer $(AuCN)_x$ containing some metallic gold.

Tsuchida et al. [82] measured the adsorption of gold and cations from solution onto acid washed activated carbon, and in 1982 noted that at pH < 10 the molar Au:K adsorption ratio was 2.5:1, and that the addition of free cyanide had no effect. At higher pH there was seen to be an increase in potassium loading, but no change with gold unless free cyanide was present, when gold loadings were reduced. They also noted the release of hydroxide during adsorption which was more pronounced at high loadings. Thus their mechanism involved decomposition of $Au(CN)_2^-$ to insoluble AuCN and free cyanide (equation 2.12). The cyanide is oxidized to cyanate (equation 2.13), carbon dioxide and ammonia are then formed by hydrolysis (equation 2.14). Increased cation adsorption at pH>10 was thought to be due to formation of anionic sites.

$$c|OH + Au(CN)_2^- \xrightarrow{pH>10} c|O^- K^+_{AuCN} + CN^- \qquad (2.12)$$

$$2\ CN^- + O_2 = 2\ CNO^- \qquad (2.13)$$

$$CNO^- + 2\ H_2O = NH_3 + CO_2 + OH^- \qquad (2.14)$$

In later reports during 1984 Tsuchida et al. [57,83] reported that free cyanide reduces gold adsorption at all pH values, but for high cyanide concentrations this drop is lower. This was assumed to be due to the high cation concentration, though it was also shown that the effect of 'spectator' cations is negligible below pH 6, and that the molar gold:cation adsorption ratio is always greater than 1:1. Increased cation adsorption in alkaline conditions was thought to be due to the precipitation of calcium and magnesium carbonates, the carbonate being formed by decomposition of cyanide.

High temperature evacuation of activated carbon was shown to result in a drop in adsorption capacity, but the molar Au:K adsorption ratio was 1:1. Gold adsorption could be restored by bubbling oxygen through the solution, thus suggesting that chemisorbed oxygen was involved in the adsorption mechanism. They proposed a structure containing chromene, carboxyl, and phenolic hydroxyl or quinone type carbonyl groups to explain their mechanism which consisted of initial ionic adsorption of $Au(CN)_2^-$ and K^+ at oxonium and carboxylate sites respectively (figure 2.2). The $Au(CN)_2^-$ ion is then chemically bonded by nucleophilic substitution, and oxidized by any quinone groups to give AuCN, carbonate and ammonia, leaving the oxonium ion to allow further adsorption.

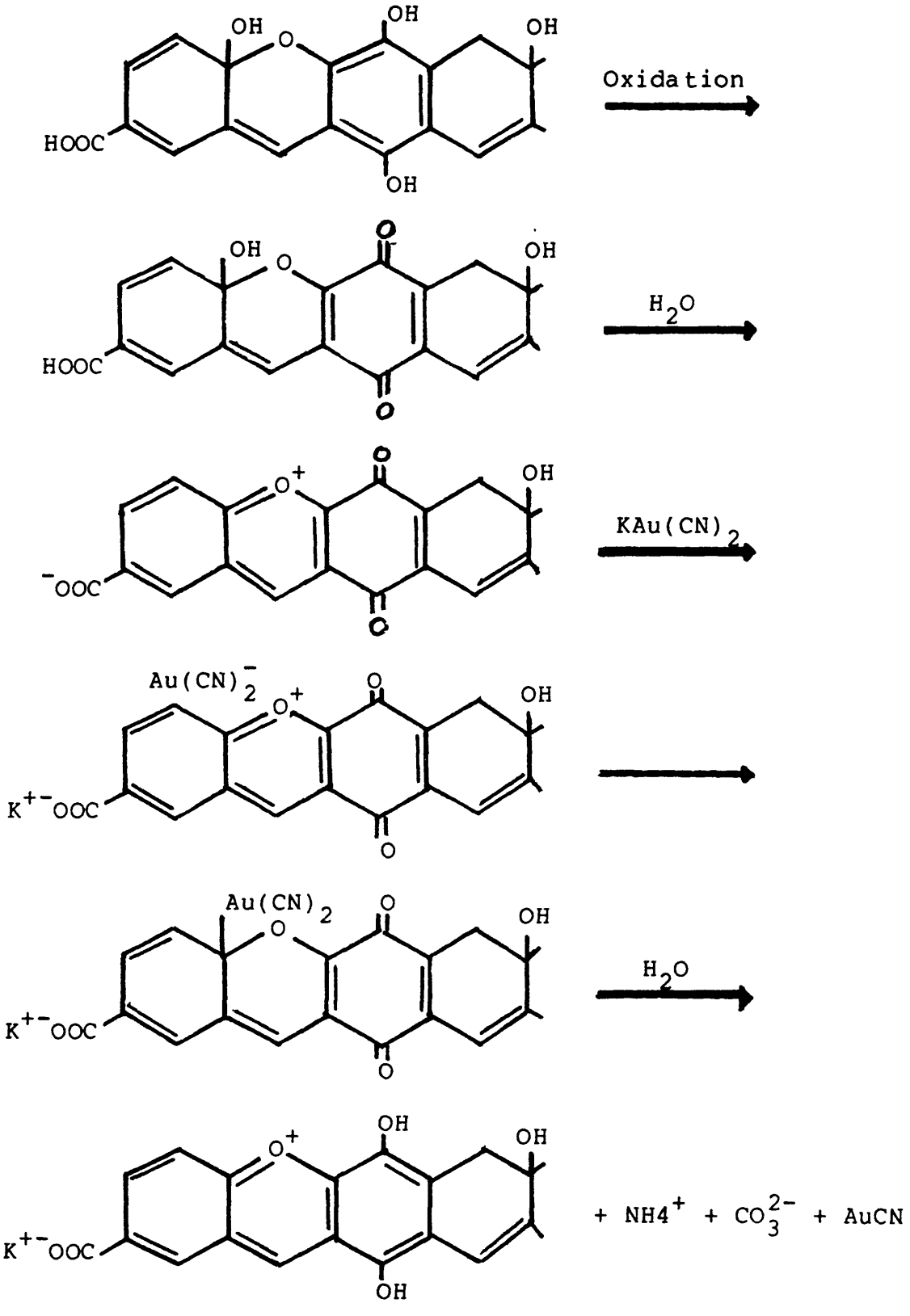

Figure 2.2 Mechanism of gold adsorption proposed by Tsuchida et al. [83]

2.6.1 Conclusions

It can be seen that many researchers have studied the phenomenon of gold adsorption by activated carbons and charcoals. From these studies several important facts have been obtained.

(1) Heat-treatment of activated carbon or charcoal at temperatures in excess of 200°C in inert atmospheres results in a significant reduction in gold adsorption. This can be restored to the original level if oxygen is bubbled through solutions during adsorption.

(2) The adsorbed species can be partially recovered by KCN. Alkaline KCN or sulphide solutions, organic solvents, and carbonate pretreatments can improve this recovery.

(3) Under normal conditions the amount of cation adsorbed is much less than that of gold. Deoxygenation of activated carbon and solutions results in equimolar gold and cation adsorption.

(4) Addition of cations to the adsorption medium tends to increase the capacity and rate of gold loading, depending on the cation and its concentration.

(5) Addition of free cyanide reduces gold adsorption up to a certain concentration, then the effect is reduced.

(6) The reaction is exothermic.

Although many theories as to the adsorption mechanism have been put forward, they can be classified into 4 main groups.

(1) Reduction to metallic gold. The observations by Green [74], and McKee and Horton [78] of metallic gold on loaded charcoals have never been corroborated by modern studies. McDougall et al. [53] could not discount AuCN as being responsible for their XPS results. Thus there is very little evidence to support this theory.

(2) Adsorption of insoluble AuCN. Support for this theory comes from the inability to recover the adsorbed gold by washing; little or no adsorption of cations from solution; presence of decomposition products of cyanide in solution; increased adsorption in acid solution; reduced adsorption with free cyanide present. This theory cannot explain the recovery of gold obtained by elution with water after a carbonate pretreatment.

(3) Adsorption of $M^{n+}(Au(CN)_2^-)_n$. Initially proposed to explain why cations did not adsorb equimolar with gold, it is assumed that sufficient impurities are contained within the activated carbon to account for the difference. The increase in adsorption seen on

addition of excess cations to solution was also thought to be due to formation of the more insoluble aurocyanide compounds. A problem with this theory is that acid washed activated carbons that contain very low levels of cations as impurities also fail to adsorb equimolar gold and cations.

(4) Ion exchange of K^+ and/or $Au(CN)_2^-$. To account for the effect of surface oxide groups it is assumed that the gold and cation species adsorb at separate sites, or that $Au(CN)_2^-$ adsorbs at cationic sites and the cation is left in solution. The deleterious effect of free cyanide is assumed to be due to competition between the two anions. Increased adsorption in acid solution could be due to the formation of more cationic sites, but the hydroxide released on formation of this site cannot be detected with certainty due to the natural buffering capacity of the activated carbons used.

3 Structural Effects on Gold Adsorption

3.1 Introduction

Considering that activated carbons have been known to adsorb gold from cyanide solution since the end of the last century [47], it seems remarkable that little evidence has been obtained for their structural and surface chemical influence on adsorption.

Studies of the structural effects on adsorption of organic and inorganic molecules has shown that many adsorbates will not be adsorbed if the pores in the adsorbent are too small [8]. This is not a general rule however, and it is thought that pore shapes and the presence of specific 'active sites' for different molecules may also play a part.

The aim of this chapter is to try and gain some understanding of the relationships between the structures of adsorbent carbons and their capacity to adsorb gold. A similar study by Davidson et al. [24] used 25 different activated carbons in an attempt to correlate their adsorptive capacity for gold with such properties as ash content, iodine number, methylene blue value, surface area and slurry pH. A correlation between adsorptive capacity and slurry pH was observed and was thought to be due to the presence of oxide groups on the surface of the activated carbons. The major problem of a study such as

this is the variance in pore structures between activated carbons produced from different starting materials, and by manufacturers using different activation methods and conditions. In this study the effects of such differences have been minimized by using commercial carbon blacks whose structures are more regular than activated carbons, and which can be simply modified by heat-treatments.

3.2 Experimental Procedures

3.2.1 Materials

Potassium dicyanoaurate (I) used in this investigation was obtained from Johnson Matthey Chemicals Ltd. All other chemicals were of AR grade.

Four commercial activated carbons and four carbon blacks were obtained. Norit R2020 and Sutcliffe Speakman 607 activated carbons and Black Pearls 71 and 1300 carbon blacks were provided by the BP Research Centre, Sunbury; Norit R2520 activated carbon by Norit, Netherlands; Pica G210 AS activated carbon by Pica, France; Black Pearls 1100 and Vulcan XC-72 carbon blacks by Cabot Carbon Ltd., Ellesmere Port.

Norit R2020 and R2520 are extruded, peat based activated carbons; Pica G210 AS and SS 607 are granulated, coconut shell based activated carbons; BP71 is a pelleted channel black; BP1100, BP1300 and

Vulcan XC-72 are pelleted furnace blacks.

Prior to adsorption tests the activated carbons were ground to a -420 +75 μm size range. The carbon blacks were not ground due to their very low mechanical strength and particle sizes of from 13 to 30 nm.

BP1300 carbon black was noted to have a relatively high volatile content compared to the other carbon blacks, and an acidic slurry pH [84]. This was later found to be due to a special after-treatment given by Cabot. The nature of this treatment was not disclosed, but it is likely to include acid washing.

3.2.2 Solutions

Gold solutions were prepared in 1 or 2 litre batches by dissolving a known amount of $KAu(CN)_2$ in distilled water. For carbonate buffered solutions accurate amounts of Na_2CO_3 and $NaHCO_3$ were dissolved with the $KAu(CN)_2$, giving a solution pH of 10 (0.025 M Na_2CO_3, 0.025 M $NaHCO_3$).

3.2.3 Solution Analysis

Solutions were analysed for gold, sodium, calcium and magnesium using a Perkin-Elmer Atomic Absorption Spectrophotometer in absorption mode. Potassium contents were determined in emission mode.

Problems were originally found with the stability of gold chloride standard solutions of low concentrations (1 and 2 ppm Au) when kept in polythene bottles. Storage of the solutions in amber glass bottles eliminated the effect, giving reproducible absorption values for several months. The potassium, sodium, calcium and magnesium solutions did not deteriorate appreciably with time, and were all kept in polythene bottles.

3.2.4 Carbon Black Heat-Treatments

The carbon blacks were heat-treated under nitrogen at 500, 1000, 1500, 2000, and 2400°C. The 500 and 1000°C heat-treatments were carried out under a nitrogen atmosphere using a horizontal tube furnace. Samples of up to 100 ml were placed in an alumina boat and positioned in the previously mapped out hot zone of the furnace so that the maximum temperature variation from the centre to the end of the boat was 20°C. The furnace tube was purged with oxygen free nitrogen throughout the duration of the treatment. The nitrogen was also passed through an oxygen trap to reduce oxygen levels to below 1 ppm. After reaching the required temperature the furnace was switched off and allowed to cool to room temperature overnight. The nitrogen flow was continued until the carbon black was removed from the furnace at room temperature.

Heat-treatments at 1500, 2000, and 2400°C were done

at the BP Research Centre using an Astro Industries vertical graphite element resistance furnace. Samples of up to 150 ml, contained in a graphite container, were purged with nitrogen during the course of the heat-treatment. The temperature of the sample container was measured through a sight tube using an optical pyrometer. After attaining the required temperature the furnace was switched off and allowed to cool to room temperature in around 2 hours.

3.2.5 Pore Size Distributions and Surface Areas

BET surface areas and pore size distributions of activated carbons and carbon blacks were determined at the BP Research Centre from nitrogen adsorption isotherms at 78 K.

Pore size distributions were calculated from the adsorption isotherms according to the method of Cranston and Inkley [85]. This method assumes capillary condensation as the nitrogen adsorption mechanism. This can only be strictly applied to pores of > 2.5 nm in diameter, as in smaller pores the concept of the formation of a meniscus cannot be validated when the pores are only a few nitrogen molecules wide. For micropore size distributions the V-t plot method was used which does not assume capillary condensation. but considers the thickness of the adsorbed layers [86].

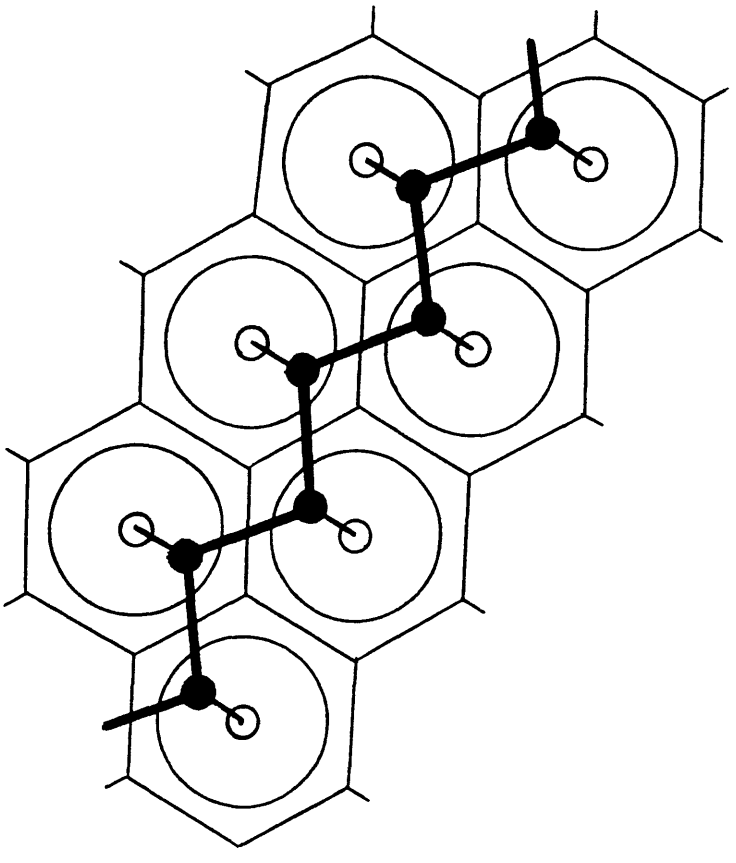

Figure 3.1 Model of adsorption of long chain hydrocarbons onto basal graphite planes [87].

Basal plane surface areas were calculated from the heat of adsorption of n-dotriacontane from heptane in a flow microcalorimeter. Edge (polar) areas were calculated from the heat of adsorption of n-butanol. The adsorption of these two compounds from heptane has been shown to correspond to two different mechanisms [87]. For n-dotriacontane ($n\text{-}C_{32}$), adsorption from n-heptane is thought to be due to the fit of hydrogen atoms attached

to one side of the zig-zag hydrocarbon chain, with the centres of the hexagons formed from the carbon atoms in the basal planes of the adsorbate (figure 3.1). The adsorption of n-butanol from n-heptane is due to the attraction of the polar groups on the surface of the adsorbent.

3.2.6 Slurry pH

The buffering pH of activated carbon and carbon black slurries were determined by adding 0.5 g samples to 50 ml of distilled water in 125 ml stoppered flasks and agitating for 24 hours at 25°C before filtration through Whatman 1 filter paper. The results of 3 determinations were used to obtain a mean value.

3.2.7 Acid Washing

The carbon blacks and activated carbons were acid washed with 1 M hydrochloric acid. Samples of 10 g were added to 250 ml stoppered flasks with 200 ml of acid. The flasks were left at room temperature for 2 - 3 days, with occasional shaking. The slurries were decanted and the washings analysed for sodium, potassium, calcium, and magnesium by atomic absorption/emission spectroscopy. Successive washes were carried out until the cation impurity contents of the washings could not be accurately determined by atomic absorption. This required from 7 to 9 washes.

For removal of excess acid held in the pores of the carbons the method of soaking the carbon in batches of distilled water [57] was found to be inefficient, requiring many washes before a significant drop in the resulting solution pH was observed. A better method found was the use of a soxhlet apparatus to give continuous hot condensed vapour washes, with the vapour formed from the washings. The soxhlet washings were decanted at weekly intervals, until the resultant solution pH was > 5. This usually required from 3 to 6 weeks.

3.2.8 Gold Adsorption Isotherms

A preliminary series of experiments using activated carbons and carbon blacks indicated that a pseudo-equilibrium was obtained after an 18 hour adsorption test. It was not possible to allow true equilibrium to be attained because this would have taken too much time. Results suggested equilibrium had not occurred during a 6 day test, but the drop in gold concentration between 18 hours and 6 days was 3 % compared to 20 % within the first 18 hours.

This method was adequate for the carbon blacks, but for the activated carbons there was a large degree of scatter in the results and it was decided to allow 1 week for each adsorption test.

All 18 hour equilibrations using carbon blacks were

carried out using 125 ml stoppered flasks, into which was weighed a given amount of carbon black, usually from 0.1 to 0.5 g. The flasks were put in an oven at 105°C for two hours to dry the carbons, before re-weighing. 100 ml of potassium aurocyanide solution of from 10 to 100 ppm gold concentration was added to the flask, and the slurry maintained at 25°C in a Grant thermostatically controlled oscillating water bath. At the end of the test the slurry was filtered through Whatman 1 filter paper using a Buchner funnel, and the filtrate collected for analysis. The loaded carbon black was rinsed with distilled water and dried at 105°C for two hours.

For the week long adsorption tests using activated carbons 550 ml stoppered flasks were used, into which was added 500 ml of potassium aurocyanide solution. Due to the larger adsorptive capacity of the activated carbons, solution concentrations of from 10 to 200 ppm gold were used. A weighed amount of dried, ground activated carbon, together with a magnetic stirrer bar was added to the solution in the flask. The flasks were maintained at 25°C in a thermostatically controlled water bath and agitated by means of a Camlab submersible magnetic stirrer plate. Slurries were filtered as for the 18 hour tests.

The solution pH was maintained at 10 using a carbonate buffer. For unbuffered adsorption tests acid washed carbons were used which did not require buffering, this was because their buffering ability had been removed

by the washing process. The equilibrium pH of such solutions was usually between 5 and 7.

3.3 Results and Discussion

3.3.1 Structural Effects of Heat-Treatments

The BET, edge, and basal plane surface areas, mean pore diameters, pore volumes, and slurry pH of all as-received and heat-treated activated carbons and carbon blacks are presented in table 3.1.

For the two Norit activated carbons there is some difference between their respective properties. Comparing the technical bulletins produced by Norit for both R2020 and R2520 activated carbons [88], their physical and adsorptive properties are given as identical, suggesting that the only difference is in name and date of production. Norit R2020 is the older sample. This highlights the problems associated with any research programme trying to correlate results obtained from different activated carbons, or comparing results obtained by different researchers even if they are using the same variety of activated carbon. If the properties of activated carbons manufactured by the same process vary between different batches, then the possibility of comparing activated carbons manufactured from different starting materials, using different activation conditions and pre- and post activation treatments cannot be

expected to produce significant results. Thus only 4 activated carbons were chosen for this investigation to get an idea into their adsorption characteristics. For a more detailed study into the structural effects on gold adsorption a carbon with a low impurity content and a regular structure is required.

Natural or synthetic graphite would be ideal structurally, but does not adsorb gold [74]. Carbon blacks can be produced with very low impurity contents, have relatively simple structures that can be readily modified by heat-treatment [34], and initial experiments indicated that they can adsorb significant quantities of gold.

Carbon/ Heat Treatment (°C)	Areas ($m^2.g^{-1}$)			Pore Volume ($ml.g^{-1}$)	Mean Pore Diameter (nm)	pH
	BET	Edge	Basal			
Norit R2020 †	783	17.6	80	0.397	1.45	10.10
Norit R2520 †	822	23	85	0.560	1.36	10.22
Pica G210 AS †	1144	28	123	0.373	1.37	9.69
SS 607 †	975	—	—	0.566	1.42	6.15
BP71	413	29	41	0.741	7.17	5.42
BP1100	290	14.2	51	0.516	4.11	4.56
BP1100/500	301	6.72	37.37	0.454	5.91	6.73
BP1100/1000	297	11.02	42.93	0.452	5.96	8.21
BP1100/1500	253	6.6	112	0.403	6.33	7.87
BP1100/2000	203	0.91	155	0.347	5.55	7.01
BP1100/2400	180	0.70	147	0.294	6.14	6.77
BP1300	655	101	90	0.833	6.29	3.25
BP1300/500	646	56.31	77.76	0.889	5.58	6.40
BP1300/1000	671	19.39	103.5	0.944	5.44	9.77
BP1300/1500	360	0.81	189	0.787	5.94	9.47
BP1300/2000	314	0.76	267	0.701	6.22	8.93
BP1300/2400	273.5	2.6	267.5	0.370	9.20	7.05
Vulcan XC-72	251	7.5	84	0.251	4.97	6.48
Vulcan/500	243	3.59	57.87	0.253	4.33	6.68
Vulcan/1000	240	3.29	76.21	0.248	4.34	7.77
Vulcan/1500	161	0.19	72	0.205	6.42	7.83
Vulcan/2000	106	0.6	88	0.205	6.90	6.65
Vulcan/2400	91	1.1	126	0.186	7.04	6.68

Table 3.1 Properties of activated carbons and carbon blacks. (†- Activated carbons.)

On heat-treating carbon blacks under inert atmospheres several different stages have been noted by previous workers.

(1) Surface oxide groups are removed between 200 and 1200°C as carbon monoxide and carbon dioxide [31].

(2) Between 600 and 1500°C hydrogen is evolved [31].

(3) Above 1000°C the layer planes re-orientate with respect to one another to form graphitic crystallites with their basal planes parallel to the particle surface, there is also growth of basal planes [34,89].

(4) From 1800°C growth of the basal planes stops, but the crystallites continue to grow by addition of further basal planes from the centre of the particle [34].

(5) Throughout heat-treatment there is no significant increase in size of the carbon black particles [89].

(6) The pH of carbon slurries is usually dependent on the presence of inorganic impurities either in the starting material or added during manufacture [8].

These previous observations can be used to explain the variations in structural properties given in table 3.1.

From figure 3.2 it is seen that up to 1000°C there is little change in the BET surface area; above this temperature a drop occurs which is constant from 1500 to 2400°C. This is due to re-orientation and growth of the layer planes resulting in a drop in the porosity of the particles. It can be seen from the decrease in pore volume and increase in mean pore diameter (figures 3.3, 3.4), that although re-orientation results in a reduction in the number of pores of all size ranges, a more significant drop has occurred in the micropore range. The smaller pores have the greater influence on surface areas, and in this temperature range the reduction in the number of these pores causes a greater drop in area than the increase caused by re-orientation and growth of the layer planes. Thus the BET surface area is reduced.

The edge area is a measure of the number of polar groups bound on the edges of the layer planes. From figure 3.5 it is seen that this area drops at all temperatures considered up to 1500°C, indicating the removal of the surface oxides.

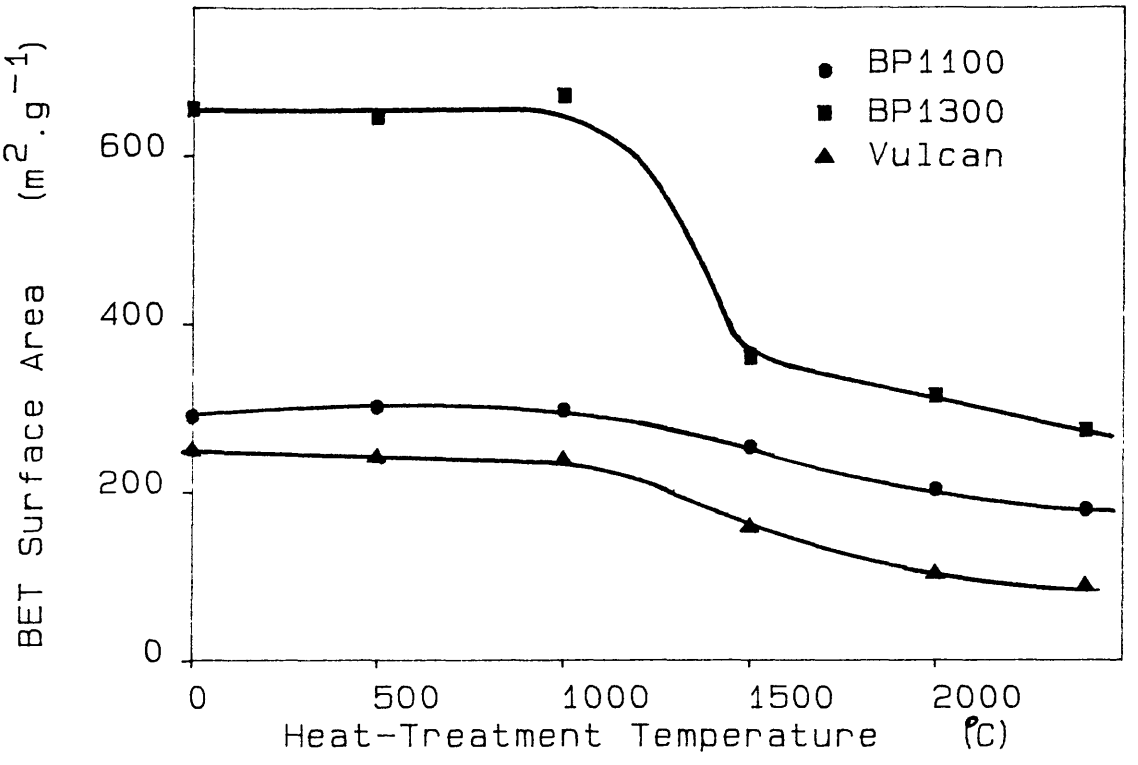

Figure 3.2 Effect of heat-treatment on BET surface areas of carbon blacks.

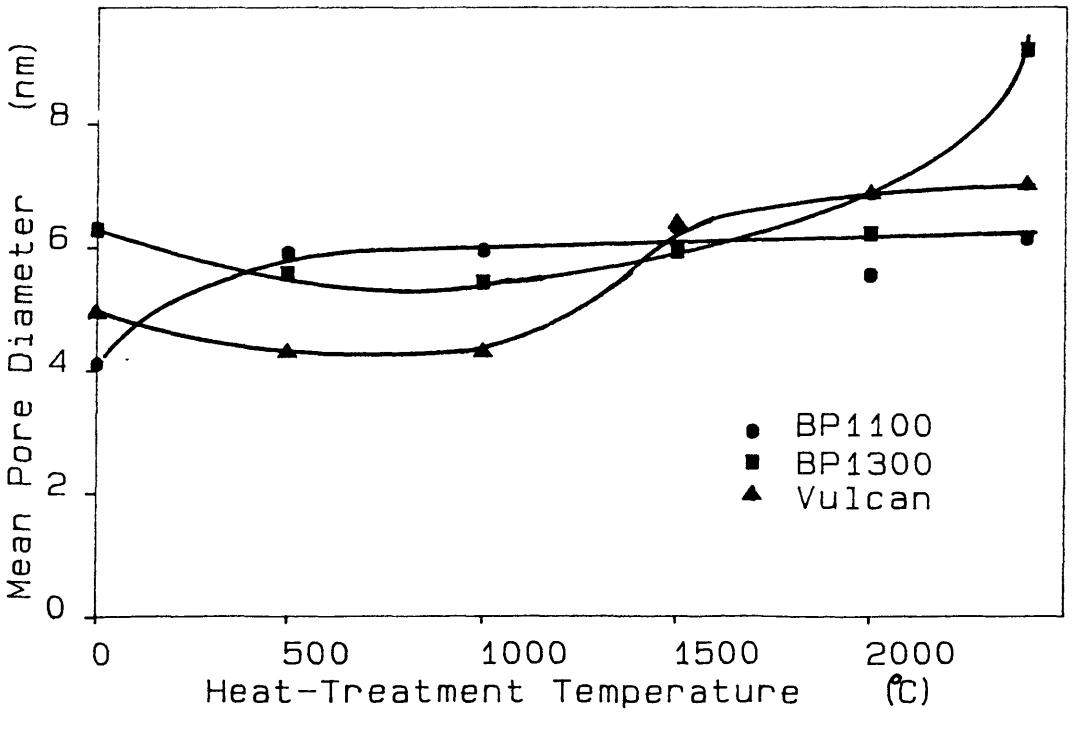

Figure 3.3 Effect of heat-treatment on mean pore diameters of carbon blacks.

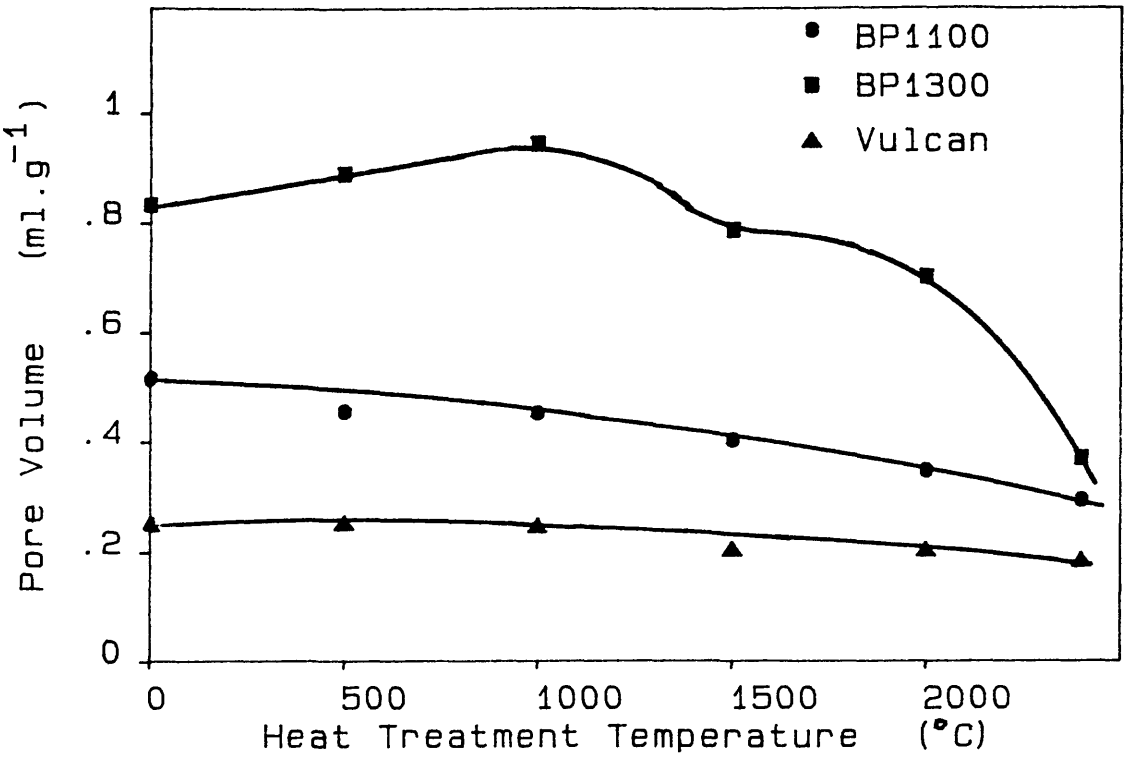

Figure 3.4 Effect of heat-treatment on pore volumes of carbon blacks.

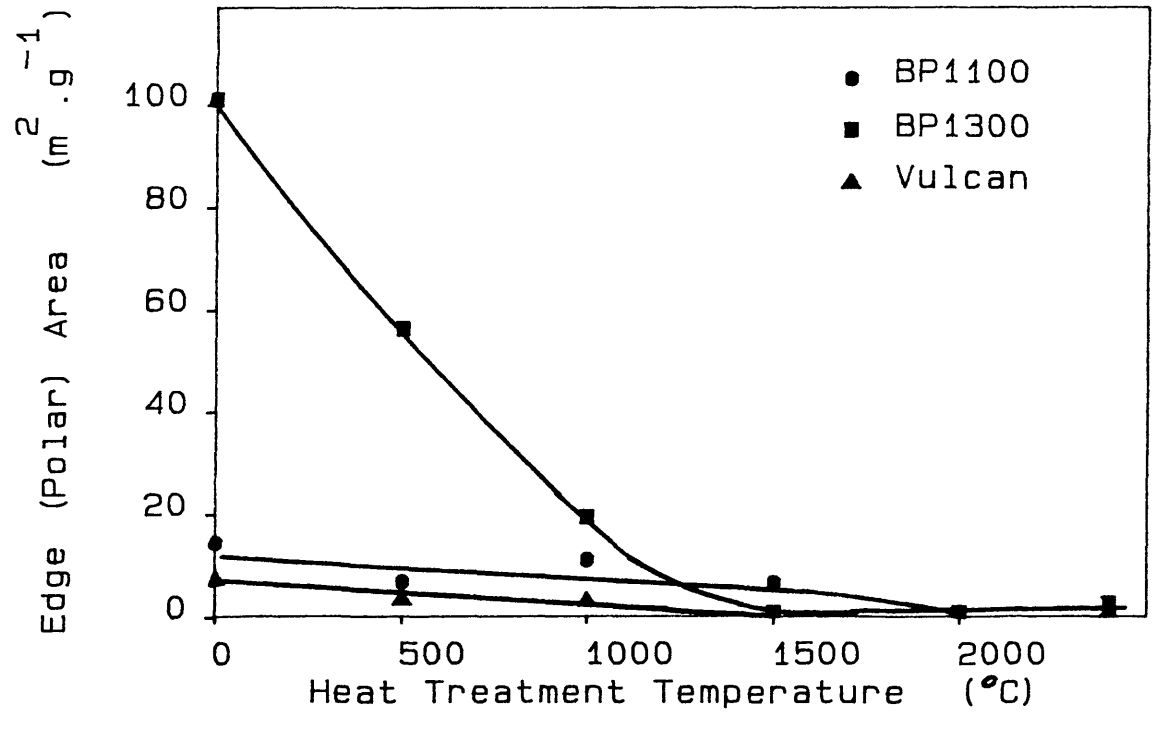

Figure 3.5 Effect of heat-treatment on edge (polar) areas of carbon blacks.

The change of the basal plane area (figure 3.6) is opposite to that of the BET. From 1000 to 2000°C there is an increase in basal plane area, but for two of the three carbon blacks there is no further increase at 2400°C. This is consistent with re-orientation and growth of basal planes from 1000 to 1800°C. The drop in area of BP1100 from 2000 to 2400°C is small and may be experimental error, but it may also be due to growth of the crystallites by addition of basal planes, thus resulting in a drop in basal area.

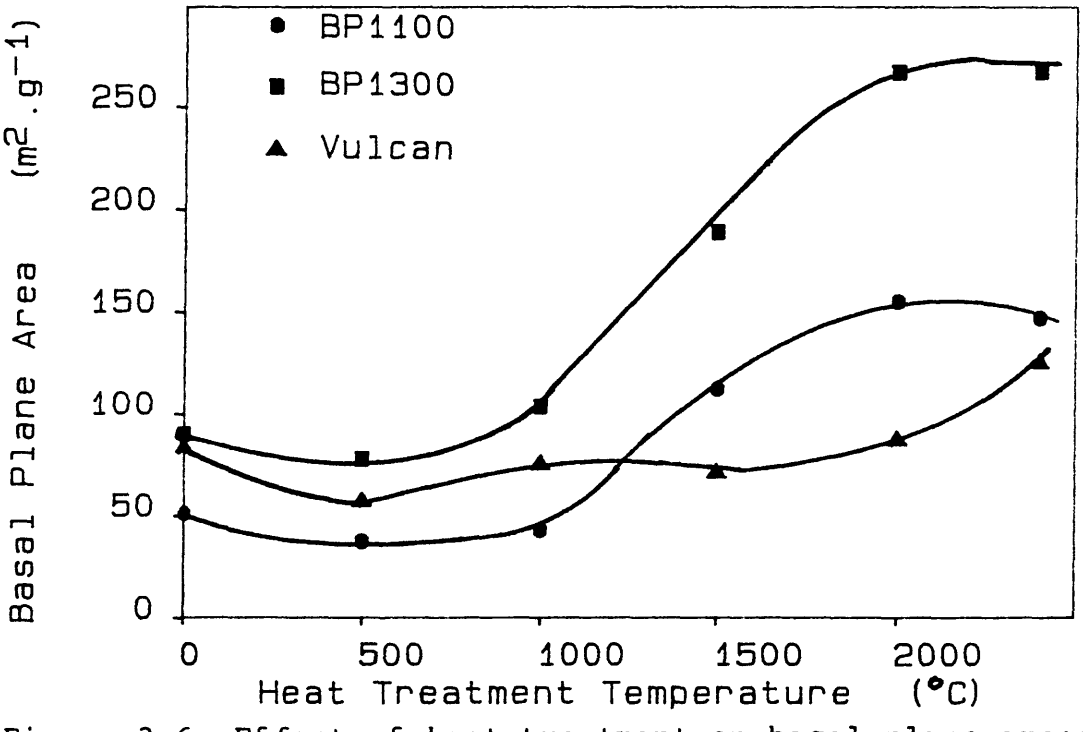

Figure 3.6 Effect of heat-treatment on basal plane areas of carbon blacks.

The low pH of as-received BP1300 slurries shown in figure 3.7 is probably due to an acid washing treatment by the manufacturer. For all carbon blacks, heat-treatment led to an increase in slurry pH, probably giving a maximum between 1000 and 1500°C, and returning

to neutral by 2400°C (figure 3.7). The variation in pH between 1000 and 2400°C would not be expected if surface oxide groups were thought to be the cause as it has been shown that the edge area, and thus the number of surface oxide groups, has become very small by 1500°C and does not vary appreciably between 1500 and 2400°C. The possibility of reoxidation of the carbon blacks by atmospheric oxygen after heat-treatment can also be discounted as this would lead to adsorption of hydroxide from solution producing acidic slurries [133].

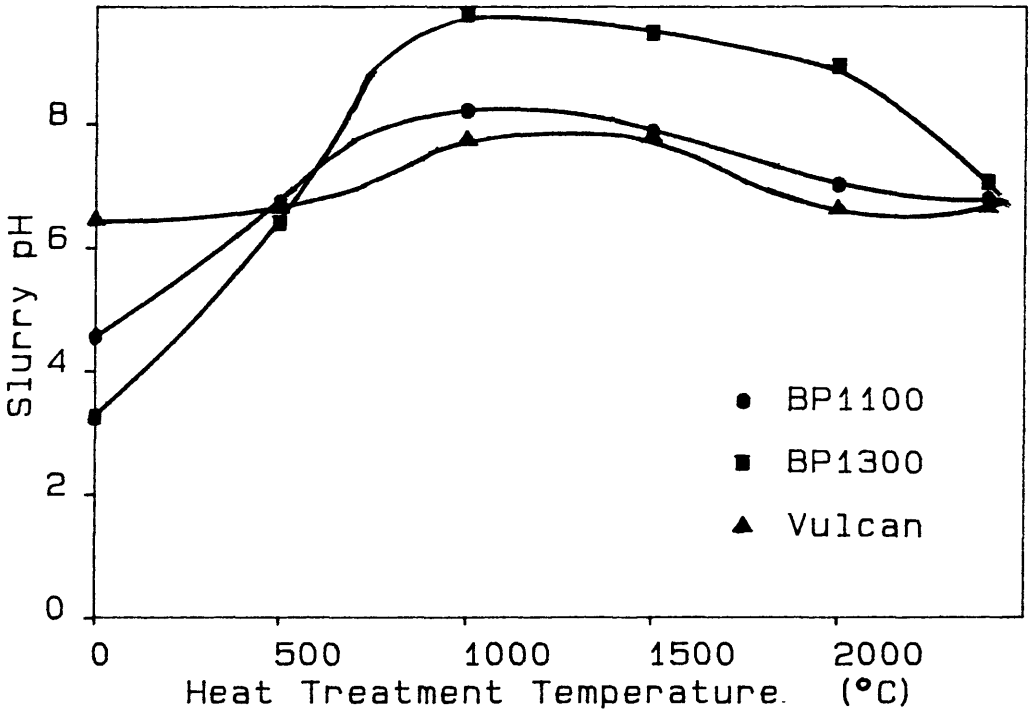

Figure 3.7 Effect of heat-treatment on the pH of carbon black slurries.

From the pore size distributions of the as-received carbon blacks (figure 3.8) it is possible to see how their structures compare, and how they are affected by the heat-treatments (figures 3.9 to 3.11). BP71 and Vulcan XC-72 contain a large fraction of their pores in a

relatively narrow range, whereas BP1100 and BP1300 have pores in a much wider size range. The effect of heat-treatment is seen to be a reduction in the number of pores from 1500°C, thus resulting in a drop in pore volume. The increase in mean pore diameter is due to a larger percentage drop in the number of the smaller pores. It must be noted that in the determination of the pore size distributions it is not possible to differentiate between pores between particles and those within the particles. The mean particle sizes given by the manufacturer (table 3.2) are greater than the mean pore diameters calculated from the pore size distributions (table 3.1). But from the pore size distributions it is noted that some pores are larger than the particles. This is caused by agglomeration of the particles, so that the larger pores are voids between particles and are not contained within the particles.

Carbon Black	Mean Particle Diameter (nm)
BP71	16
BP1100	14
BP1300	13
Vulcan XC-72	30

Table 3.2 Size of carbon black particles determined by electron microscopy [91].

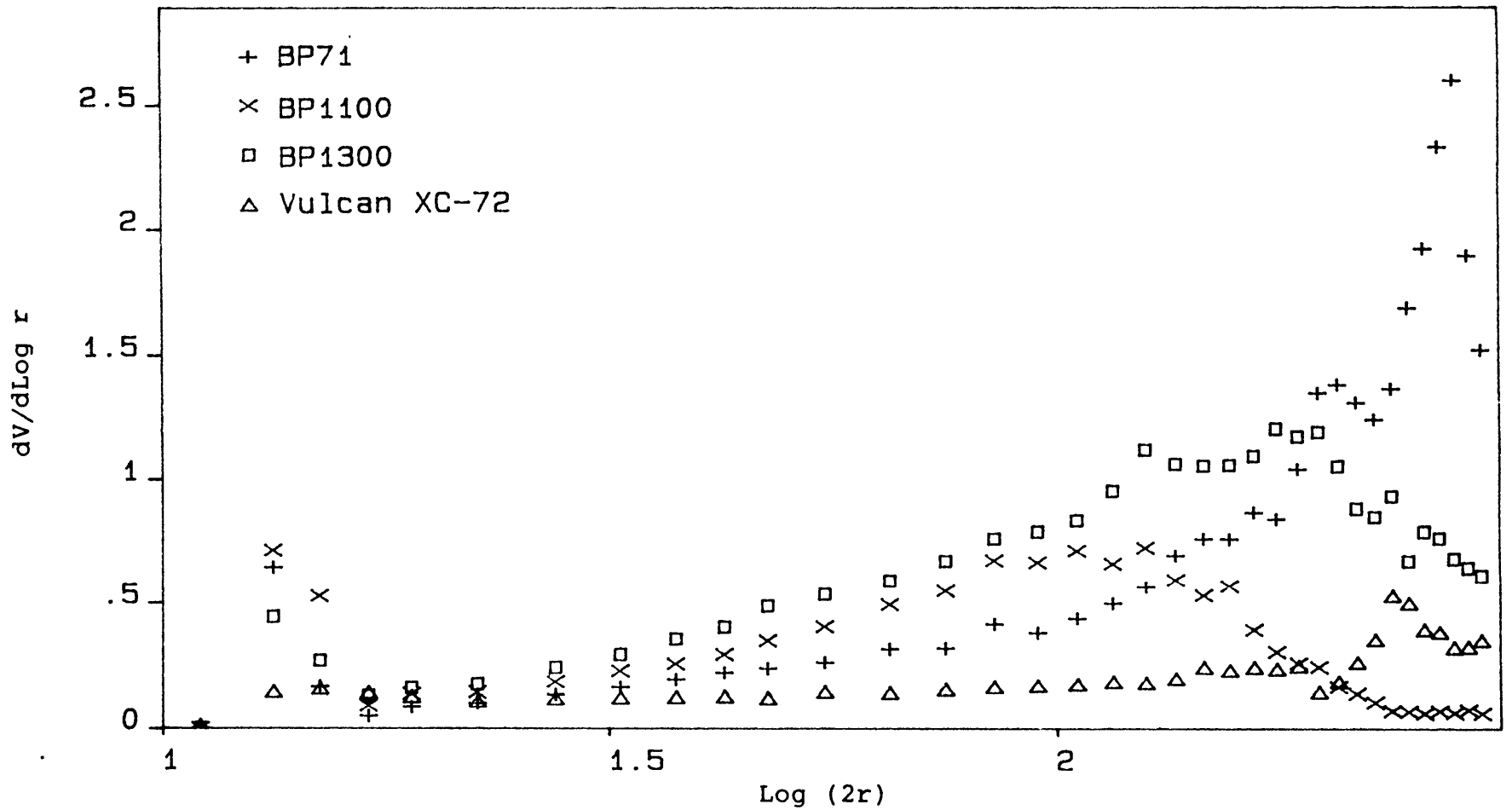

Figure 3.8 Pore size distributions of carbon blacks. (V- Pore volume $cm^3.g^{-1}$, r- pore radius Å)

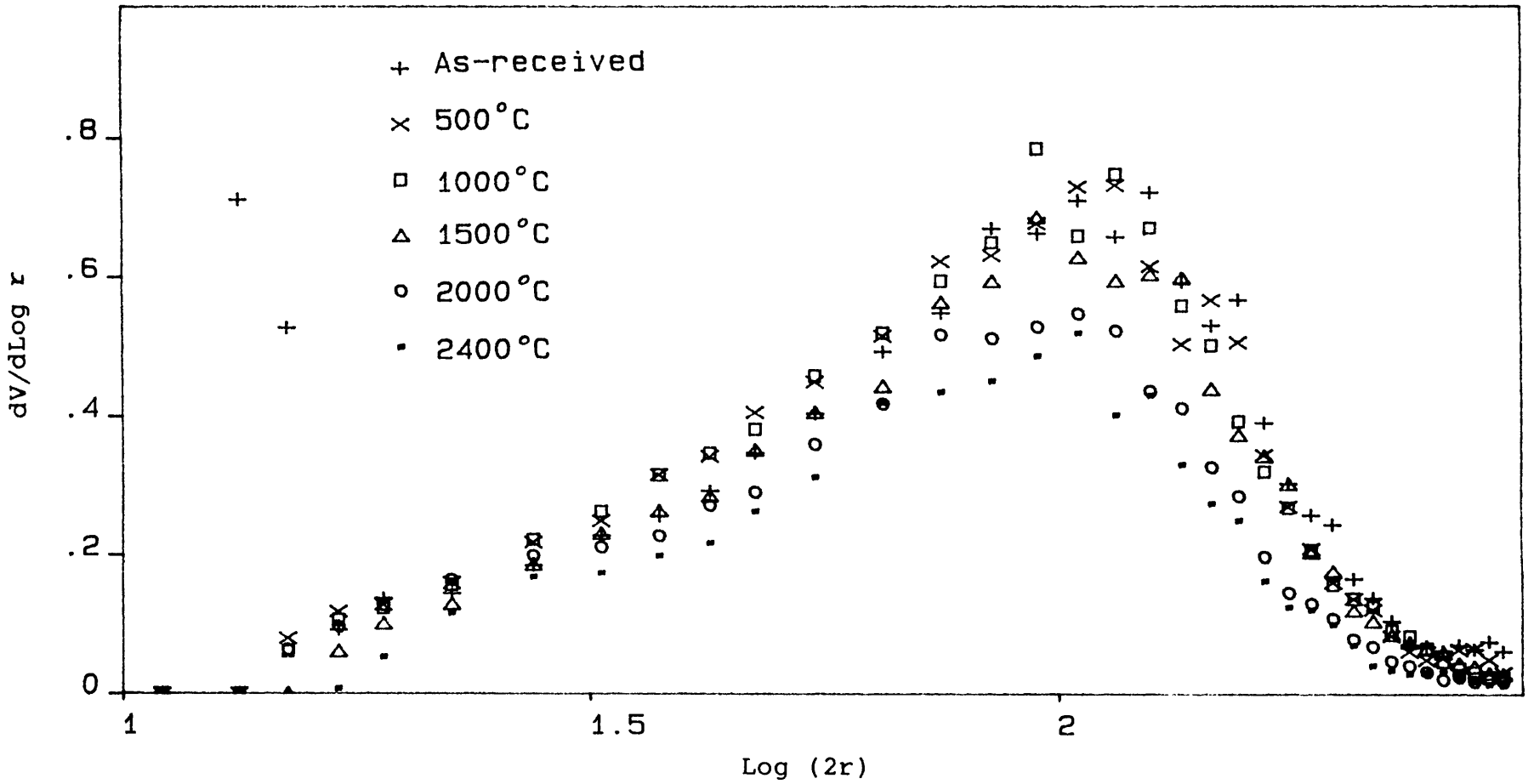

Figure 3.9 Pore size distributions of BP1100, heat-treated. (V- Pore volume $cm^3.g^{-1}$, r- pore radius Å)

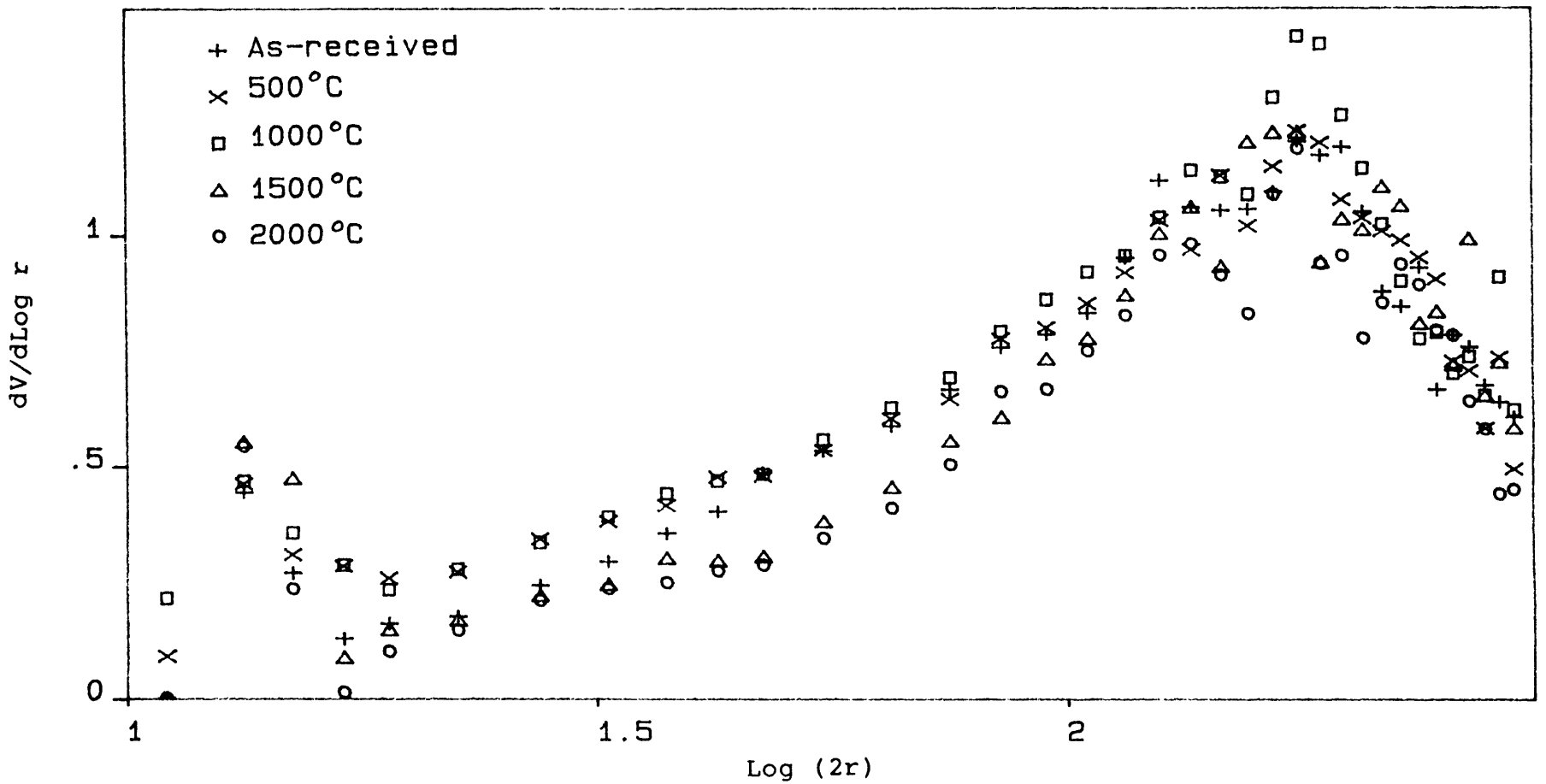

Figure 3.10 Pore size distributions of BP1300, heat-treated. (V- Pore volume $cm^3.g^{-1}$, r- pore radius Å)

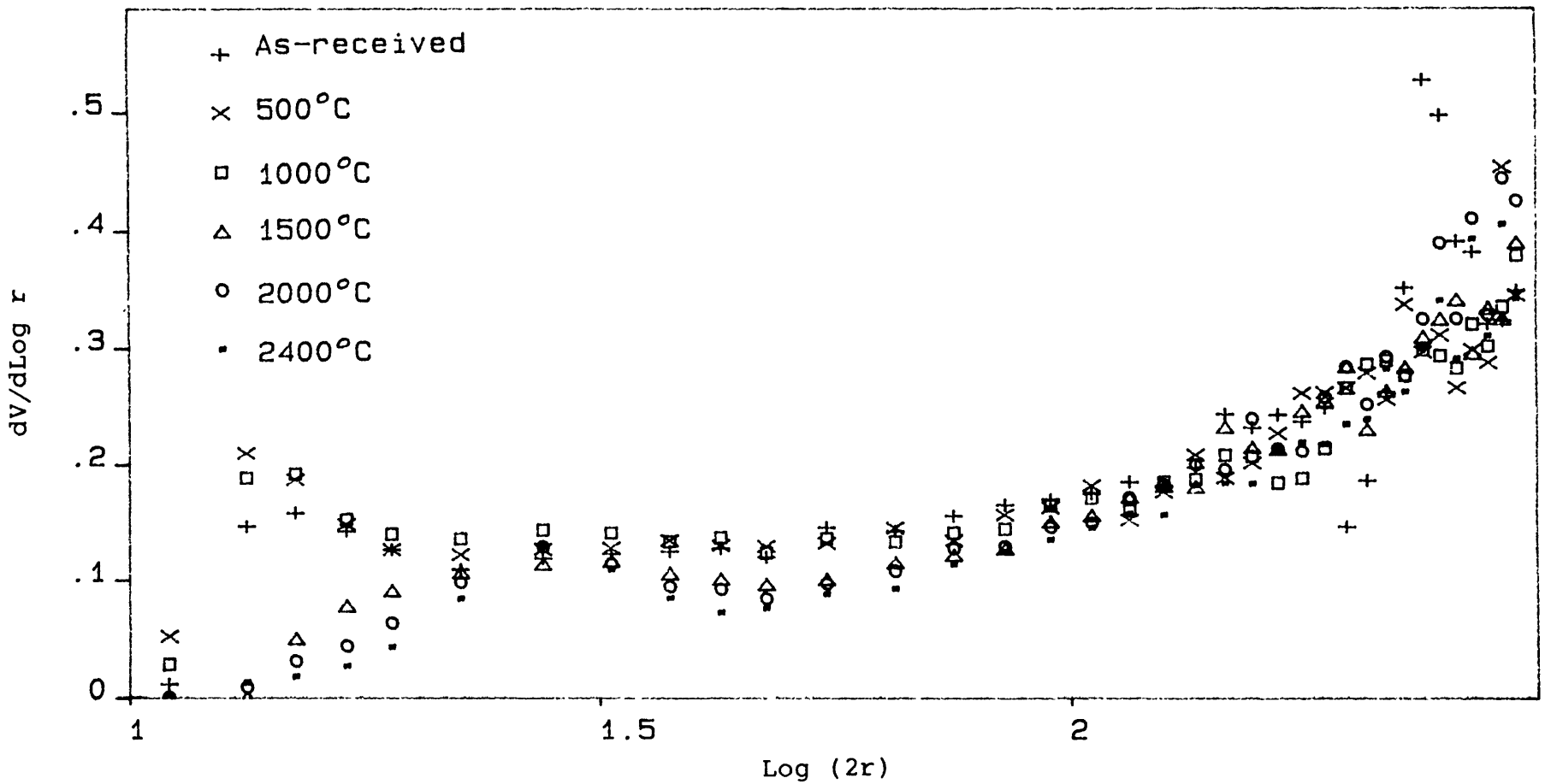

Figure 3.11 Pore size distributions of Vulcan XC-72, heat-treated. (V- Pore volume $cm^3.g^{-1}$, r- pore radius $\mathring{A}$)

For pores of less than 2.5 nm diameter the pore size distributions cannot be relied upon as they were calculated using the Cranston and Inkley method assuming capillary condensation. Such an assumption cannot be justified in small pores of only a few nitrogen molecules width. Thus for micropores the V-t plot method was used which considers the thickness of the adsorbed layers. Considering BP1100 (figure 3.12) it is seen that there is a significant increase in the number of micropores by 500°C. This is probably due to the removal of volatiles left over from the production process, and explains the increase in BET surface area at this temperature. Further heat-treatments results in the collapse of micropores leading to a reduction in BET surface area.

The pore structures of the activated carbons are very different to those of the carbon blacks (figure 3.13). Their very high surface areas are due to an extensive system of micropores of less than 1 nm diameter, with relatively few larger pores as indicated by mean pore diameters of from 1.3 to 1.5 nm (table 3.1).

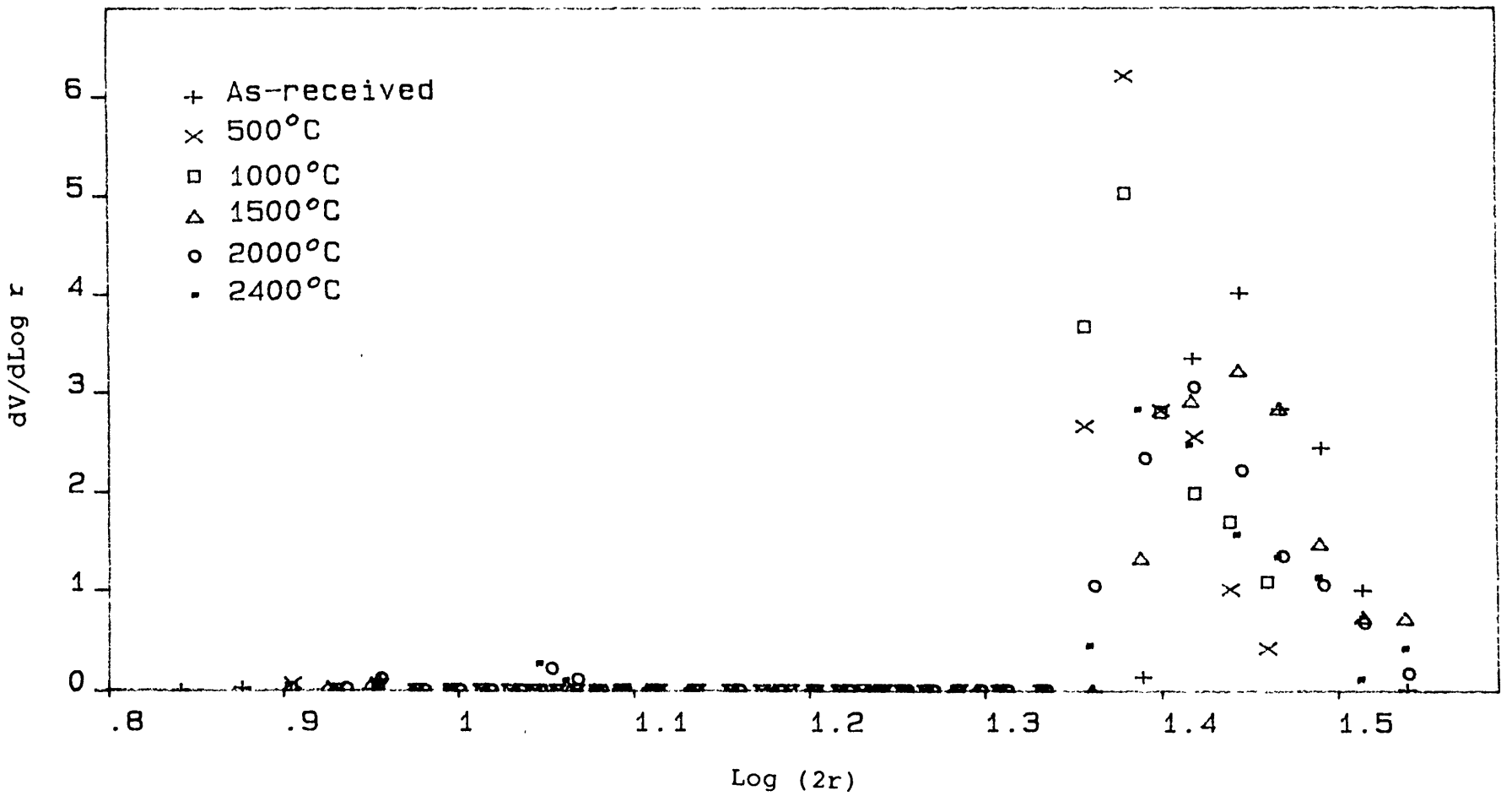

Figure 3.12 Micropore size distributions of BP1100, heat-treated. (V- Pore volume $cm^3.g^{-1}$, r- pore radius Å)

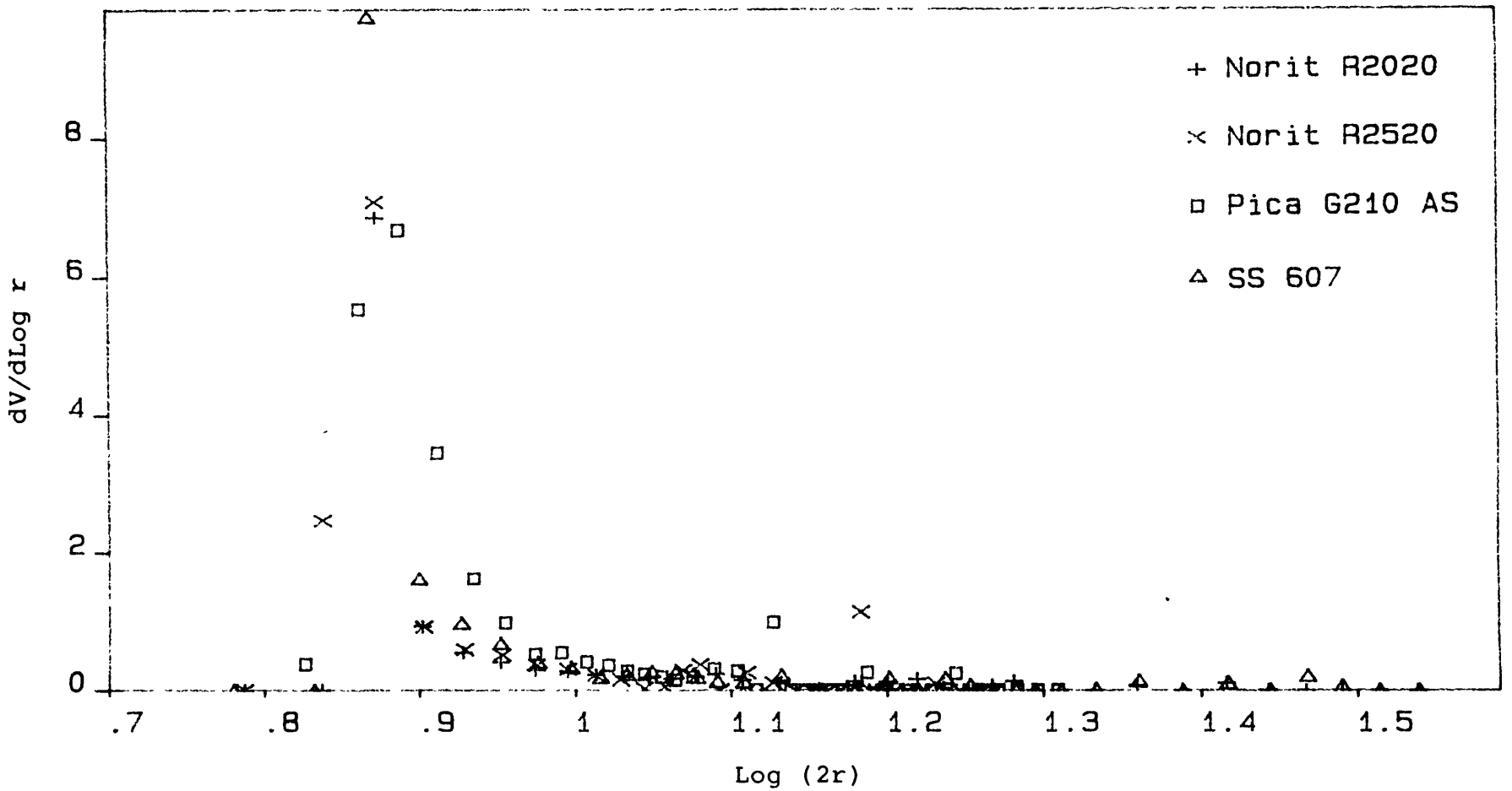

Figure 3.13 Micropore size distributions of activated carbons. (V- Pore volume $cm^3.g^{-1}$, r- pore radius Å)

3.3.2 Adsorption Isotherms

Two different adsorption isotherms were used to try to model the gold adsorption data. These were the Freundlich and Langmuir isotherms.

3.3.2.1 Freundlich Adsorption Isotherm.

Originally developed to explain experimental adsorption results [92], this empirical isotherm has been used as a test of the effectiveness of particular activated carbons to adsorb gold [56,88,93]. The form of the equation usually employed (equation 3.1) relates the amount of gold loaded (X), to the equilibrium gold concentration in solution (C), using two constants (K and n).

$$X = K.C^{1/n} \qquad (3.1)$$

Although this equation has been successfully applied to the adsorption of gold, it predicts infinite adsorption at infinite concentration whereas in this investigation the maximum capacity was required. To categorize the effectiveness of different adsorbents the capacity constant (K) is usually used. This is not a measure of the maximum capacity of a carbon to adsorb gold, but the loading expected at unit equilibrium concentration. The major advantage of the isotherm is the relatively simple method of calculating K using the

log-log form (equation 3.2) and linear least squares analysis.

$$\log X = \log K + \frac{1}{n}.\log C \qquad (3.2)$$

3.3.2.2 Langmuir Adsorption Isotherm

Originally developed to explain the adsorption of gas molecules onto crystalline materials with homogenous surfaces and adsorption sites with the same adsorption potentials [94], this isotherm should be more useful than the Freundlich because it predicts a maximum loading value (Xm) for monolayer coverage (equation 3.3).

$$X = \frac{Xm.C}{K'+C} \qquad (3.3)$$

Calculation of the constants (Xm, K') is more complicated than for the Freundlich isotherm because rearrangement leads to the production of 6 different linear equations that can be analysed by least squares analysis (equations 3.4-3.9).

$$X = \frac{-K'.X}{C} + Xm \qquad (3.4)$$

$$\frac{X}{C} = \frac{-X}{K'} + \frac{Xm}{K'} \qquad (3.5)$$

$$\frac{1}{X} = \frac{K'}{Xm.C} + \frac{1}{Xm} \qquad (3.6)$$

$$\frac{C}{X} = \frac{C}{Xm} + \frac{K'}{Xm} \qquad (3.7)$$

$$C = \frac{Xm.C}{X} - K' \qquad (3.8)$$

$$\frac{1}{C} = \frac{Xm}{K'.X} - \frac{1}{K'} \qquad (3.9)$$

Each of these equations give different values for the constants Xm and K' [95,96]. A better method of calculation was thought to be by iteration. In this method a value of K' was chosen and the linear regression of X on $\frac{C}{K'+C}$ calculated, K' was varied until the least squares error was minimized.

Calculation method	BP71		R2020 †	
	Xm	K'	Xm	K'
Least squares, (equation 3.4)	19.8	10.1	86.8	2.8
(equation 3.5)	22.0	13.4	92.7	4.1
(equation 3.6)	17.7	7.9	86.7	2.9
(equation 3.7)	26.8	23.8	84.4	2.1
(equation 3.8)	25.1	20.2	83.8	1.9
(equation 3.9)	17.9	8.1	90.6	3.6
Iteration	29.0	30.2	88.2	3.0

Table 3.3 Comparison of Langmuir constants calculated by various methods. (†- Activated carbon.)

The effect of these different calculation methods on the values of the adsorption constants calculated can be seen in the examples given in table 3.3. For both carbons the differences between the Xm values calculated by the different methods are large. From consideration of the

fit of the isotherms derived from these different methods, it was decided that the iterative method gave results that more accurately fit experimental data, and this method was used throughout all further calculations.

Tables 3.4 and 3.5 give experimental adsorption results for 4 carbons used in this investigation. The remainder of the results can be found on microfiche at the end of this report. Typical examples of the isotherms obtained for samples of BP71 and Norit R2020 are given in figure 3.14. This demonstrates the difference in adsorptive capacities of the two types of carbon, with the activated carbon being much more effective at low gold concentrations, and quickly reaching its adsorptive capacity. Also to be noted is the much better fit of the Langmuir over the Freundlich isotherms. This point is considered later when analysing the adsorption results in more detail.

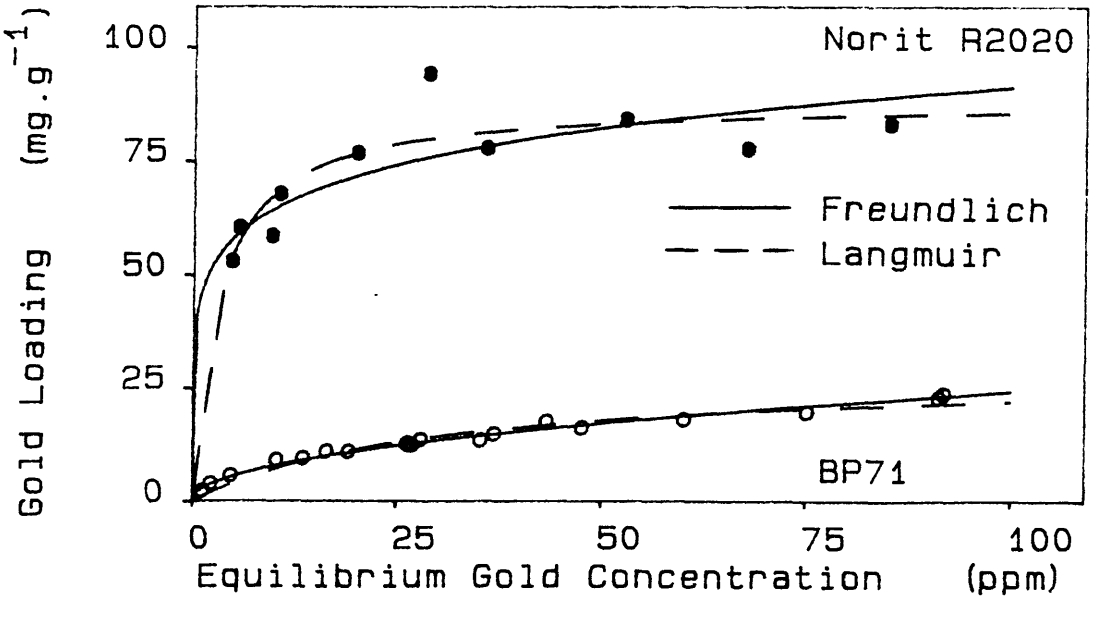

Figure 3.14 Adsorption isotherms of BP71 carbon black and Norit R2020 activated carbon.

Norit R2020		Pica G210 AS	
Equilibrium Gold Concentration (ppm)	Gold Loading ($mg.g^{-1}$)	Equilibrium Gold Concentration (ppm)	Gold Loading ($mg.g^{-1}$)
85.20	83.08	92.90	89.46
67.70	77.68	80.15	87.19
52.80	84.11	60.90	82.47
36.05	77.86	36.95	69.64
28.90	94.25	25.45	66.01
20.13	76.77	18.63	69.10
10.55	67.80	15.61	69.75
9.61	58.62	2.68	38.21
5.55	60.43		
4.64	53.01		

Table 3.4 Experimental adsorption data for Norit R2020 and Pica G210 AS activated carbons in carbonate buffered solutions.

BP71		BP1100	
Equilibrium Gold Concentration (ppm)	Gold Loading ($mg.g^{-1}$)	Equilibrium Gold Concentration (ppm)	Gold Loading ($mg.g^{-1}$)
91.90	23.80	98.00	14.17
91.30	22.98	85.65	14.68
75.10	19.71	72.75	14.34
60.00	18.14	71.80	14.91
47.64	16.33	64.30	14.78
43.30	17.72	55.04	13.40
37.00	14.94	48.76	14.43
35.38	13.56	44.82	12.33
28.00	13.67	38.45	13.26
27.00	12.49	36.46	10.32
26.51	12.61	33.99	11.00
26.32	12.82	30.30	12.43
19.14	11.12	29.85	10.95
16.43	11.11	29.23	10.97
13.55	9.61	25.07	10.37
10.24	9.19	21.91	9.55
4.58	5.72	21.78	10.11
2.17	3.90	16.32	8.72
1.17	2.32	15.96	9.66
		10.49	7.69
		4.99	5.44
		1.84	4.01
		0.76	2.43

Table 3.5 Experimental adsorption data for BP71 and BP1100 carbon blacks in carbonate buffered solutions.

3.3.3 Effect of Heat-Treatment on Gold Adsorption

The Langmuir and Freundlich loading constants for the activated carbons and heat-treated carbon blacks are presented in table 3.6.

For the heat-treated carbon blacks the variation of the Langmuir maximum loading constant (Xm) with heat-treatment temperature (figure 3.15) is similar to the change seen in the BET surface area (figure 3.2). The BET surface areas and Xm values increase up to 1000°C, and then drop to 2400°C. The large increase in Xm for BP1300 does not correlate with the BET results, though this is most probably due to the removal of volatiles contained by the carbon black as a result of the special after treatment during manufacture [84]. The variation in the Freundlich capacity constant (K) is similar to that for Xm (figure 3.16), except that the three carbon blacks show a greater increase in K by heat-treating up to 1000°C. The difference in results obtained by considering the loading constants calculated from the Freundlich and Langmuir isotherms shows the difficulty in interpreting adsorption using the Freundlich isotherm. The constant K is the loading expected at an equilibrium concentration of 1 ppm. All the experimental isotherms contained data points at up to 100 ppm, thus the K value is calculated from the early part of the isotherm where the change in slope of the curve, and thus the error, is greatest (figure 3.14). Thus the K value is more useful in

determining the effectiveness of different adsorbents in removing very low concentrations of species from solution, whereas for this series of experiments, where it is more important to know the capacity of the adsorbent, the Langmuir maximum loading constant will be more useful.

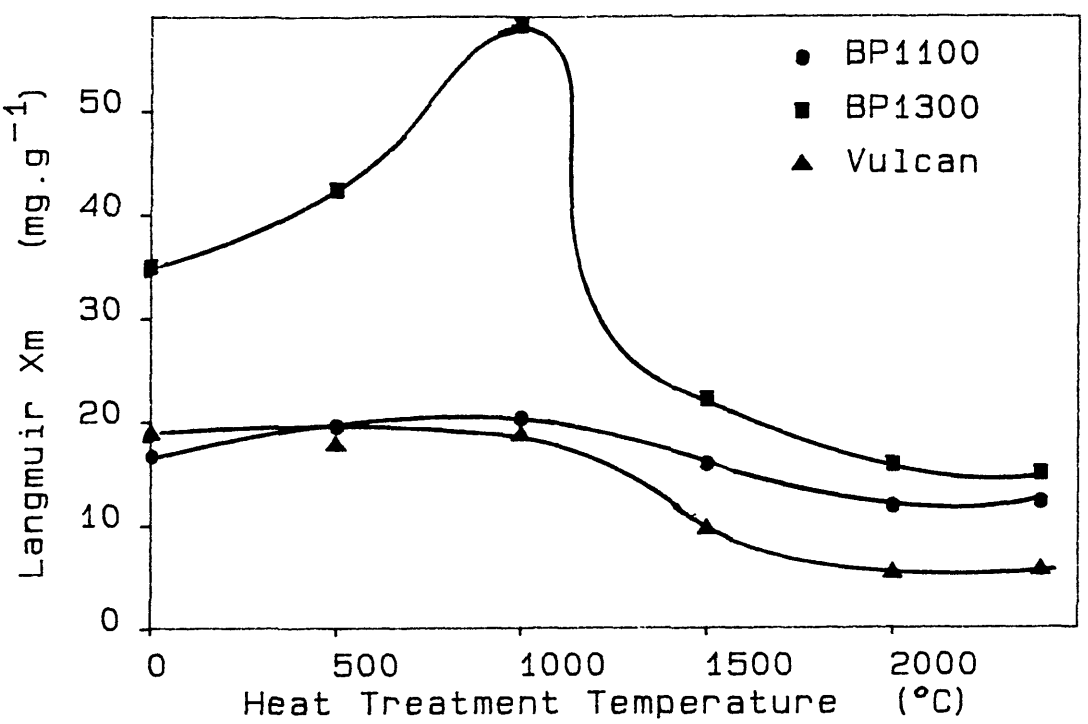

Figure 3.15 Effect of heat-treatment on Langmuir maximum loading constants of carbon blacks.

Carbon/ Heat Treatment (°C)	Langmuir		Freundlich	
	Xm ($mg.g^{-1}$)	K' (ppm)	K ($mg.g^{-1}$)	n
Norit R2020 †	88.21	2.99	45.80	6.67
Norit R2520 †	76.71	2.83	42.65	7.59
Pica G210 AS †	87.07	4.23	32.92	4.44
SS 607 †	67.80	5.88	22.65	4.06
BP71	28.95	30.23	2.56	2.04
BP1100	16.65	12.81	3.08	2.70
BP1100/500	19.56	8.55	4.31	2.93
BP1100/1000	20.32	6.27	6.27	3.76
BP1100/1500	15.92	8.29	4.16	3.33
BP1100/2000	11.84	12.77	2.55	3.08
BP1100/2400	12.25	16.30	2.40	3.07
BP1300	34.95	21.35	3.90	2.16
BP1300/500	42.39	15.61	6.47	2.45
BP1300/1000	58.16	8.25	11.26	2.62
BP1300/1500	22.18	6.64	5.87	3.30
BP1300/2000	15.89	4.84	5.42	3.93
BP1300/2400	15.01	12.82	3.38	3.22
Vulcan XC-72	19.04	10.04	4.76	3.35
Vulcan/500	17.93	5.87	5.53	3.75
Vulcan/1000	18.87	3.98	6.38	3.91
Vulcan/1500	9.79	5.70	2.96	3.73
Vulcan/2000	5.51	12.63	0.87	2.44
Vulcan/2400	5.80	21.43	0.73	2.34

Table 3.6 Langmuir and Freundlich adsorption constants of activated carbons and heat-treated carbon blacks. (†- Activated carbon.)

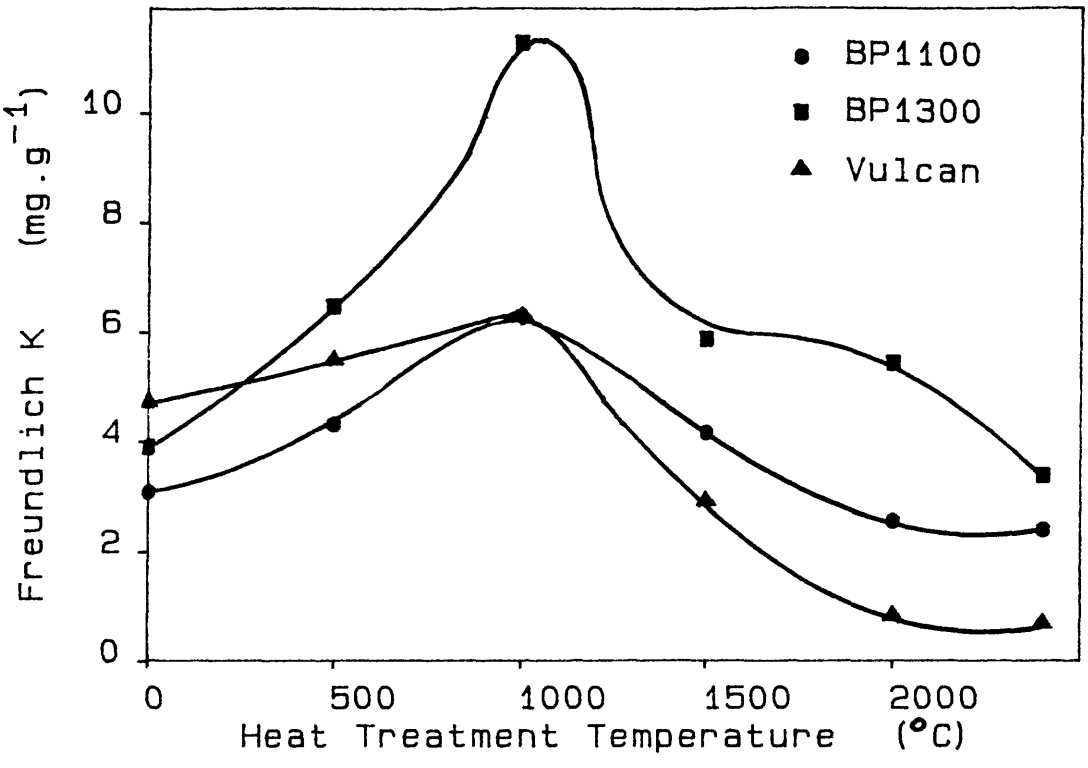

Figure 3.16 Effect of heat-treatment on Freundlich capacity constants of carbon blacks.

The linear correlations between the Langmuir Xm values found in carbonate buffered solution and the structural properties of the as-received carbon blacks and activated carbons are given in table 3.7. It is seen that statistically significant linear correlations are found with BET and edge areas, pore volumes and the pH.BET function.

Properties	Carbon Blacks	Carbon Blacks and Activated Carbons	Activated Carbons
BET Area	0.9448	0.9509	0.0235
Edge Area	0.5966	0.3929†	0.1126¶
Basal Area	0.1849	0.1493†	0.3207¶
Slurry pH	0.0747	0.4593	0.7989
Slurry pH.BET Area	0.9006	0.9600	0.7312
Pore Volume	0.8318	0.3409	0.9242
Mean Pore Diameter	0.1878	0.8021	0.0704
Pore Volume/ Mean Pore Diameter	0.8467	0.8992	0.8949
Points	19	23	4
95% Significance [97]	0.456	0.413	0.950
99% Significance [97]	0.575	0.526	0.990

† 22 points; ¶ 3 points.

Table 3.7 Linear least squares correlation coefficients between properties of carbons and Langmuir maximum loading constants in carbonate buffered solution.

From the slope of the correlation line of Xm on the BET surface area for carbon blacks and activated carbons (figure 3.17) it is possible to calculate the average surface area occupied by each adsorbed gold complex. The slope of the line is 0.0847 $mg.m^{-2}$, from which it can be calculated that each gold species is occupying 3.86 nm^2. By considering the crystalline structure of

$KAu(CN)_2$ [98], it is possible to calculate the length of the $Au(CN)_2^-$ ion as 0.67 nm. With the Au^+ ionic radius of 0.137 nm, this gives an approximate cross sectional area of 0.18 nm^2. Thus the $Au(CN)_2^-$ ion (if it is the gold species adsorbed) would only cover 4.7 % of the total surface, though this figure will be higher if stabilizing cations and water molecules are considered. The significant surface area correlation suggests that the gold is adsorbed as discrete species rather than the large cluster type complexes suggested by McDougall et al. [53], since this would lead to little correlation with surface area as they would not be able to fit into the smaller micropores. Attempts to correlate the Langmuir Xm value with the surface area of the pore size fractions determined from the pore size distributions were not successful. Thus the low surface coverage appears to occur over the entire surface, and suggests another factor is affecting adsorption.

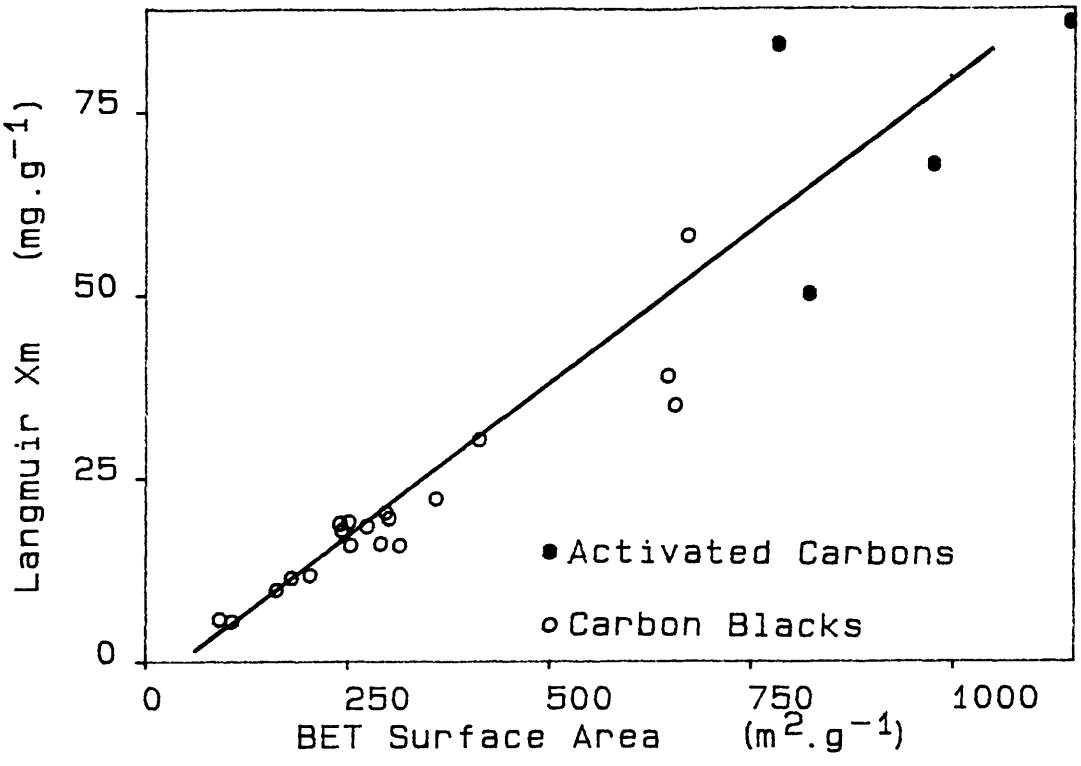

Figure 3.17 Relationship between Langmuir maximum loading constants and BET surface areas of activated carbons and carbon blacks.

The possibility of adsorption at specific surface oxide sites would seem to be unlikely, considering the difference in concentration and character of such sites between different heat-treated carbons. The statistically significant correlation between edge area and Xm shows that surface groups may have some effect, but figure 3.18 shows that significant adsorption will occur where there is negligible edge area. The carbon blacks with large edge areas are BP1300 as-received and heat-treated at 500°C. However, these results must be treated with caution due to the treatment given during manufacture. Up to 1000°C the edge area of this carbon black falls from 101 to 19.39 $m^2.g^{-1}$ (table 3.1), whereas the Xm value

increases from 34.9 to 58.2 $mg.g^{-1}$ (figure 3.15). Thus surface oxide sites would not appear to be the major factor influencing adsorption.

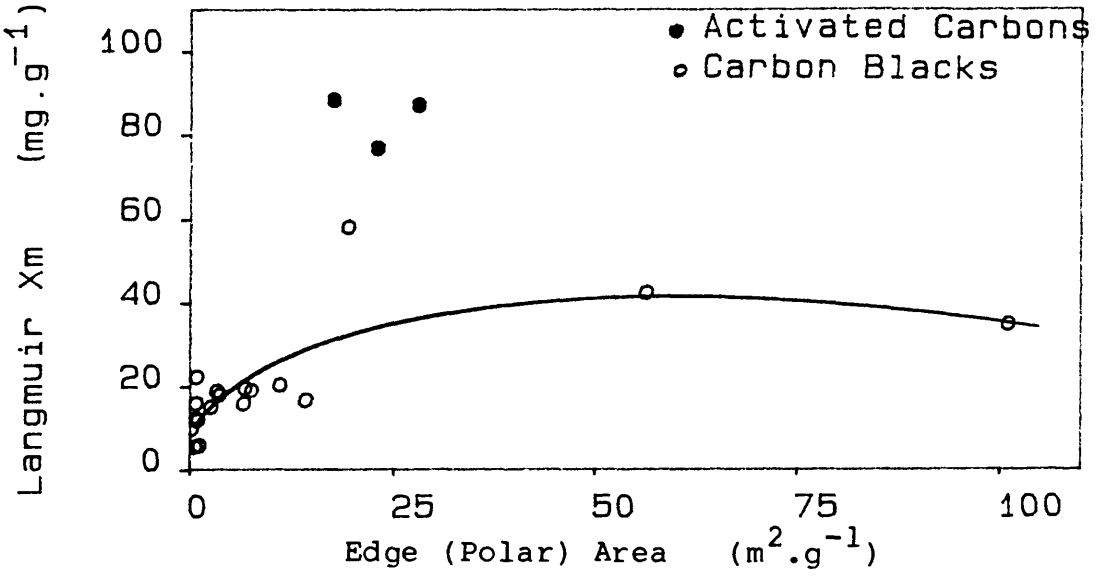

Figure 3.18 Relationship between Langmuir maximum loading constants and edge (polar) areas of activated carbons and carbon blacks.

The lack of a significant correlation with the basal plane area was expected from previous observations that graphite does not adsorb gold [74]. Considering the high electron density associated with a basal plane surface, it would seem unlikely that a negatively charged anion could be adsorbed, and this is supported by the correlation results.

A correlation with the slurry pH of the carbon blacks was expected, as this had been shown by Davidson et al. to occur with the Freundlich K value for

25 different activated carbons [24]. The variations of Xm and pH with heat-treatment are similar in type (figures 3.7, 3.15), but the effects of temperatures up to 1000°C differ enough to result in a very poor correlation. If the Freundlich K value is considered instead of Xm, the variation of this value with heat-treatment more closely resembles that of the slurry pH (figure 3.16), resulting in correlation coefficients between the two variables better than those using Xm (table 3.8). Thus the slurry pH of the carbon blacks would seem to have an influence on the Freundlich K value, but not Xm. Thus the agent contained by the carbons that is responsible for their buffering effect aids adsorption at low concentrations, but does not significantly affect the total amount of gold adsorbed. Davidson assumed that the agents responsible for the pH changes were the surface oxide groups [24], but a more likely explanation is that inorganic impurities cause this buffering effect [8]. The presence of some of these impurities has been shown by Davidson to have beneficial effects on gold adsorption when present in solution [54].

Davidson has also reported that for activated carbons produced from a common starting material it was possible to obtain a significant correlation between the Freundlich K value and the function (slurry pH.BET surface area) [24]. This is confirmed by the results presented here (table 3.8) for the K value, but by using the Langmuir Xm value there is no improvement in

correlation for the carbon blacks (table 3.7). The improvement in correlations on considering activated carbons also may be due to the bias produced by their high Xm values. Thus again the effect would appear to be of inorganic impurities contained by the carbons aiding adsorption at low gold loadings, but having little effect when the loading is much higher.

Correlations with pore volumes and mean pore diameters can be used to give further information on the effect of structure on adsorption. Considering carbon blacks and activated carbons separately, it is seen that the pore volume has a significant effect on loading. If the results of the two types of carbon are combined this relationship is significantly reduced. This is probably due to the difference in pore sizes for carbon blacks and activated carbons. If the range of pore sizes is taken into account using Pore Volume / Mean Pore Diameter then this combined correlation is improved. This function can be considered as a crude measure of surface area for long cylindrical shaped pores. Thus these results suggest that the pore size does not directly effect gold adsorption, only indirectly from its effect on surface area.

Properties	Carbon Blacks	Carbon Blacks and Activated Carbons	Activated Carbons
BET Area	0.6558	0.7889	0.6630
Edge Area	0.1460	0.1430†	0.9525¶
Basal Area	0.0396	0.0975†	0.9916¶
Slurry pH	0.5261	0.5917	0.9008
Slurry pH.BET Area	0.8854	0.8921	0.2886
Pore Volume	0.5693	0.0719	0.3394
Mean Pore Diameter	0.3977	0.8415	0.0370
Pore Volume/ Mean Pore Diameter	0.6518	0.8580	0.3104
Points	19	23	4
95% Significance [97]	0.456	0.413	0.950
99% Significance [97]	0.575	0.526	0.990

† 22 points; ¶ 3 points.

Table 3.8 Linear least squares correlation coefficients between properties of carbons and Freundlich capacity constants in carbonate buffered solution.

Carbon/ Heat Treatment (°C)	Impurities (weight %)				
	Na	K	Ca	Mg	Total
R2020 †	0.502	0.074	0.265	0.355	1.197
R2520 †	0.828	0.099	0.442	0.366	1.735
Pica G210 AS †	0.366	0.260	0.072	0.039	0.737
SS 607 †	0.197	0.141	0.023	0.005	0.366
BP71	0.317	0.015	0.026	0.003	0.361
BP1100	0.163	0.095	0.040	0.015	0.313
BP1100/2400	0.095	0.094	0.101	0.002	0.293
BP1300	0.825	0.043	0.040	0.069	0.976
Vulcan XC-72	0.274	0.037	0.093	0.039	0.443
Vulcan/2400	0.495	0.013	0.141	0.004	0.653

Table 3.9 Cation impurity contents of carbons removed by acid and water washing. (†- Activated carbon.)

3.3.4 Adsorption by Acid Washed Carbons

The cation impurities removed by acid and water washing of activated carbons and carbon blacks are given in table 3.9. These values cannot be considered as quantitative due to the large experimental errors involved, however they do give some indication of the relative amounts of cations removed by washing. As a result of the acid and water washing operation the buffering capacity of the activated carbons and carbon

blacks has been neutralized, strongly suggesting that the impurities were responsible for this effect.

Comparing the loading constants of the acid washed carbons (table 3.10) with those before acid washing (table 3.6 it is seen that the washing operation has resulted in a reduction in gold adsorption for most carbons. This reduction is more easily represented by the correlation of the Langmuir Xm value with the BET surface area, from which the area occupied by each adsorbed gold species is calculated to be 6.65 nm^2. This is an increase of 44 % on the area occupied by each species on the non acid washed carbons, which was 4.63 nm^2 (all values calculated from correlations with carbon blacks only). Since the surface area will not be changed significantly by the acid washing operation, this is equivalent to an average 44 % reduction in gold adsorption by acid washing. This reduction cannot be completely explained as being a result of the removal of the cationic impurities, assuming they do play an important role in adsorption, since the high sodium content of the carbonate buffer used (0.075 M) should result in adequate cation adsorption for this purpose. One possible explanation may be the presence of chemically bonded chloride groups on the carbon surface, which will not be completely removed by water washing (see chapter 5.3.4). These may either occupy favourable adsorption sites, or otherwise inhibit the gold adsorption process.

The acid washing has almost certainly affected the edge areas of the carbons, due to adsorption of chloride, and has eliminated their buffering capacity. Assuming the effects on BET and basal surface areas, pore volumes and mean pore diameters are negligible, correlations against Xm are given in table 3.11. Such assumptions are valid because hydrochloric acid washing will only produce chemical changes to the carbon surface, and should not change its physical structure.

Carbon/ Heat Treatment (°C)	Langmuir		Freundlich	
	Xm ($mg.g^{-1}$)	K' (ppm)	K ($mg.g^{-1}$)	n
Norit R2020 †	80.27	4.90	30.51	4.73
Norit R2520 †	85.06	4.30	34.42	4.90
Pica G210 AS †	76.49	5.77	25.60	4.06
SS 607 †	83.41	14.98	15.18	2.83
BP71	24.14	22.02	3.29	2.52
BP1100	16.52	29.96	1.55	2.11
BP1100/2400	9.10	7.83	2.53	3.59
BP1300	33.68	15.23	5.22	2.57
Vulcan XC-72	16.20	14.23	2.94	2.84
Vulcan/2400	5.47	21.48	0.55	2.06

Table 3.10 Langmuir and Freundlich constants of acid washed activated carbons and heat treated carbon blacks. (†- Activated carbon.)

Comparing these correlations with those for the as-received carbons (table 3.7) it is seen that there are no major changes in significance of any of the correlations. Thus acid washing does not appear to have greatly affected the adsorption process, only to have reduced the amount of gold loaded.

Properties	Carbon Blacks	Carbon Blacks and Activated Carbons	Activated Carbons
BET Area	0.9865	0.9294	0.6383
Basal Area	0.5823	0.0622	0.7658
Pore Volume	0.9256	0.2196	0.9254
Mean Pore Diameter	0.0275	0.9083	0.0326
Pore Volume/ Mean Pore Diameter	0.8337	0.9591	0.9088
Points	6	10	4
95% Significance [97]	0.811	0.632	0.950
99% Significance [97]	0.917	0.765	0.990

Table 3.11 Linear least squares correlation coefficients between properties of acid washed carbons and Langmuir maximum loading constants in carbonate buffered solution.

3.3.5 Adsorption from Unbuffered Solutions

Since acid washing removed the buffering capacity of the activated carbons and carbon blacks, it was possible

to use pure solutions of $KAu(CN)_2$ for adsorption tests without having to maintain solution pH by addition of acid or alkali. The loading constants and correlations calculated from this series of adsorption tests are presented in tables 3.12 and 3.13.

Carbon/ Heat Treatment (°C)	Langmuir		Freundlich	
	Xm ($mg.g^{-1}$)	K' (ppm)	K ($mg.g^{-1}$)	n
Norit R2020 †	75.18	-9.96	54.85	9.20
Norit R2520 †	56.89	-12.98	46.68	7.66
Pica G210 AS †	35.18	-25.00	47.14	70.86
SS 607 †	38.55	-2.02	71.32	-5.55
BP71	11.84	2.77	4.85	4.61
BP1100	13.98	17.72	3.81	4.46
BP1100/2400	4.58	-9.28	5.32	-574.15
BP1300	24.48	11.80	6.03	3.86
Vulcan XC-72	7.18	-9.72	5.48	13.75
Vulcan XC-72 ¶	9.42	-9.27	6.32	5.94
Vulcan/2400	1.70	-5.92	1.88	17.89

¶ Not acid washed.

Table 3.12 Langmuir and Freundlich constants of acid washed activated carbons and heat-treated carbon blacks using unbuffered solutions. (†- Activated carbon.)

The result of using unbuffered rather than carbonate buffered solutions is again a marked drop in gold

adsorption. From the correlation of BET surface area with Xm, the area occupied by each gold species is calculated as 8.22 nm^2. This is a 24 % increase from the acid washed results using carbonate buffers, and a 56 % increase from the as-received carbonate buffered results (in all cases considering carbon blacks only). As with the carbonate buffered results, there has been little change in the structural correlations (table 3.13). The drop in gold loading between carbonate and unbuffered tests will be due mostly to the removal of excess cations from solution. As shown by Davidson [54], 'spectator' cations have a marked effect on gold adsorption. The drop in solution pH from 10 to around 7 should not have affected the results greatly, since in this pH range there is little variation in gold adsorption [57].

The effect of acid washing and the carbonate buffer on gold adsorption can be more easily seen by considering the Vulcan XC-72 results separately (table 3.14). The advantage of using this carbon black is that the slurry pH of the as-received sample is 6.48, similar to that expected for the unbuffered tests. Thus if solution pH does have any effect, it will be minimized.

Properties	Carbon Blacks	Carbon Blacks and Activated Carbons	Activated Carbons
BET Area	0.9580	0.7520	0.8931
Basal Area	0.4967	0.1630	0.9331
Pore Volume	0.8929	0.2020	0.1579
Mean Pore Diameter	0.1531	0.8199	0.5099
Pore Volume/ Mean Pore Diameter	0.9144	0.8244	0.1970
Points	6	10	4
95% Significance [97]	0.811	0.632	0.950
99% Significance [97]	0.917	0.765	0.990

Table 3.13 Linear least squares correlation coefficients between properties of acid washed carbons and Langmuir maximum loading constants in unbuffered solution.

Conditions		Langmuir		Freundlich	
Wash	Buffer	Xm ($mg.g^{-1}$)	K' (ppm)	K ($mg.g^{-1}$)	n
As received	Carbonate	19.04	10.04	4.76	3.35
Acid washed	Carbonate	16.20	14.23	2.94	2.84
As received	Unbuffered	9.42	-9.27	6.32	5.94
Acid washed	Unbuffered	7.18	-9.72	5.48	13.75

Table 3.14 Langmuir and Freundlich constants of Vulcan XC-72 under different conditions.

Considering the Langmuir Xm constants, acid washing results in a much smaller reduction in gold loading than removal of the carbonate buffer. The two treatments appear to act independently. Acid washing results in reductions in maximum loading of 2.8 and 2.2 $mg.g^{-1}$ from carbonate and unbuffered solutions respectively. Whereas removal of the carbonate buffer leads to reductions of 9.6 and 9.0 $mg.g^{-1}$ for as-received and acid washed samples. These values are thus similar in magnitude, and do not change with the order of the treatments. Thus there appears to be two different processes in operation. The buffer effect will be due to excess cations in solution increasing adsorption, the acid washing effect possibly being due to adsorbed chloride groups reducing the number of favourable adsorption sites. Evidence for the latter effect cannot be given, apart from the high chloride contents of the carbons determined by XPS (see chapter 5.3.4).

The effects of these different conditions on the Freundlich K value are different to those found on the Langmuir Xm value. In the case of the K value acid washing causes a reduction in loading (as seen with Xm), but increased adsorption occurs in unbuffered solution. With this increase in adsorption there is also an increase in the constant n, which leads to the reduction in maximum loading. It must be realized that the K value is the loading expected at an equilibrium gold concentration of 1 ppm. Higher K values in unbuffered

solutions could be due to the reduction in the anion concentrations in solution competing for active adsorption sites. At larger gold concentrations (e.g. 100 ppm for the calculation of Xm), the effect of the removal of these anions reducing adsorption is masked by the far greater effect of the removal of the cations aiding adsorption. Thus the loading value will drop.

Acid washing has the same effect on the Freundlich K value as it does on Xm. This reduction in loading is thus almost certainly a result of a chemical change to the carbon surface, reducing the number of favourable adsorption sites.

3.4 Conclusions

Studies of the structural influences on the gold adsorption process has shown a strong correlation between the maximum loading capacity and the BET surface area of the carbons. Surface coverage was low, estimated at about 4 % if it is assumed that $Au(CN)_2^-$ is the adsorbed species. No dependence of the area of specific pore size ranges on gold adsorption could be found, indicating that adsorption was occurring over the whole of the surface.

Inert atmosphere heat-treatments at up to 2400°C for the carbon blacks were used for the surface area correlations. These heat-treatments would change the surface oxide structure of the carbons as well as the

surface areas. Thus demonstrating that adsorption at a specific oxide group is unlikely.

Acid washing results in a 44 % drop in the maximum gold capacity. This was assumed to be due to the change in chemistry of the surface of the carbons, being saturated with chloride groups.

Unbuffered adsorption tests led to a 24 % drop in the maximum gold capacity, compared to carbonate buffered tests. This is probably due to removal of 'spectator' cations from solution. Increases in the Freundlich capacity constants in unbuffered solution were considered as being due to the removal of interfering anions from solution.

4 Effect of Cations on the Adsorption of $Au(CN)_2^-$

4.1 Introduction

Several studies of 'spectator' cations added to gold cyanide solutions have shown that the increase in adsorption produced follows the series [53,54,57]:

$$H^+ > Ba^{2+} > Ca^{2+} > Mg^{2+} > Cs^+ > Li^+ > Na^+ > K^+$$

The effect of combinations of these cations in solution has not been studied thoroughly. Tsuchida has shown that the cation effect is reduced, and eventually eliminated, in acid solution [57]. This is due to the greater effect of H^+ in solution at similar concentrations to the other cations. Tsuchida also measured the amount of K^+ adsorbed with the gold, either with or without addition of excess cations in solution. A ratio of 2:1 was found in pure $KAu(CN)_2$ solution between Au:K adsorption. With excess cations the amount of K^+ adsorbed was reduced or eliminated, but the Au:M^{n+} adsorption ratios were not reported.

Rather than adding cations to solutions of $KAu(CN)_2$ and studying the change in gold adsorption, a more precise method that does not require the addition of excess cations or anions in solution is the production of specific $M^{n+}(Au(CN)_2^-)_n$ compounds, where M^{n+} is the cation to be studied.

4.2 Experimental Procedures

4.2.1 Cyanide Analysis

Free cyanide ion concentrations were determined using a Russell specific cyanide ion electrode in conjunction with a double junction reference electrode. Cyanide standard solutions were found to be unreliable, thus more stable iodide standards were used to give equivalent results. All solutions were diluted 1:1 with 0.2 M sodium hydroxide solution before analysis.

4.2.2 Solution Preparations

Excess cations were added to $Au(CN)_2^-$ solutions as chlorides. Generally the concentration of cations was chosen to be ionically equivalent to the gold concentration. Cyanide solutions were prepared using KCN.

Solutions of $HAu(CN)_2$, $Mg(Au(CN)_2)_2$, and $Ca(Au(CN)_2)_2$ were prepared from $KAu(CN)_2$ by cation exchange. 11 cm^3 of Zerolit 225 cation exchange resin was charged into a 1 cm diameter column. 1 M nitric acid was passed through the column to remove any previously adsorbed cations. Excess acid was washed through with distilled water. Chloride solutions of the required cation were then passed through the column until the effluent pH was neutral, indicating complete M^{n+} - H^+ exchange. The column was again rinsed through with

distilled water to remove any excess chloride solution. A solution of $KAu(CN)_2$ was then passed once through the column, and the resulting solution analysed by atomic emission for potassium. If significant quantities of potassium were detected then the resin charging procedure was repeated, and the solution passed through the fresh column. This procedure was repeated until potassium levels were too low for accurate analysis, generally < 0.2 ppm.

4.2.3 Deoxygenated - Oxygenated Adsorption Tests

The deoxygenated tests were carried out under similar conditions to the normal adsorption tests (chapter 3.2.8). Nitrogen was bubbled through the gold solutions 4 hours before the carbon was added, and throughout the course of the experiment. This was to remove any dissolved oxygen. For these experiments the carbon samples were kept in sample vials during weighing and drying, and added to the gold solutions which had been kept under nitrogen bubbling. After an 18 hour period a 10 ml sample of solution was taken, and the nitrogen bubbling continued for a further 6 hours before being replaced by oxygen. Tests indicated that negligible further adsorption occurred in this time period between taking the sample and starting oxygen flow, indicating that equilibrium had been achieved. After a further 18 hours under oxygen bubbling the slurry was filtered as reported previously, and the filtrate and 10 ml sample

analysed as in the previous adsorption experiments.

4.3 Results and Discussion

4.3.1 Adsorption of Gold and Potassium

During adsorption tests of $KAu(CN)_2$ using normal and acid washed carbons in carbonate buffered solution it was found that potassium was not adsorbed. This was also the case with the as-received Vulcan XC-72 in unbuffered solution. There are three possible reasons for this.

(1) Sufficient cation impurities are present in the carbons to account for $M^{n+}(Au(CN)_2^-)_n$ adsorption.

(2) In carbonate buffered solution the adsorbed species is $NaAu(CN)_2$.

(3) Adsorption of $M^{n+}(Au(CN)_2^-)_n$ does not occur.

In the previous chapter it was shown how gold adsorption was affected by acid washing and buffering solutions. Acid washing carbons was shown to lead to a reduction in the Langmuir Xm value, with carbonate buffering increasing it. The sodium content of the carbonate buffer used (0.075 M) was too high for any small changes due to adsorption to be measured. Only in unbuffered solutions, using acid washed carbons, was it possible to measure the molar Au:M adsorption ratio

(where M is the cation adsorbed from solution).

In the unbuffered adsorption tests the initial and equilibrium pH of the solutions were usually between 5 and 7. Small variations between initial and equilibrium pH did occur, but these were too small to be differentiated from experimental error, or to be related to gold adsorption. Thus changes in pH were not taken into account when calculating the Au:M adsorption ratios of the unbuffered solutions.

For pure solutions of $KAu(CN)_2$ the mean Au:K adsorption ratios are given in table 4.1. If the adsorbed species is $KAu(CN)_2$, then this ratio should be 1:1. All carbons studied gave values greater than this. However, a major problem with these results is the relatively large values of the standard deviations. In the case of the carbon blacks this is due mainly to low gold loadings resulting in relatively large experimental errors. The activated carbons adsorbed much more gold from solution, but very little potassium. Although for both types of carbon the actual numerical values given in the table are not very accurate, the general impression they give is that equimolar gold and potassium adsorption does not occur.

Carbon/ Heat Treatment (°C)	Au:K Adsorption Ratio (mol:mol)	Standard Deviation
BP71	1.71	0.56
BP1100	2.72	0.81
BP1100/2400	9.66	7.21
BP1300	1.47	0.93
Vulcan XC-72	3.40	1.08
Vulcan/2400	10.13	10.42
Norit R2020 †	16.70	8.85
Norit R2520 †	10.67	2.89
Pica G210 AS †	12.23	17.25
SS 607 †	8.45	6.41

Table 4.1 Gold : potassium adsorption ratios of acid washed carbons from unbuffered solutions. (†- Activated carbon.)

An interesting feature of the differences between the mean Au:K ratios of the carbons is their relationship to the BET surface area (figure 4.1). For the carbon blacks there is an increase in the relative proportion of potassium adsorbed at the higher surface areas, eventually resulting in equimolar Au:K adsorption. For the very low surface area carbon blacks, very little potassium is adsorbed resulting in large ratios. A more detailed study using many more carbons, and more data points to try to reduce errors, may show whether there is a correlation between the Au:K ratio and surface area, or

whether the variation shown is merely a result of the relatively larger errors occurring with carbons that only adsorb small quantities of gold. It must be remembered that although the carbons adsorb different amounts of gold, the surface coverage is similar. Thus variances in the amounts of gold loaded cannot be used to explain the surface area relationship.

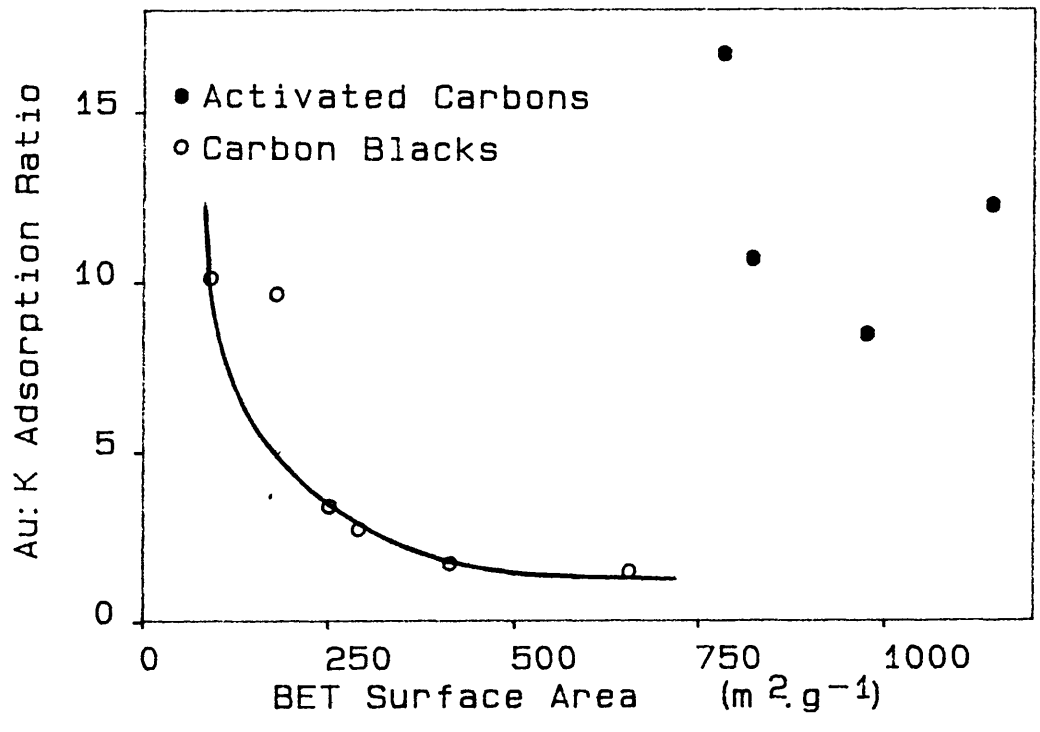

Figure 4.1 Relationship between BET surface areas of activated carbons and carbon blacks and the Au:K adsorption ratio from unbuffered solutions of $KAu(CN)_2$.

Errors in potassium determinations cannot explain the large Au:K ratios found for the activated carbons because the concentrations involved are too large. If

equimolar gold and potassium adsorption does not occur from unbuffered solution, then two questions arise:

(1) What cation is being adsorbed with $Au(CN)_2^-$?

and,

(2) What anion is left in solution to counter the charge of the K^+ cation ?

In carbonate buffered solution Na^+ may be the cation adsorbed with $Au(CN)_2^-$, leaving HCO_3^- or CO_3^{2-} in solution. This cannot occur in the unbuffered solutions, but anion exchange with surface hydroxide groups [57] or adsorption of $HAu(CN)_2$ [79] may. Both of these processes would lead to an increase in pH of the solution. Such increases can be predicted if it is assumed that there is equimolar $Au:(K^+ + H^+)$ adsorption (i.e. a combination of $KAu(CN)_2$ and $HAu(CN)_2$). Throughout the course of this investigation no change in pH has been large enough to suggest such a mechanism.

Another possible explanation for the large Au:K ratios is the precipitation of insoluble aurocyanide (AuCN).

$$Au(CN)_2^- = AuCN + CN^- \qquad (4.1)$$

A wide range of solutions were analysed after the

adsorption tests to try to detect any free cyanide released. In all cases the free cyanide concentration was below the detection limit of the cyanide electrode used (10^{-6} M). Thus if decomposition was occurring then the cyanide produced was not entering solution. The cyanide may be adsorbed, but this still leaves no counter ion to balance the K^+ left in solution, or it may decompose further.

$$CN^- + \frac{1}{2} O_2 = CNO^- \qquad (4.2)$$

$$CNO^- + 2\ H_2O = HCO_3^- + NH_3 \qquad (4.3)$$

This decomposition could lead to carbonate and ammonia being left in solution, balancing the charge on the potassium cation. Thus the overall reaction will be:

$$KAu(CN)_2 + \frac{1}{2} O_2 + 2\ H_2O = AuCN + KHCO_3 + NH_3 \qquad (4.4)$$

4.3.2 Deoxygenated - Oxygenated Adsorption

For the previous reaction (equation 4.4) adsorption may be affected by the presence of dissolved oxygen in solution. This has been confirmed by several researchers, who have shown that nitrogen saturation of solutions results in a significant drop in gold adsorption [57,59,99]. Oxygen saturation however has been shown to have no effect on adsorption, unless the carbon or solution has been deoxygenated previously in which case

adsorption increases to its normal level. Figure 4.2 shows the effect of nitrogen and oxygen bubbling on adsorption by a heat-treated carbon black. It is seen that the effects are similar to those expected. The isotherm plotted in figure 4.2 was obtained from normal unbuffered results, and it can be seen that nitrogen saturation reduces the gold loading significantly, whereas oxygen saturation has no effect. For adsorption tests from carbonate buffered solution, nitrogen or oxygen bubbling did not affect the amount of potassium adsorbed. As with the normal tests, little or no potassium was adsorbed.

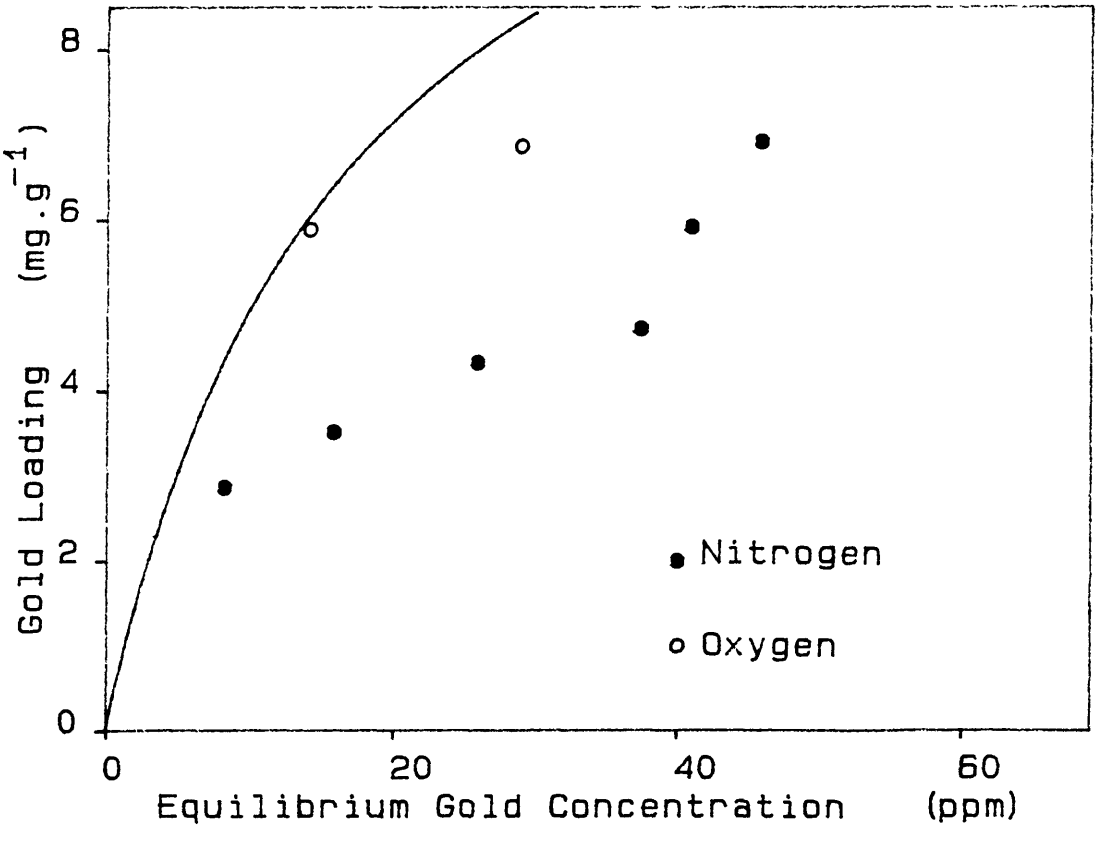

Figure 4.2 Effect of nitrogen and oxygen atmospheres on the adsorption of gold by BP1100/2400°C from unbuffered $KAu(CN)_2$ solution.

Carbon/ Heat Treatment (°C)	Au:K Adsorption Ratio (mol:mol)
BP1100	1.01
BP1100/2400	2.82
BP1300	0.39
Vulcan XC-72	0.81
Vulcan/2400	2.38
Norit R2020 †	1.72
Norit R2520 †	1.67
Pica G210 AS †	0.95
SS 607 †	1.15

Table 4.2 Gold : potassium adsorption ratios of acid washed carbons from unbuffered, deoxygenated solutions. (†- Activated carbon.)

As well as a reduction in gold adsorption, the gold : potassium adsorption ratio is also reduced by deoxygenation of the solutions (table 4.2). For the majority of the carbons this ratio is around 1:1 indicating equimolar adsorption (i.e. $KAu(CN)_2$). The possibility that chemically adsorbed oxygen is responsible for the high Au:K ratios can be discounted by considering the results of the two heat-treated carbon blacks. The heat-treatments have removed surface oxide groups, but the Au:K ratios are higher than the non heat-treated carbons. These larger ratios are probably

due to inaccuracies in the determination of the very small amounts of gold and potassium adsorbed by these two low surface area carbon blacks.

Carbon/ Heat Treatment (°C)		In Solution		Adsorbed		
		Au (ppm)	K (ppm)	Au ($mg.g^{-1}$)	K ($mg.g^{-1}$)	Au:K (mol:mol)
BP1100/2400		93.75	19.20			
	N_2	81.05	18.15	2.40	0.20	2.40
	O_2	68.75	20.00	4.49	—	—
Vulcan XC-72		94.90	19.45			
	N_2	88.20	18.05	3.45	0.72	0.95
	O_2	84.30	18.15	5.25	0.67	1.55
R2020 †		93.75	19.20			
	N_2	39.25	14.35	18.59	1.65	2.23
	O_2	3.58	17.65	29.55	0.64	9.14
SS607 †		74.65	14.80			
	N_2	48.65	10.30	12.58	2.18	1.15
	O_2	33.45	10.00	19.20	2.31	1.65

Table 4.3 Effect of nitrogen and oxygen atmospheres on adsorption of gold and potassium by acid washed carbons from unbuffered solution.
(†- Activated carbon.)

The effect of molecular oxygen on gold and potassium adsorption can be easily seen from the results of the series of tests where oxygen was passed through a

deoxygenated adsorption system after adsorption was complete (table 4.3).

The results of these tests show that molecular oxygen in solution causes adsorbed potassium to be desorbed, and leads to an increase in gold adsorption. Thus the adsorption mechanism can be considered as comprising two steps. Initially adsorption of the $KAu(CN)_2$ complex occurs, followed by an oxidation step which results in potassium desorption and increased gold adsorption. Such a mechanism would result in AuCN precipitation (equation 4.4), and the production of carbonate and ammonia. Analysis of carbons and solutions for these two species is reported in the next chapter.

Carbon	Weight (g)		K (ppm)	CN^- (ppm)	CN^- Lost ($mg.g^{-1}$)
R2020	0.1008	N_2	4.0 4.35	1.22 0.43	0.79
R2020	0.0981	O_2	3.6 4.2	1.35 0.34	1.03
R2520	0.0963	N_2	4.0 4.45	1.22 0.39	0.86
R2520	0.0988	O_2	3.6 4.3	1.35 0.35	1.01

Table 4.4 Adsorption/decomposition of cyanide by activated carbons in deoxygenated and oxygenated solutions.

The decomposition of $KAu(CN)_2$ via equation 4.4 requires molecular oxygen for the oxidation of free

cyanide to cyanate and eventually carbonate and ammonia. Thus if a solution of KCN is used in place of $KAu(CN)_2$ then the same N_2/O_2 dependence as for $KAu(CN)_2$ should be found.

From the results given in table 4.4 it is seen that reduced cyanide adsorption/decomposition occurs in deoxygenated solutions. However the amount of cyanide lost from deoxygenated solution is still significant. Potassium adsorption does not occur under either oxygen or nitrogen atmospheres. This is strong evidence for the decomposition, rather than adsorption, of cyanide, since for adsorption a cation must be adsorbed to balance the charge of the cyanide anion.

The reason for cyanide decomposition under deoxygenated conditions was thought to be due to oxygen adsorbed in the pores of the activated carbon samples. This would also account for the Au:K ratios of > 1 found in deoxygenated solutions. To test this theory a sample of Norit R2520 activated carbon was added to 100 ml of distilled water, and then nitrogen bubbled through for 24 hours. This should have removed any adsorbed oxygen species. After 24 hours a weighed sample of $KAu(CN)_2$ was added and the normal deoxygenated adsorption procedure followed. The Au:K ratio adsorbed was calculated to be 1.66, which is very similar to the value obtained normally (table 4.2). Thus the theory is not proven, which suggests that the activated carbons can catalyse

the decomposition of cyanide without the presence of molecular oxygen in solution. This may be due to surface oxide groups, which can only be removed by high temperature heat-treatments. Tsuchida [57] gave results for a sample of Norit R2020, heat-treated at 950°C under a vacuum at 10^{-5} torr, and loaded under similar deoxygenated conditions to this investigation. The Au:K ratios found lay between 0.92 and 1.08. Thus oxidation of cyanide may be due to a combination of molecular and chemically adsorbed oxygen.

4.3.3 Effects of H^+, Na^+, Ca^{2+}, Mg^{2+} on Adsorption

It has been seen in the previous section that equimolar gold : potassium adsorption only occurs in deoxygenated solution. The effects of 'spectator' cations in solution have been studied by several researchers [53,54,57], but the amounts of these cations adsorbed or their separate or combined effects at equivalent concentrations has not.

Table 4.5 shows the relationship between the cations in solution, added as chlorides, and the gold : cation ratios. It is seen that with H^+ addition equimolar adsorption occurs. Adsorption of other cations with H^+ is small. For the other cations the ratios are much greater than 1:1 when H^+ is not added to the solution. Ca^{2+} and

Mg^{2+} are adsorbed in similar amounts when they are together in solution, but individually Ca^{2+} is more strongly adsorbed and thus has the lower ratio. Na^{+} and K^{+} adsorptions are low in most cases, and are only really significant when the other cations are not present. From these results it is possible to deduce that the effect of the cations in reducing the adsorption ratio follows the order:

$$H^{+} > Ca^{2+} > Mg^{2+} > Na^{+} > K^{+}$$

Although complete adsorption isotherms for systems with these added cations were not determined, figure 4.3 gives an indication of their effect on gold adsorption.

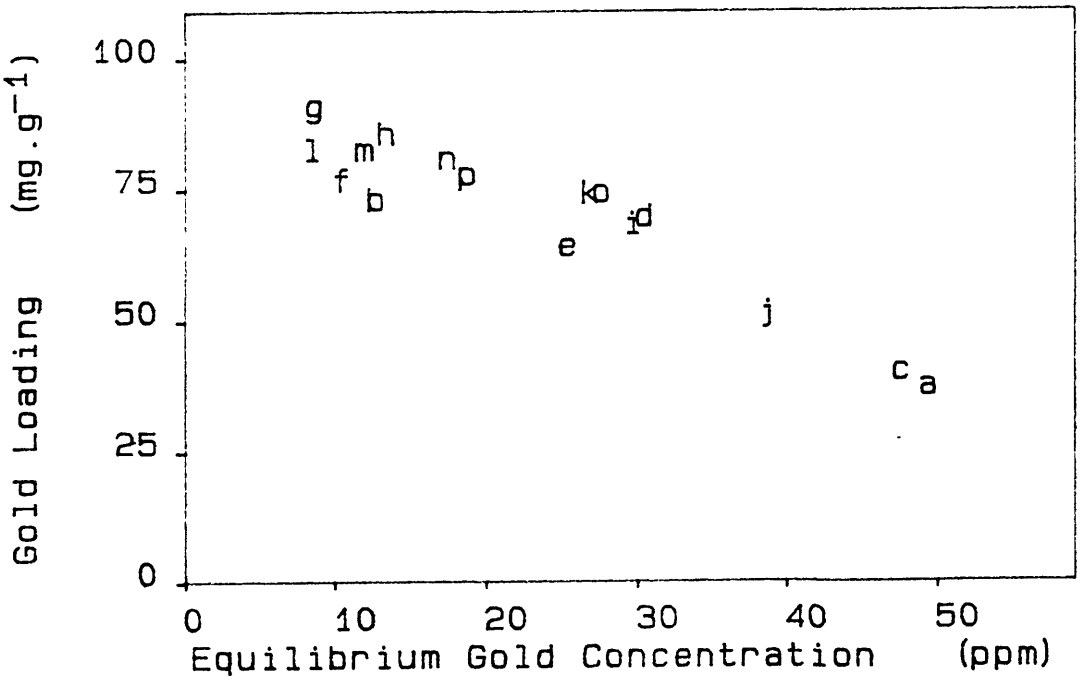

Figure 4.3 Relationship between equilibrium gold concentration and gold loading for R2020 activated carbon in $KAu(CN)_2$ solutions containing excess cations as chlorides. (a - p as in table 4.5)

	Cations	Initial/Equilibrium Concentrations (ppm)						Loadings ($mg.g^{-1}$)						Adsorption Ratios (mol:mol)					
		Au	K	Na	Mg	Ca	pH	Au	K	Na	Mg	Ca	H	Au:K	Au:Na	Au:2Mg	Au:2Ca	Au:H	Au:(K+Na+2(Mg+Ca)+H)
a	K	84.70	17.00				6.43												
		48.90	14.80				7.24	35.69	2.19					3.23					3.23
b	K H	84.00	17.30				3.33												
		12.20	16.00				4.17	71.23	1.29				0.40	10.96				0.91	0.84
c	K Na	85.40	16.60	20.50			7.29												
		47.10	15.50	19.00			6.18	38.57	1.11	1.51				6.91	2.98				2.08
d	K Mg	99.50	19.20		9.30		6.10												
		29.90	19.10		7.70		7.15	67.90	0.10		1.56			138.16		2.69			2.63
e	K Ca	89.75	17.83			5.88	5.73												
		24.85	17.75			2.77	7.01	62.34	0.08			2.99		161.04			2.13		2.10
f	K H Na	88.30	18.10	20.00			3.33												
		9.95	17.30	19.20			4.39	74.98	0.77	0.77			0.41	19.44	11.43			0.93	0.82
g	K H Mg	98.00	19.10		10.30		2.66												
		8.10	19.00		10.30		2.75	89.01	0.10		†		0.41	178.46		†		1.11	1.10
h	K H Ca	93.90	19.35			6.48	3.35												
		12.90	18.85			5.45	4.12	83.68	0.52			1.06	0.39	32.16			8.00	1.11	0.95
i	K Na Mg	98.70	19.60	23.00	9.10		5.74												
		29.20	19.00	23.80	8.10		7.00	66.44	0.57	†	0.96			22.99	†	4.29			3.62
j	K Na Ca	87.20	17.40	19.80		6.00	6.45												
		38.30	16.60	22.00		2.48	7.04	49.59	0.81	†		3.57		12.13	†		1.42		1.27
k	K Mg Ca	100.60	19.20		10.20	7.96	5.97												
		26.60	19.10		9.00	5.45	6.92	72.41	0.10		1.17	2.46		146.90		3.81	3.00		1.66
l	K H Na Mg	88.40	19.40	23.00	9.90		2.66												
		7.95	19.10	25.40	9.80		2.72	80.69	0.30	†	0.10		0.29	53.23	†	49.65		1.45	1.37
m	K H Na Ca	95.00	18.80	23.60		7.07	3.22												
		11.43	18.70	23.40		6.34	3.99	80.74	0.10	0.19		0.71	0.49	165.89	48.77		11.65	0.85	0.78
n	K H Mg Ca	97.30	18.70		9.90	8.43	3.24												
		16.98	18.10		9.70	7.09	3.91	78.98	0.59		0.20	1.32	0.49	26.57		24.79	6.10	0.90	0.74
o	K Na Mg Ca	100.20	19.45	23.20	11.10	7.59	6.02												
		26.90	19.20	24.00	10.10	5.91	6.97	72.57	0.25	†	0.99	1.66		58.20	†	4.53	4.44		2.16
p	K H Na Mg Ca	95.00	18.70	21.80	10.30	7.53	3.15												
		18.24	18.30	23.60	9.80	13.90	6.65	76.00	0.40	†	0.50	†	0.71	38.09	†	9.48	†	0.55	0.51

Table 4.5 Gold : cation adsorption ratios for Norit R2020 activated carbon in unbuffered $KAu(CN)_2$ solution with excess cations added as chlorides. († No cation adsorbed.)

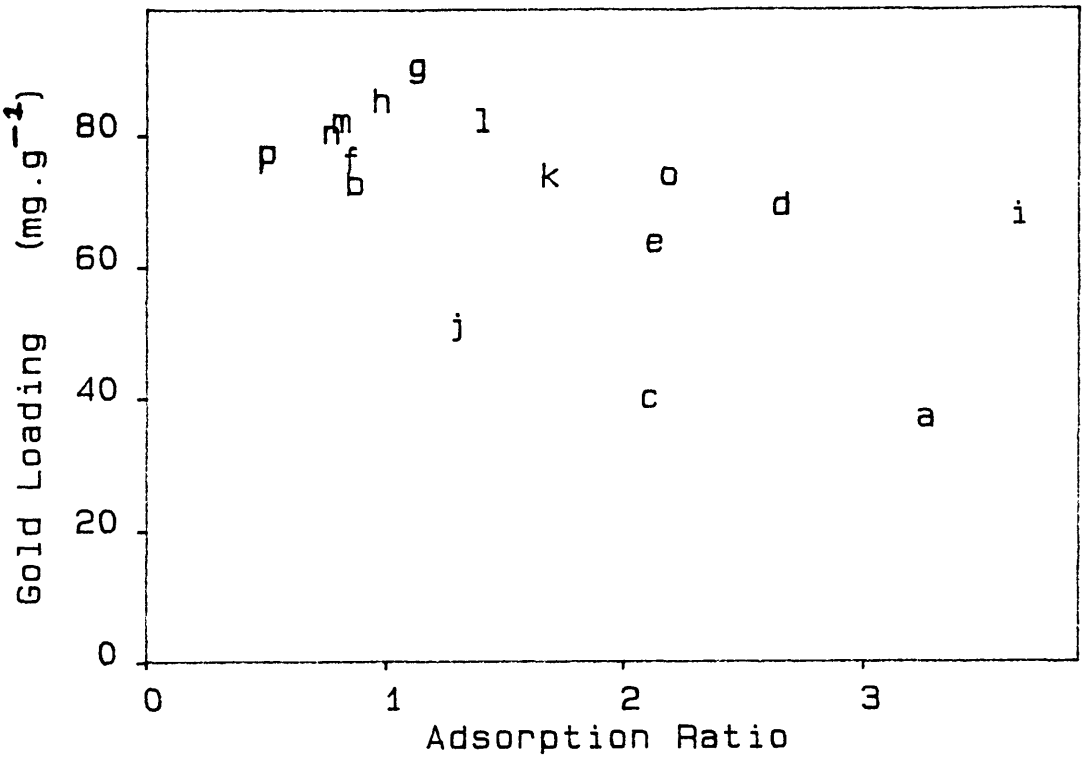

Figure 4.4 Relationship between gold : cation adsorption ratios and gold loading by R2020 activated carbon in $KAu(CN)_2$ solution with excess cations added as chlorides.
(a - p as in table 4.5)

The linear relationship in figure 4.3 between gold loading and equilibrium gold concentration for the different systems is a result of the similar experimental conditions used for all the tests. Thus variations in initial gold concentrations and the weight of activated carbon samples used need not be considered in comparing the results obtained in table 4.5. The figure also shows that the high loading values are associated with addition of H^+ ions to the adsorption solutions.

Cations	Gold Loading ($mg.g^{-1}$)	Gold : Cation Adsorption Ratios (mol:mol)					
		Au:K	Au:H	Au:Na	Au:2Mg	Au:2Ca	Au:(K+H+Na+2(Mg+Ca))
K	N_2 29.20	2.16					2.16
	O_2 41.31	3.50					3.50
K H Na Mg Ca	N_2 74.59	38.87	1.22	†	16.11	†	1.10
	O_2 88.99	†	1.08		†	73.69	1.06
K Na Mg Ca	N_2 39.86	40.79		4.00	1.81	2.93	0.86
	O_2 60.20	†		10.98	2.18	3.53	1.20

Table 4.6 Gold : Cation adsorption ratios for R2020 activated carbon in deoxygenated and oxygenated $KAu(CN)_2$ solution with excess cations added as chlorides. († No cation adsorbed.)

There does not appear to be a direct correlation between the gold : cation adsorption ratio and the gold loading on the carbon. This is shown in figure 4.4, where again the strong influence of H^+ ions in solution is apparent. Using the data from table 4.5 it is seen that the order in which the cations affect gold adsorption is:

$$H^+ > Ca^{2+} > Mg^{2+} > Na^+ > K^+$$

The effects of N_2 and O_2 on adsorption in the presence of excess cations is not as noticeable as in the case of pure $KAu(CN)_2$ solutions (table 4.6). In the presence of H^+ ions the only significant change is an increase in gold adsorption on oxygenation after the deoxygenation step. This could be due to the presence of O_2, but the effect is small, and is more likely a result of the longer adsorption time. In solutions where H^+ ions have not been added, oxygenation causes K^+ and Na^+ ions to be desorbed as they are from $KAu(CN)_2$ solution. Ca^{2+} and Mg^{2+} adsorption increases on oxygenation, but not as greatly as the increase in gold adsorption. Thus the gold : cation ratio increases.

The effects of oxygen and nitrogen atmospheres on the adsorption of gold with addition of excess cations is thus similar to the case using pure $KAu(CN)_2$ solutions, with the exception of adsorption from acid solution. In this case equimolar Au:H adsorption occurs with or without nitrogen saturation, thus suggesting $HAu(CN)_2$

adsorption from acid solution with no decomposition and precipitation of AuCN.

4.3.4 Adsorption from $HAu(CN)_2$, $Mg(Au(CN)_2)_2$ and $Ca(Au(CN)_2)_2$ Solutions

The interdependence of the different cations when added to gold solutions prior to adsorption tests has made direct comparisons difficult. A way to avoid this difficulty is to use specific $M^{n+}(Au(CN)_2^-)_n$ solutions, where M^{n+} is the cation to be studied. Such comparisons between H^+ and Ca^{2+} can be seen in tables 4.7 and 4.8. As before it is seen that the presence of H^+ leads to increased gold adsorption, but the difference in this case is that the gold : cation ratios are higher in the acid containing adsorption tests. From the results given it cannot be said whether this is as a result of the single cationic species in solution, or inaccuracies in determining H^+ concentrations from pH results.

Carbon	Weight (g)	Au (ppm)	pH	Gold Loading ($mg.g^{-1}$)	Au:H (mol:mol)
BP1100	0.3011	92.20	3.64		
		41.65	3.89	16.79	2.56
Vulcan	0.3092	92.20	3.64		
		51.60	3.80	13.13	2.92
R2520 †	0.0996	86.90	3.40		
		11.78	4.10	75.42	1.20
Pica †	0.2010	92.20	3.64		
		3.00	5.10	44.38	2.05

Table 4.7 Gold adsorption from unbuffered $HAu(CN)_2$ solution. (†- Activated carbon.)

Carbon	Weight (g)	Au (ppm)	Ca (ppm)	pH	Gold Loading ($mg.g^{-1}$)	Au:2Ca (mol:mol)
BP1100	0.3110	78.12	9.59	6.05		
		48.79	8.00	6.60	9.43	1.88
Vulcan	0.2982	78.12	9.59	6.05		
		53.48	8.55	6.57	8.26	2.41
R2520 †	0.0968	78.12	9.59	6.05		
		23.31	6.53	7.04	56.62	1.82
Pica †	0.0984	78.12	9.59	6.05		
		22.75	5.12	6.77	56.27	1.26

Table 4.8 Gold adsorption from unbuffered $Ca(Au(CN)_2)_2$ solution. (†- Activated carbon.)

Weight		In Solution				Adsorbed			
		Au	Mg	Ca	pH	Gold Loading	Au:2Mg	Au:2Ca	Au:H
(g)		(ppm)	(ppm)	(ppm)		($mg.g^{-1}$)	(mol:mol)	(mol:mol)	(mol:mol)
0.1005		85.10	9.50		4.93				
	N_2	44.00	7.30		5.49	40.90	1.16		
	O_2	28.20	6.90		6.83	55.04	1.34		
0.1015		76.60		9.68	6.18				
	N_2	36.95		5.19	5.99	39.06		0.90	
	O_2	18.49		4.05	6.97	55.43		1.04	
0.1001		84.50			3.40				
	N_2	35.70			3.71	48.75			1.22
	O_2	9.39			4.15	72.41			1.17

Table 4.9 Gold : cation adsorption ratios for R2520 activated carbon in deoxygenated and oxygenated $M^{n+}(Au(CN)_2^-)_n$ solutions, where $M^{n+} = H^+$, Ca^{2+}, Mg^{2+}.

The effect of oxygen is similar as in $KAu(CN)_2$ solutions (table 4.9), with equimolar $Au:M^{n+}$ ratios and reduction in gold adsorption in deoxygenated solution. The small increases in the gold : cation ratios for Mg^{2+} and Ca^{2+} are due to a greater increase in gold than cation adsorption on oxygenation. For all three systems there was no observable desorption of the cation when the oxygen replaced nitrogen. An interesting feature of these systems is that the ratios are close to 1:1, and the increases on oxygenation are not very great. Certainly the ratios are much less than those found in systems using $KAu(CN)_2$ or $M^{n+}(Au(CN)_2^-)_n$ solutions, but are similar to those found for deoxygenated/oxygenated $KAu(CN)_2$ solutions with added cations. It seems likely that in these cases adsorption of $M^{n+}(Au(CN)_2^-)_n$ occurs in deoxygenated solution, but when oxygen is passed there is little decomposition of the adsorbed species and thus little AuCN formation. This may be related to the stability of the $M^{n+}(Au(CN)_2^-)_n$ adsorbed species, with the more strongly adsorbed species being more resistant to oxidation.

4.4 Conclusions

Studies of the ratios of gold to cations adsorbed by carbons has given several indications of the type of species adsorbed. In carbonate buffered solution no potassium is adsorbed, though with 0.075 M sodium ions in solution adsorption of $NaAu(CN)_2$ may be the reason for this. In unbuffered solution and using acid washed carbons, the amount of potassium adsorption was less than that expected if $KAu(CN)_2$ is the adsorbed species. The relative proportion increased in deoxygenated solution, giving values close to the 1:1 molar Au:K ratio expected for $KAu(CN)_2$ adsorption. If oxygen was then passed through such a solution, increased gold adsorption occurred and potassium was desorbed to give the same results as found under normal conditions. The reason for such an effect is thought to be due to precipitation of AuCN with oxidation of CN^- to carbonate and ammonia.

The addition of excess cations to the solutions prior to the adsorption tests resulted in a lower gold : cation adsorption ratio and increased gold adsorption in the order:

$$H^+ > Ca^+ > Mg^+ > Na^+$$

With acid additions to solutions prior to adsorption tests, equimolar $Au:H^+$ adsorption occurs, suggesting $HAu(CN)_2$ as the species adsorbed. Also deoxygenation had

little or no effect on this ratio, whereas for the other cations an increase was seen. Desorption of these other cations on oxygenation did not occur, suggesting that the reason for the increase in adsorption on addition of these cations is related to the stability of the $M^{n+}(Au(CN)_2^-)_n$ complex.

5 The Nature of the Gold Adsorbate

5.1 Introduction

An important step to aid the evaluation of the mechanism of gold adsorption is the determination of the form of the adsorbate. Many theories as to its nature have been proposed [48,53,54,57-59,74-77,79-83], but most of these have relied on bulk chemical analysis of solutions and adsorbents. More direct methods such as X-ray Photoelectron Spectroscopy [53] and Potential Stripping techniques [57] have been used in the study of the adsorbate, but comparisons between the results obtained from using these techniques and chemical analysis of adsorption solutions have not as yet provided sufficient evidence to determine the form of the gold adsorbate(s). Combining techniques such as XPS with bulk chemical analysis of carbons and solutions, under the various conditions considered in the previous chapter, may improve our understanding of this adsorption system.

5.2 Experimental Procedures

5.2.1 Elution of Gold Loaded Carbons

The elution of gold from loaded carbons was achieved using a soxhlet apparatus (figure 5.1). A weighed amount of dried carbon was placed in the thimble and left for up to 1 week of continuous hot condensed vapour elution. Any

metallic gold or AuCN left in the flask was dissolved by KCN solution, with O_2 bubbling through the solution if required. Solution analysis for gold, potassium and free cyanide was as previously described.

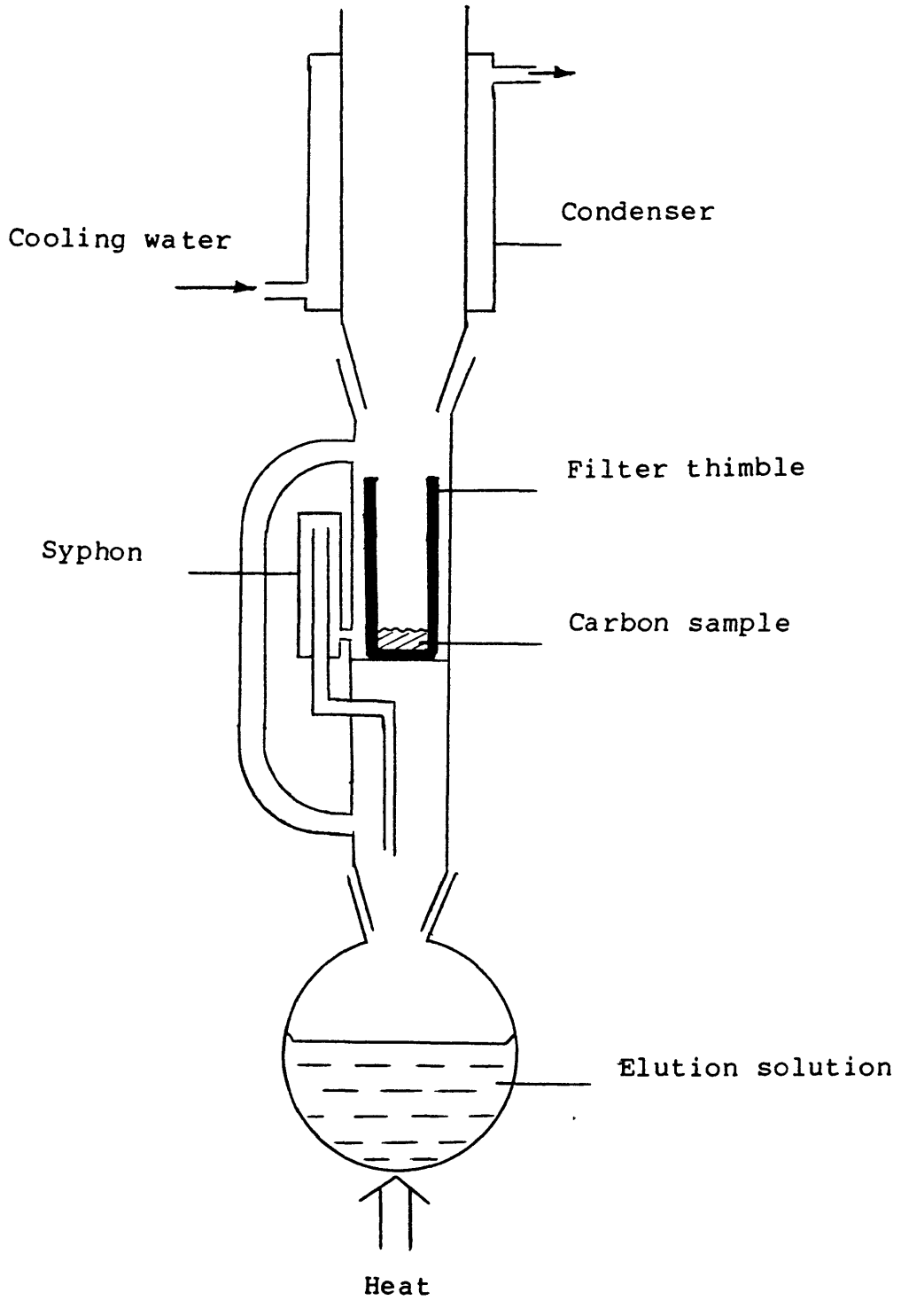

Figure 5.1 Soxhlet apparatus used for the elution of gold loaded carbons.

5.2.2 Microanalysis of Gold Loaded Carbons

Microanalyses were carried out using a Carlo Erba model 1106 CHN analyser. A weighed sample in a tin cup is introduced into the instrument which is then purged with helium. The cup then enters the hot zone of a furnace set at 1100°C, and a metered amount of pure oxygen added. The helium carrier gas sweeps the combustion products over hot copper granules, at 650°C, to remove excess oxygen and reduce nitrogen oxides to nitrogen. The gas then passes through a chromatography column at 120°C, from which the products leave in the order nitrogen, carbon, and then hydrogen. The amount of each element in the gas is determined from the change in thermal conductivity of the gas, and calculated by a digital integrator which measures the resultant peak areas.

5.2.3 Determination of Species in Eluates

A sample of acid washed Norit R2520 activated carbon, loaded with 81.99 $mg.g^{-1}$ gold and 2.36 $mg.g^{-1}$ potassium, was eluted in a Soxhlet apparatus for 1 week. The eluate was then sent to the BP Research Centre at Sunbury for analysis for gold species, ammonia, cyanate, carbonate and free cyanide.

5.2.3.1 Gold Species

Separation of complex anions can be achieved using reverse phase ion-pair chromatography. In this study a Dionex reverse phase column was used, with a Shimadzu SPD2A U.V. detector at 240 nm as $Au(CN)_2^-$ adsorbs strongly in the ultra-violet. 2 mM t-butyl ammonium hydroxide and 0.2 mM Na_2CO_3 in a 40 % v/v aqueous acetonitrile solution was used as the eluant.

5.2.3.2 Total Carbon

A Dohrmann DC80 total organic carbon analyser was used to determine total carbon and the sum of carbonate plus cyanate. For the total carbon content the aqueous sample solution is introduced into a vessel containing ammonium persulphate in a nitric acid medium. On irradiation with ultra-violet light the carbon species are oxidized to carbon dioxide. The CO_2 produced is taken by a carrier gas through a drier and measured using an infra-red analyser. Prior to analysis of the eluate the method was checked using synthetic solutions of $Au(CN)_2^-$, cyanate and free cyanide.

Low levels of carbonate can be detected by measuring CO_2 evolution on acidifying the sample. This can be carried out using the Dohrmann DC80 total organic carbon analyser with the ultra-violet lamp switched off. Hydrolysis of cyanate to carbonate in acid solution was

found to be rapid enough for the total carbonate and cyanate concentration to be determined.

5.2.3.3 Total Nitrogen

Nitrogen contents were determined using a Dohrmann 100 combustion/chemiluminescence apparatus. The liquid or slurry to be analysed is injected into a combustion tube and burnt in a helium/oxygen carrier gas mixture.

$$R - N + He/O_2 = He/O_2,\ CO_2,\ H_2O \text{ and } NO \qquad (5.1)$$

The carrier gas sweeps the combustion products into a reaction cell where ozone is added to react with nitric oxide via a photochemical reaction, to produce nitrogen dioxide in an excited state. Fluorescence then occurs with electromagnetic radiation (hv) emission in the 600 - 900 nm range.

$$NO + O_3 = NO_2^* + O_2 \qquad (5.2)$$

$$\downarrow hv$$

$$NO_2$$

The electromagnetic radiation detected in the 600 - 900 nm range by a photomultiplier and amplifier is thus proportional to the total amount of chemically bound

nitrogen injected into the system.

5.2.3.4 Ammonia

The detection of ammonia was by a colorimetric method based on the formation of indophenol blue by the reaction of ammonia with phenol and sodium hypochlorite. The ammonia concentration is proportional to the optical density of the solution at 625 nm.

Because ammonia can be formed by the decomposition of cyanide and cyanate, synthetic solutions containing these and $Au(CN)_2^-$ ions were prepared and analysed for ammonia by this method.

5.2.3.5 Cyanate

Cyanate concentrations were determined by ion-chromatography. A Dionex Model 10 and AS3 separator column, fibre suppressor and conductivity detector were used. A Shimadzu SPD2A HPLC U.V. detector (set at 200 nm) was used in series with the conductivity detector.

Use of a suppressor after the separator column is to remove cations from the eluant. The suppressor used was a hollow fibre of cation exchange membrane. The eluant flows through the centre of the fibre and the cations pass through the membrane into a continuous flow of dilute acid. An alternative suppressor was tried which

comprised a column of a strong acid form of a cation exchange resin. No cyanate was detected with the column suppressor in place, suggesting that the cyanate had been hydrolysed to CO_2.

5.2.3.6 Cyanide

Cyanide concentrations were determined by a flow injection ion selective electrode method [100]. This is a continuous method in which two streams containing the carrier solution (de-ionized water) and an ionic strength adjuster (1 M NaOH, 7.7 mM KCN) are mixed and flow through a detector containing the ion selective electrode and double junction reference electrode. 20 μl samples of standards and the solution to be analysed are injected into the carrier stream, and the detector response monitored on a chart recorder using a millivolt meter. Calibration was achieved by plotting peak height versus the logarithm of the standard cyanide concentration, giving a linear graph.

5.2.4 X-Ray Photoelectron Spectroscopy Study of Gold Loaded Carbons

XPS analysis is based upon the principle of the photoelectric effect. This is the emission of electrons when electromagnetic radiation impinges upon a surface. The kinetic energy of the emitted electrons will be determined by the difference between their initial energy

level and the energy of the incident electromagnetic radiation, with a correction made for the work function of the spectrometer (equation 5.3).

$$E_{KE} = h\nu - E_{BE} - \phi \qquad (5.3)$$

Where :

E_{KE} = Kinetic energy of photoelectron.

E_{BE} = Binding energy of electron.

h = Planck's constant.

ν = Frequency of incident radiation.

ϕ = Work function of spectrometer.

The typical layout of a X-ray photoelectron spectrometer is given in figure 5.2. This uses an electron beam impinging on an aluminium target to provide the AlKα radiation. The photoelectrons produced on interaction with the samples are focused by a lens system through a hemispherical analyser into an electron multiplier. The height of the peak produced on the x-y recorder is a measure of the number of photoelectrons of a particular energy detected. Different energy electrons are detected by either varying the potential across the hemispherical analyser (FRR or Fixed Retard Ratio mode), or changing the focus of the lens system (FAT or Fixed Analyser Transmission mode).

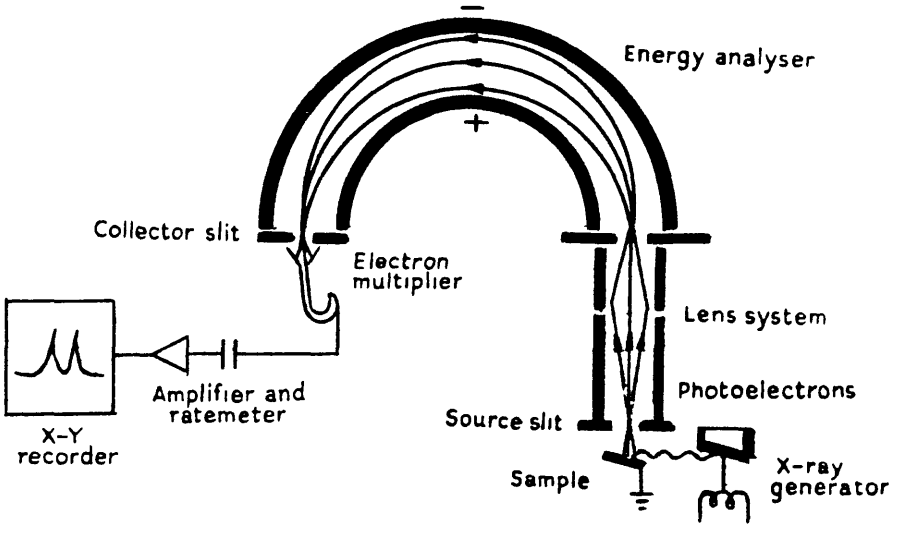

Figure 5.2 Schematic diagram of an X-ray photoelectron spectrometer [101].

XPS analysis of the carbons was carried out by the BP Research Centre at Sunbury using a Kratos ES300 spectrometer. Fixed analyser transmission mode was used, with the pass energy set at 65 eV and a slit width of 1.75 mm. An aluminium anode was used as the X-ray source, operating at 15 keV and 20 mA. The samples were mounted on double-sided adhesive tape and introduced into the spectrometer via a rapid insertion probe. Due to evolution of adsorbed gases, up to $\frac{1}{2}$ hour was allowed for the pressure to equilibrate at around 7.5×10^{-9} torr. Data acquisition and analysis was controlled by a Kratos DS300 data system. Because of sample charging, caused by the insulating properties of the adhesive tape, the binding energies determined may be increased by 1 or

2 eV. This was corrected by referencing the binding energies to the carbon 1s peak at 285 eV. The concentrations of the elements detected were determined from the peak areas, corrected for atomic sensitivity factors. These concentrations were calculated relative to the carbon 1s peak at 285 eV.

5.3 Results and Discussion

5.3.1 Soxhlet Elution of Gold Loaded Carbons

The continuous, condensed vapour elution of gold from carbon blacks and activated carbons was found to be very slow, but effective (table 5.1). Usually between 50 and 70 % of the adsorbed gold was removed in 140 to 170 hours (6 to 7 days). Recovery of potassium was more variable, and subject to a large degree of experimental error. This was due to the relatively small quantities adsorbed, and correspondingly smaller amounts usually eluted. The change in concentration of potassium detected in solution between the eluant and the eluate was usually between 0.5 and 1 ppm. This is below the recommended working range of 1 to 3 ppm for potassium determination by atomic emission spectroscopy. Consequently background fluctuations in emission reading will cause significant changes in measured concentrations, and will reduce accuracy. As noted earlier (see chapter 4.3.1), measurement of the molar Au:K ratio adsorbed by the carbons is also subject to large degrees of error, but

this was due mainly to problems in detecting small changes in potassium concentrations. The net result of these observations is that the potassium results cannot be treated with any confidence in this case, and thus the molar Au:K ratios of the eluates given in table 5.1 are only very approximate. A more complete analysis of one of these eluates is given later (see chapter 5.3.2).

During the course of several of the elution experiments the precipitation of yellow AuCN occurred around the water line of the boiler. This precipitation usually started from 2 to 3 days into the elution operation. Decomposition of part of this precipitate appeared to occur later on in the elution procedure, leaving a thin film of metallic gold on the inside of the boiler. This decomposition was thought to be caused by the over-heating of the boiler above the level of the eluant.

For the elution of the Norit R2020 activated carbon which had been loaded from deoxygenated solution a pink/purple coloration of the eluate was noted, almost certainly caused by colloidal gold. No such observable coloration was seen for any of the other elutions.

Carbon	Loading ($mg.g^{-1}$)		Au:K Ratio Adsorbed (mol:mol)	Elution Time (hr:min)	Recoveries (%)				Au:K Ratio in Eluate (mol:mol)
	Au	K			Au			K	
					In Solution	Precipitated	Total		
BP1300	11.94	2.04	1.16	18:10	48.07	—	48.07	72.13	0.77
BP1300	12.08	1.94	1.24	139:50	91.80	—	91.80	180.20	0.63
BP1300	26.76	4.37	1.22	187:35	69.40	—	69.40	130.38	0.65
Vulcan	7.04	0.50	2.79	164:35	31.74	37.95	69.69	83.86	1.06
R2020 *	81.75	0.90	18.01	147:40	52.43	0.00	52.43	749.61	1.26
R2020 *	81.20	1.25	12.90	114:45	15.97	75.91	91.88	48.97	4.21
R2020 *	74.45	1.00	14.78	140:05	11.49	54.10	65.59	20.08	8.46
R2020 *	33.59	2.55	2.61	165:40	54.79	8.26	63.06	90.00	1.59
R2020 †*	26.43	2.90	1.81	163:30	69.16	2.27	71.43	24.09	5.19
R2020 ¶*	94.25	—	—	138:15	46.06	0.24	46.30	—	—
R2520 *	81.99	2.36	6.90	161:00	40.37	7.37	47.74	27.46	10.14
R2520 *	81.54	5.15	3.14	143:25	17.20	25.04	42.25	3.57	15.14
R2520 §*	46.57	0.12	2.07	166:30	22.76	27.76	50.52	0.01	56.20

Table 5.1 Elution of adsorbed gold and potassium from carbon blacks and activated carbons. (* Activated carbon. † Deoxygenated, § Carbonate buffered, ¶ $HAu(CN)_2$ adsorptions. For $HAu(CN)_2$ adsorption H^+ results given in place of K^+.)

The source of the AuCN precipitated in the boiler may give some useful indications of the gold species adsorbed. This AuCN may either be eluted directly from the carbon, or be a result of decomposition of $Au(CN)_2^-$ in solution. Decomposition of this species could leave other products in solution, and attempts to detect these species are reported later (see chapter 5.3.4).

To determine whether or not the AuCN may have come directly from the carbon sample, a sample of AuCN was put into the soxhlet apparatus in place of a loaded carbon and the standard elution procedure followed for 7 days. After this time the eluate was a pink/purple colour and metallic gold had been precipitated in the bottom of the boiler. No yellow AuCN had been precipitated at the bottom of the boiler or at the water line. Approximately 4 % of the AuCN was found in the eluate (as gold) in this experiment, 3.6 % being in solution and 0.4 % precipitated as metallic gold. The gold concentration of the aqueous solution was 11.6 ppm. AuCN is virtually insoluble in water [102], and since only metallic gold was precipitated it seems likely that there was little or no AuCN dissolved in the eluate. Further evidence came from analysing the AuCN left in the soxhlet thimble. This had changed from a bright yellow to a dark green colour (noted by Williams to occur on heating [77]). X-ray diffraction analysis of this sample showed it to be a mixture of AuCN and metallic gold. Thus it appears that the AuCN gradually decomposed to metallic gold in the

thimble. Some of these gold particles formed may have been small enough to pass through the soxhlet thimble as a colloidal solution. The possibility of free cyanide formation by this decomposition, which could then lead to dissolution of the AuCN as $Au(CN)_2^-$ ion cannot be completely discounted, but this mechanism will be given further consideration later.

Since it has been shown that the AuCN precipitated in the boiler during the gold loaded carbon elutions is not formed by transport of AuCN from the carbon held in the thimble, it must be formed from the aqueous eluate. One possibility is that $Au(CN)_2^-$ may be dissociating in solution (equation 5.4), with gaseous HCN being evolved and re-entering solution in the thimble. In the thimble the reverse reaction would occur, resulting in $HAu(CN)_2$ formation which would then return to the boiler. This should result in AuCN precipitation in the boiler.

$$Au(CN)_2^- + H^+ = AuCN + HCN \qquad (5.4)$$

To test this theory a sample of AuCN was again put into the soxhlet apparatus, but this time a solution of 50 ppm gold, as $KAu(CN)_2$, was used as the eluant. The results were similar to the previous case where distilled water was used. Metallic gold was precipitated in the bottom of the boiler and also around the water line. The eluate had a pink/purple coloration of colloidal gold, but again there was no AuCN precipitation. A significant

change was noted however in the time taken for the colloidal solution to appear. The process was much faster this time, with the colloidal gold solution being formed within 1 day, whereas in the previous experiment it took 3 days. The amount of gold recovered in this case was much greater, at 39.3 % compared to 4 % using distilled water. Of this 24.8 % was in solution and 14.3 % precipitated. Thus although the enhancement of the dissolution of AuCN from the thimble by addition of $Au(CN)_2^-$ ions to the boiler is apparent, the mechanism is far from certain. The lack of AuCN precipitation suggests that simple dissociation (equation 5.4) is not the main process occurring, and thus other sources of AuCN formation must be considered.

Since neither of these methods of eluting AuCN led to AuCN precipitation in the boiler, it seems more likely that gold adsorbed as $Au(CN)_2^-$ is the source. To test this theory the soxhlet apparatus was used again but without a thimble. The eluant used this time was $HAu(CN)_2$, and the main aim was to see the effect on this solution of a continuous reflux. After 7 days continuous operation there was AuCN precipitation at the water line and in the bottom of the flask. However, metallic gold was not produced. This AuCN must have been produced by $HAu(CN)_2$ decomposition (equation 5.4). An important point to realize is that $HAu(CN)_2$ is not as stable a compound as $KAu(CN)_2$. It is possible to crystallize $KAu(CN)_2$ from solution by simple evaporation, but $HAu(CN)_2$ always

dissociates to AuCN and HCN. The reason for this is probably due to the volatility of HCN. Thus AuCN formed during elution of gold loaded carbons is apparently produced from any $HAu(CN)_2$ eluted. Dissolution of adsorbed AuCN by reaction with free cyanide in the thimble was proposed earlier, but this can be discounted since this would also lead to AuCN precipitation in the boiler which did not occur with the AuCN elution test.

From these three similar experiments it has been shown that AuCN is precipitated by decomposition of $HAu(CN)_2$ in solution. Formation of AuCN during elution of gold loaded carbons thus suggests $HAu(CN)_2$ as being adsorbed. The results of an elution test of a carbon loaded from $HAu(CN)_2$ solution have been given in table 5.1. As with carbons loaded from $KAu(CN)_2$ solutions, gold was found in solution, and precipitated as AuCN and metallic gold. The molar Au:H ratio adsorbed by this carbon was 2.07. This suggests a combination of $HAu(CN)_2$ and AuCN as being adsorbed. Such a combination agrees with the results of the gold species obtained by elution, with AuCN coming from $HAu(CN)_2$ elution and decomposition, and metallic gold from the decomposition of adsorbed AuCN.

The possibility of $HAu(CN)_2$ adsorption from $KAu(CN)_2$ solutions has been discussed earlier (see chapter 4.3.1). Such a mechanism would have explained the high Au:K adsorption ratios found in unbuffered solutions. However,

$HAu(CN)_2$ adsorption would result in an increase in solution pH, which was not observed to any significant extent. This resulted in the hypothesis that AuCN was adsorbed. Differentiation between these two adsorbed species by microanalysis and X-ray photoelectron spectroscopy is reported later.

For this apparently complex desorption system further evidence for the theories of metallic gold and AuCN formation may come from analysis of the eluate for decomposition products of cyanides.

5.3.2 Species Eluted From Gold Loaded Activated Carbon

The composition of the eluate obtained from a sample of gold loaded Norit R2520 is given in table 5.2. The recovery of gold was 40.37 % gold in solution and 7.37 % precipitated as metallic gold and AuCN (table 5.1). Yellow AuCN and metallic gold were both deposited on the sides of the boiler at the water line. The potassium recovery was 27.46 %.

The results given in table 5.2 indicate that within experimental error all the gold present in solution is in the form of the $Au(CN)_2^-$ ion. The only other possible gold species in solution (colloidal gold, AuCN, and $Au(CN)_4^-$) would not have been detected by the reverse phase ion-pair chromatography method used, and thus their presence in solution would have resulted in a lower

measured gold concentration than that obtained.

Allowing for experimental error (± 0.04 mM), the nitrogen content of the solution agrees with that expected for $Au(CN)_2^-$ and ammonia. From comparing the potassium and gold contents of the eluate it is clear that $KAu(CN)_2$ is not the main gold species eluted. In this case a significant drop in the pH of the eluate from that of the original eluant was noted. The initial pH was 6.9, which dropped to 4.2 after elution. If it is assumed that the remaining 0.15 mM of gold is eluted in the form of $HAu(CN)_2$, a value of 3.8 would be expected for the eluate pH. The difference between these two values can be accounted for by experimental error in the determination of H^+ concentrations using a pH electrode. A more accurate titrimetric technique is recommended for any future work on this system.

The difference in pH between the eluant and eluate was unique to this elution test. For the other elutions given in table 5.1 (except that loaded from $HAu(CN)_2$ solution), changes in pH were small. Why this particular elution behaved in this way is not clear. It would appear that in this case decomposition of $HAu(CN)_2$ to AuCN did not occur to any appreciable extent, with only 7.37 % of gold recovered by precipitation. For the other elutions of the activated carbons with large gold loadings, a combination of decomposition of $HAu(CN)_2$ and the presence of $KAu(CN)_2$ in solution would lead to only

small pH changes as observed.

Species	Concentration		
	as species (mM)	as C (mM)	as N (mM)
Total carbon	1.00	1.00	—
Total Nitrogen	0.26	—	0.26
Carbon as CO_3^{2-} and CNO^-	0.04	0.04	—
Cyanate	<0.01	<0.01	<0.01
Carbonate	0.04	0.04	—
Free cyanide	<0.08	<0.08	<0.08
Ammonia	0.01	—	0.01
$Au(CN)_2^-$	0.14	0.27	0.27
Total gold	0.13	—	—
Total potassium	0.02	—	—

Table 5.2 Analysis of eluate obtained from gold loaded Norit R2520 activated carbon.

Ammonia detection in solution was by the formation of indophenol blue. Since it is possible that ammonia can be formed by the decomposition of $Au(CN)_2^-$, a test solution containing 85 μg of $Au(CN)_2^-$ was analysed by this method. The results indicated the presence of 1.17 μg of ammonia in solution. In the eluate the ammonia concentration was 0.01 mM. Thus the amount of nitrogen in the form of ammonia is small compared to the total nitrogen content (0.26 mM), and does not seriously affect the nitrogen balance on the solution. Therefore,

although ammonia is found in the eluate, its presence cannot be seen to indicate the decomposition of cyanide species in solution.

Other possible decomposition products of $Au(CN)_2^-$ (cyanate and free cyanide) could not be detected in significant concentrations. Carbonate was detected, but the elution procedure of continuously boiling the eluate, to produce condensed vapour as the eluant, would result in CO_2 liberation. The carbonate found was probably adsorbed from the atmosphere on cooling and general handling.

The excess carbon not accounted for in the eluate was probably inorganic or organic impurities eluted from the activated carbon sample, the carbon content of the eluant being < 0.08 mM. Even though the acid and water washing treatment was thorough, the nature of the adsorbent means that trace amounts of carbon would always be expected in solution.

Thus analysis of the eluate has revealed the presence of $KAu(CN)_2$ and $HAu(CN)_2$ as the two gold species in solution. Decomposition products of cyanide could not be detected in significant quantities.

Carbon	Total Nitrogen Contents				Au Loading	K Loading	Molar Ratios	
	By Microanalysis		Calculated					
	Initial (%)	Au Loaded (%)	as AuCN + $KAu(CN)_2$ (%)	as $Au(CN)_2^-$ + $KAu(CN)_2$ (%)	($mg.g^{-1}$)	($mg.g^{-1}$)	Au:K	Au:N†
BP1300	0.00	0.37	0.33	0.37	26.76	4.37	1.22	0.50
R2020 *	0.48	1.22	0.96	1.44	76.95	0.49	31.17	0.64
R2020 *	0.48	1.02	0.85	1.14	51.36	1.52	6.71	0.60
R2020 *	0.48	0.88	0.78	0.92	33.59	2.55	2.61	0.54
R2020 ¶*	0.48	0.73	0.71	0.77	21.64	2.72	1.58	0.57

Table 5.3 Microanalysis results for a gold loaded carbon black and activated carbons. (* Activated carbon, § Loaded from deoxygenated solution, † using nitrogen contents from microanalysis.)

5.3.3 Microanalysis of Gold Loaded Carbons

Nitrogen contents of samples of gold loaded carbons were determined by microanalysis. The change in nitrogen content, determined by microanalysis, with gold adsorption can be compared to that calculated from the experimental adsorption tests. McDougall et al. [53] have shown that at low loadings the Au:N adsorption ratio approaches 0.5, indicating $Au(CN)_2^-$ adsorption. This ratio was seen to increase to 1 at high loadings or in acid solution. Since no free cyanide was found in solution after adsorption, they suggested that cyanide was oxidized to ammonia which was then lost from the system.

A series of results of analyses of samples of gold loaded BP1300 carbon black and Norit R2020 activated carbons are given in table 5.3. The calculated nitrogen contents were obtained from the unloaded microanalysis results assuming adsorption of $KAu(CN)_2$ and $Au(CN)_2^-$ or AuCN. Because equimolar Au:K adsorption did not occur for any of the adsorptions considered, it was assumed that all potassium was adsorbed as $KAu(CN)_2$, with excess gold as either AuCN or $Au(CN)_2^-$. In the latter case no correction for the complementary cation adsorbed with $Au(CN)_2^-$ could be made. For both cases however the calculated total nitrogen contents of the activated carbons are different to those determined by microanalysis. The microanalysis figures lie between the calculated values, indicating insufficient nitrogen to

account for $KAu(CN)_2$ and $Au(CN)_2^-$ adsorption, but too much nitrogen for $KAu(CN)_2$ and AuCN. Either there is a combination of all three species, or the excess nitrogen not accounted for by $KAu(CN)_2$ and AuCN adsorption must be a nitrogen containing decomposition product formed with AuCN. If the latter is the case then the Au:N adsorption ratio given in table 5.3 is meaningless since it assumes all the nitrogen is adsorbed as gold species.

For BP1300 the Au:K adsorption ratio of 1.22 would result in a Au:N ratio of 0.55 if it is assumed that the two species adsorbed are $KAu(CN)_2$ and AuCN. The actual value calculated is 0.50, which corresponds to $KAu(CN)_2$ and $Au(CN)_2^-$ adsorption. If any decomposition to AuCN occurs in this case then the nitrogen containing product (e.g. ammonia) must be adsorbed also.

For the activated carbons the nitrogen contents lie between the expected values calculated assuming the two adsorption situations. The Au:N ratios and potassium loadings show that low gold loading tends to result in increased adsorption of $KAu(CN)_2$, as reported by McDougall et al. [53]. However, even under the high gold loading situation there is too much nitrogen found to correlate with decomposition to AuCN, unless as suggested earlier the adsorption of the nitrogen containing decomposition product occurs. The only other possibility is a combination of $KAu(CN)_2$, $Au(CN)_2^-$, and AuCN adsorbed as suggested by the elution results.

The results of a sample of Norit R2020 activated carbon loaded from deoxygenated solution have also been analysed (table 5.3). The results are similar to the normal tests, but the differences between the calculated and measured nitrogen contents are too small for any meaningful conclusions to be drawn.

5.3.4 XPS Analysis of Carbons

Samples of heat-treated and gold loaded Norit R2020 activated carbon and BP1300 carbon black have been analysed by XPS. The primary aim of the analysis was to determine the oxidation state of the adsorbed gold species. McDougall et al. [53] measured a mean oxidation number of 0.3 for gold adsorbed by Pica G210 activated carbon. The binding energies given for the adsorbed gold species lay between 91.5 and 91.6 eV. For metallic gold the reported value was 90.8 eV, and for $KAu(CN)_2$ 93.6 eV. All these values were for the gold 4f 7/2 peak, calculated relative to the carbon 1s peak at 285 eV.

In this investigation the binding energies of the gold 4f 7/2 peak were also calculated relative to the carbon 1s peak at 285 eV. However the values obtained ranged from 85.6 to 86 eV for the gold loaded carbons (table 5.4). For crystalline $KAu(CN)_2$ a value of 85.1 eV was obtained, and for AuCN 84.9 eV (table 5.5). The standard value given for the gold (0) state is 83.98 eV [103]. As expected this is less than the

measured value of around 85 eV for the two gold (I) compounds. The gold loaded carbons give binding energies greater than expected for the gold (I) state. However these were referenced to the carbon 1s peak at 285 eV, but if the carbons are slightly graphitic in nature this value may be shifted toward that of 284.5 eV for graphite. Thus the binding energy of the gold adsorbed by the carbons closely resembles that expected for the gold (I) state, and any reduction type adsorption mechanism can be discounted.

No reason can be put forward to explain the differences in gold binding energies reported by McDougall et al., with those found in this and other investigations. Referencing to the carbon 1s peak at 285 eV should have corrected differences in values caused by use of different instruments and techniques.

From the XPS results it was possible to calculate the relative proportions of oxygen, nitrogen, chlorine and gold contained by the adsorbents relative to the amount of carbon. These results are given in table 5.6. Attempts to determine the potassium contents of the samples were unsuccessful due to the low levels adsorbed. For the BP1300 sample containing the largest concentration of potassium the analysis was repeated, looking for the K 2s peak. This is much weaker than the 2p peak measured previously, but the detection limit is lower. Using this method potassium was detected in

quantities expected from the experimental adsorption results, but the time required for this analysis was too great for analysis of the other samples to be carried out.

Sample	Binding Energies (eV)				
	C	O	N	Cl	Au
a	285	532.9	401.0	200.6	——
b	285	533.5	T	ND	——
c	285	533.1	401.2/398.6	200.9	86.0
d	285	533.0	400.8/398.5	201	85.8
e	285	532.9	400.8/398.7	201	86.0
f	285	533.1	399.2	201	85.6

Table 5.4 Binding energies of elements detected in carbons by XPS. (a to e- Norit R2020 activated carbon; f- BP1300 carbon black. a- sample before adsorption; b- heat-treated at 1000°C under nitrogen; c and f- gold loaded from unbuffered solution and dried at 105°C; d- gold loaded from unbuffered solution and vacuum dried at room temperature; e- gold loaded from deoxygenated solution. ND- not detected, T- trace.)

Sample	Binding Energies (eV)			Atomic Ratios to Carbon		
	N	K	Au	N	K	Au
$KAu(CN)_2$	398.1	292.8	85.1	0.31	0.36	0.32
AuCN	398.6	——	84.9	0.41	——	0.43
KCNO	398.3	293.3	——	0.23	0.55	——

Table 5.5 Binding energies and composition of compounds determined by XPS.

For the activated carbons the oxygen contents of the samples increased as a result of the adsorption process. The possibility that this was due to the process of drying at 105°C was discounted, since an alternative vacuum drying method gave even higher values (sample d). Further evidence that oxygen was being adsorbed from solution is provided by the deoxygenated test (sample e), where the amount of oxygen adsorbed is much less from the oxygen free solution. As a check on the heat-treatment of the carbons a sample of Norit R2020 heat-treated at 1000°C under nitrogen was also analysed (sample b). This indicated that approximately 74 % of the adsorbed oxygen had been removed by the heat-treatment. The remaining 26 % should be removed at higher temperatures, up to 1300°C.

Sample	Loadings		Au:K Ratio	Atomic Ratios to Carbon				
	Au ($mg.g^{-1}$)	K ($mg.g^{-1}$)	(mol:mol)	C	O	N	Cl	Au
a	—	—	—	1.00	0.074	0.005	0.003	—
(crushed)				1.00	0.073	0.004	0.002	—
b	—	—	—	1.00	0.019	0.000	0.000	—
c	76.95	0.49	31.17	1.00	0.127	0.023	0.003	0.0052
(crushed)				1.00	0.068	0.013	0.002	0.0054
d	46.47	2.19	4.21	1.00	0.154	0.019	0.003	0.0041
(crushed)				1.00	0.079	0.011	0.003	0.0042
e	24.50	3.81	1.28	1.00	0.084	0.008	0.003	0.0024
(crushed)				1.00	0.076	0.010	0.002	0.0027
f	25.15	5.73	0.87	1.00	0.063	0.002	0.001	0.0012
(crushed)				1.00	0.067	0.003	0.001	0.0011

Table 5.6 Composition of carbons determined by XPS.

To determine the nature of the carbon-oxygen species adsorbed a peak synthesis method was used on the carbon 1s peak obtained by subtracting the spectra of samples a and c. The synthesis gives the binding energies and relative proportions of the carbon-oxygen species comprising the peak which were adsorbed along with the gold. These carbon binding energies were found to correspond to singly and doubly bonded carbonyl groups in the ratio 61 % C-O (286.6 eV) and 39 % C=O (288 eV). No peak corresponding to carboxyl groups (289.2 eV) could be determined, this is because of a lack of knowledge about the essential peak shape of carbon not attached to oxygen.

XPS analysis is surface sensitive, results being obtained from the top 2 nm of the adsorbent. To get a more representative (bulk) analysis the samples were ground in a mortar and pestle and the analysis repeated. The results of these analyses are given as the crushed values in table 5.6. A feature of the oxygen adsorption is that it only occurs at the external surface of the carbons, since grinding the samples resulted in much lower concentrations being detected.

The nitrogen contents were also more concentrated on the external surface of the carbons, but the crushed samples show that nitrogen is also found adsorbed in the pores. From the spectra in the nitrogen region it was possible to determine two different nitrogen states

(figure 5.3). These had binding energies of from 398.4 to 398.8 eV, and 400.8 to 401.5 eV, except the sample loaded by BP1300 (f) which had only one nitrogen state at 399.2 eV. The lowest binding energy state was related to gold adsorption, only being detected on the loaded samples (table 5.7). The highest binding energy state could be detected on the unloaded sample, but the concentration increased on gold loading. It was this state that was more concentrated on the external surface of the gold loaded activated carbons (samples c and d), but not during deoxygenated adsorption (sample e).

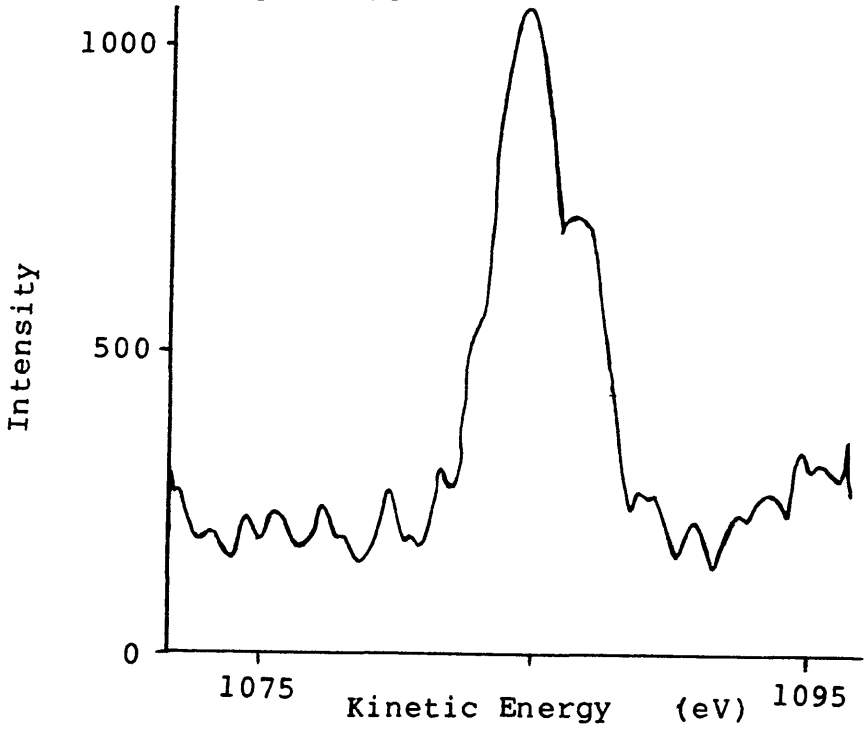

Figure 5.3 Nitrogen spectrum of a gold loaded activated carbon (sample d) showing a double peak corresponding to two different nitrogen species.

In table 5.5 the results are given of XPS analysis of pure samples of $KAu(CN)_2$, AuCN, and KCNO. In all three

cases there is only one nitrogen binding energy, corresponding to the CN^- group at 398 eV. This agrees with the analysis of the carbons where this binding energy was only found on the gold loaded samples. The higher binding energy (401 eV) will correspond to a more highly oxidized species than cyanide, such as an amine. The detection of ammonia would not occur due to its volatility, resulting in its removal by the vacuum system.

Sample	Atomic Ratios Adsorbed						
		Nitrogen State					
		Total		A		B	
	Au:C	N:C	Au:N	N:C	Au:N	N:C	Au:N
c	0.0052	0.018	0.29	0.013	0.40	0.005	1.04
(crushed)	0.0054	0.009	0.60	0.003	1.80	0.005	1.08
d	0.0041	0.014	0.29	0.008	0.51	0.006	0.68
(crushed)	0.0042	0.007	0.60	0.001	4.20	0.005	0.84
e	0.0024	0.003	0.80	0.002	1.20	0.001	2.40
(crushed)	0.0027	0.006	0.45	0.002	1.35	0.004	0.68
f ¶	0.0012	0.002	0.50	——	——	——	——
(crushed)	0.0011	0.003	0.42	——	——	——	——

Table 5.7 Atomic ratios of adsorbed gold and nitrogen on activated carbons. (c to f- as in table 5.4; A- 401 eV nitrogen state; B- 398 eV nitrogen state (CN^-); ¶- 399.2 eV nitrogen state.)

A problem with the analysis of these three compounds is the proportions of the different elements detected. In all cases the carbon content is too high, leading to atomic ratios to carbon that are low. This is caused by deposition of carbon from the atmosphere or during analysis. In the case of $KAu(CN)_2$ the gold : nitrogen ratio is approximately 1, a value of 0.5 being expected. These discrepancies could cast doubts over the results given in tables 5.6 and 5.7. However for sample c it is possible to re-calculate these atomic ratios from the microanalysis data. In table 5.3 the adsorbed gold : nitrogen ratio of sample c (loaded with 76.95 $mg.g^{-1}$ gold) was given as 0.64. This compares favourably with the XPS result of 0.60 given in table 5.7 (for nitrogen adsorbed in both states). Thus the relative amounts of gold and nitrogen detected by XPS agree with the bulk microanalysis. The atomic ratio of the total nitrogen content to carbon for the sample crushed is 0.013 by XPS (table 5.6). Microanalysis gave a total carbon content of 80.80 wt %, and 1.22 wt % nitrogen. This is equivalent to an atomic nitrogen : carbon ratio of 0.0129. Thus the absolute nitrogen contents by XPS agree with the microanalytical data, and the inaccuracies in the relative gold, carbon, and nitrogen contents found by analysis of pure $KAu(CN)_2$ do not seem to be apparent in the XPS results of the gold loaded carbons. The similarity of nitrogen contents determined by these two methods indicates that the adsorbed species are not in the form of large particles. Since XPS is a surface

sensitive technique, results being obtained from the top 2 nm of the sample, and microanalysis is a bulk technique, the maximum size of any gold particle is approximately 2 nm.

The reason for the low nitrogen content found for $KAu(CN)_2$ may be related to the presence of oxygen found during XPS analysis. The O:C ratio was 0.09, suggesting possible hydrolysis of $KAu(CN)_2$ with liberation of ammonia. This would result in potassium carbonate and AuCN being left, and a Au:N ratio of 1.

For these comparative calculations using sample c it is assumed that all K is adsorbed as $KAu(CN)_2$. Since the experimentally determined Au:K adsorption ratio was 31.17, only 3.2 % of the gold adsorbed is as this complex. Another sample (e) loaded from deoxygenated solution has an experimentally determined Au:K ratio of 1.28. This is equivalent to 78.1 % of the gold loaded as $KAu(CN)_2$, and a Au:N ratio of 0.56 if it is assumed that AuCN is the other gold species adsorbed (table 5.8). From XPS results this ratio was calculated as 0.68, using results for nitrogen adsorbed as the cyanide complex. The difference can be attributed to experimental error from the adsorption results. Thus these two samples which have large differences in their relative values of the Au:K adsorption ratio provide strong evidence for the accuracy of the experimental and XPS methods used to determine the relative proportions of the adsorbed elements.

The comparison (table 5.8) between the gold : nitrogen ratios calculated from experimental adsorption tests and the XPS figures shows a remarkable similarity of results. The experimental gold : nitrogen ratios have been calculated from the gold : potassium values given, assuming all potassium is adsorbed as $KAu(CN)_2$, and excess gold as AuCN. The XPS results are those calculated using only the nitrogen contents found at 398 eV, corresponding to cyanide groups.

Sample	Atomic Ratios Adsorbed		
	Experimental		XPS
	Au:K	Au:N	Au:N
c	31.17	0.97	1.08
d	4.21	0.81	0.84
e	1.28	0.56	0.68
f	0.87	0.47	0.42

Table 5.8 Comparison of atomic ratios calculated from experimental adsorption data assuming $KAu(CN)_2$ and AuCN adsorption, with those determined from XPS results using cyanide nitrogen.

The results suggest that for these carbons only $KAu(CN)_2$ and AuCN are the adsorbed gold species. Adsorption of $Au(CN)_2^-$ or $HAu(CN)_2$ would increase the experimental gold : potassium ratio, giving higher gold : nitrogen ratios as calculated from experimental results, but would not affect the XPS results. The

microanalysis results discussed earlier suggested much lower gold : nitrogen ratios of around 0.60 (table 5.3), but these consider the total nitrogen content adsorbed. Similar results have been shown for total adsorbed nitrogen by XPS (table 5.7). The difference between these values, i.e. the nitrogen contents in the form of the higher binding energy species, would thus appear to be a nitrogen containing decomposition product of $KAu(CN)_2$. Further evidence for this decomposition comes from the oxygen contents of the carbons (table 5.6). The presence of the 401 eV nitrogen state on the uncrushed samples correlates with the presence of excess oxygen (samples c and d). For the deoxygenated adsorption sample (e), where little or no decomposition of $KAu(CN)_2$ occurs, there is no change in the concentration of the 401 eV nitrogen state on crushing. Also the difference in oxygen concentration is small. Thus the higher binding energy state of nitrogen, found predominately on the external surface of the carbons, is associated with excess oxygen, and is most likely a result of $KAu(CN)_2$ decomposition.

The chlorine content of the carbons (table 5.6) is due to the hydrochloric acid washing stage. The results show that even with the thorough soxhlet condensed vapour washing operation carried out after acid washing, there is still an appreciable amount of chlorine adsorbed. The possible effects on gold adsorption have been discussed earlier (section 3.3.5).

5.4 Conclusions

Recovery of adsorbed gold from loaded carbons has been shown to occur by continuous elution using a soxhlet apparatus. No pre-treatment of the loaded carbons was necessary for elutions of from 50 to 70 % in 1 week. Three forms of eluted gold were found.

(1) $KAu(CN)_2$ - in solution.

(2) AuCN - precipitated from solution. This was shown to occur by the decomposition of desorbed $Au(CN)_2^-$.

(3) Au - either as colloidal solution or precipitated. This was formed by the decomposition of AuCN adsorbed by the carbons.

Nitrogen contents determined by microanalysis corroborated these elution results. However, XPS analysis indicated that part of the nitrogen was adsorbed as a decomposition product of cyanide. This product was associated with C-O and C=O groups formed on the external surface of the carbons. In the interior of the carbons excess oxygen was not found, and the only nitrogen species adsorbed were in the form of cyanides.

Binding energy figures indicated that all of the

adsorbed gold was in the 1+ oxidation state, thus being in the form of $M^{n+}(Au(CN)_2)_n$ or AuCN. Combining the nitrogen contents determined by XPS with the potassium contents measured from experimental adsorption tests it was shown that the adsorbed gold species must be $KAu(CN)_2$ and AuCN.

6 Summary of Results

This study of gold adsorption by a series of activated carbons and heat-treated carbon blacks has resulted in the presentation of many results which will aid in the understanding of the adsorption mechanism.

Initially attempts were made to correlate gold loading, calculated using the Langmuir adsorption isotherm, with the structural properties of as-received and heat-treated carbon blacks. The most significant correlation produced was with the Langmuir Xm value and the BET surface area. This indicated that other factors such as surface chemistry and pore size and structure did not directly influence the adsorption process. Surface coverage was also shown to be very low, at approximately 4 %.

This correlation was still obtained after acid washing of the carbon blacks, and loading from unbuffered solutions. However in both cases the amount of gold adsorbed was reduced. The two effects were shown to be acting separately, with acid washing probably leaving chloride groups on the carbon surface to interfere with adsorption, and removal of 'spectator' cations affecting unbuffered tests.

During adsorption tests in buffered solutions there was no adsorption of potassium from solution. This was

assumed to be due to $NaAu(CN)_2$ adsorption. For unbuffered tests using acid washed carbons potassium was adsorbed, but the amount was always less than would be expected for $KAu(CN)_2$ adsorption. The possibility of decomposition of $KAu(CN)_2$ to AuCN and KCN was considered, but analysis of solutions after adsorption failed to detect any free cyanide produced. This suggested the possibility of cyanide decomposition to carbonate and ammonia.

For adsorption from deoxygenated solutions the amounts of gold and potassium adsorbed correlated well with $KAu(CN)_2$ adsorption. The amount of gold adsorbed was always less under these conditions than would normally be expected. On exposure to oxygen however gold adsorption increases to its expected level, and potassium is desorbed. This strongly suggested that decomposition to AuCN and carbonate and ammonia was occurring, as this step was shown to require molecular oxygen.

Addition of cations as chlorides to solutions of $KAu(CN)_2$ was shown to result in increased gold adsorption in the order

$$H^+ > Ca^{2+} > Mg^{2+} > Na^+ > K^+$$

In acid solution $HAu(CN)_2$ was the only species adsorbed, even with the other cations present. In neutral solutions containing several cations it was shown that all cations are adsorbed, but the amounts followed the

order given above. The total gold to cation adsorption ratios were still greater than 1, thus suggesting that decomposition to AuCN was still occurring.

Deoxygenation in the presence of 'spectator' cations did not have quite the same effect as in the pure $KAu(CN)_2$ solutions. In acid solution there was no change in gold or cation adsorption under deoxygenated or oxygenated conditions. For the other cations the effects were similar to those in pure $KAu(CN)_2$ solutions, though much reduced.

Using pure solutions of $M^{n+}(Au(CN)_2^-)_n$ (where M^{n+} = H^+, Ca^{2+}, Mg^{2+}, Na^+, or K^+) it was possible to obtain better information about the relative effects of the different cations on gold adsorption. The results agreed with those obtained from adding cations as chlorides, and it is thought that a rigorous investigation into the relative effects of these species on gold adsorption may prove useful in understanding why the cations have differing effects.

Elution of adsorbed gold using a soxhlet apparatus was shown to be effective, with up to 70 % being recovered. Three forms of gold were obtained using this method. $KAu(CN)_2$ was found in solution, AuCN was precipitated from solution, and metallic gold was also precipitated or found in colloidal solution.

The AuCN eluted was shown not to be AuCN adsorbed by the carbons, which was shown to elute as metallic gold. It must have been produced by the decomposition of $HAu(CN)_2$ in the eluate, which must have been eluted from the carbon.

Significant quantities of the decomposition products of cyanide could not be detected in the eluate, however it was shown that $HAu(CN)_2$ was in solution.

Microanalysis of gold loaded carbons was used to determine nitrogen contents. The results indicated that insufficient nitrogen was adsorbed to account for $KAu(CN)_2$ and $HAu(CN)_2$, but too much was present for $KAu(CN)_2$ and AuCN. Thus the only possibilities were a combination of all three species, or the adsorption of $KAu(CN)_2$, AuCN, and part of a nitrogen containing decomposition product of cyanide.

X-ray photoelectron spectroscopy was used to determine the oxidation state of the adsorbed gold species. Results indicated that all gold was in the 1+ oxidation state, thus ruling out any reduction type adsorption mechanism, and confirming that either AuCN or a $M^{n+}(Au(CN)_2^-)_n$ type species are adsorbed.

Analysis of oxygen contents by XPS indicated that large concentrations were produced on the external surface of the carbons as a result of gold adsorption.

The form of the oxygen was predominately as singly and doubly bonded carbonyl groups, in the ratio 3:2, though the presence of carboxyl groups could not be discounted.

Nitrogen was also shown to be concentrated on the external surface as a result of gold adsorption. However this was in the form of two distinct species. One corresponded to a cyanide group and could be either AuCN or $M^{n+}(Au(CN)_2^-)_n$. The other was shown not to be a cyanide species, but was more highly oxidized suggesting an amine type decomposition product of cyanide. It was this second species that was concentrated on the external surface, the cyanide species being found evenly over the carbon surface.

The total nitrogen contents determined by XPS were shown to agree with those determined by microanalysis. This could only be expected if the gold was adsorbed as species smaller than approximately 2 nm, which is the depth of penetration of the spectrophotometer used. This rules out adsorption of cluster type compounds as they can be much larger than this.

By subtraction of the fraction of nitrogen shown to be adsorbed as an amine type species from the microanalysis results, it was shown that the nitrogen contents correlate to $KAu(CN)_2$ and AuCN adsorption only.

From these points it is possible to develop a simple

adsorption mechanism.

(a) Gold : cation adsorption ratios under deoxygenated conditions indicate that the initially adsorbed species is $M^{n+}(Au(CN)_2^-)_n$, where M^{n+} is the cation in solution. From solutions containing more than one cation a combination of species is adsorbed following the order:-

$$H^+ > Ca^{2+} > Mg^{2+} > Na^+ > K^+$$

(b) If molecular oxygen is present in solution then a reaction occurs leaving AuCN and an amine type species adsorbed, with cation desorption. For example:-

$$KAu(CN)_2 + \tfrac{1}{2} O_2 + 2 H_2O = KHCO_3 + AuCN + NH_3 \qquad (6.1)$$

Evidence for such a step comes from the increase in gold adsorption on oxygenation following deoxygenation, without a corresponding increase in cation adsorption; insufficient cyanide nitrogen adsorption to account for the $M^{n+}(Au(CN)_2^-)_n$ species; adsorption of a nitrogen containing amine group; elution of metallic gold caused by thermal decomposition of adsorbed AuCN.

Mechanisms proposing adsorption of metallic gold can be discounted since in this investigation XPS analysis

has shown that all the gold adsorbed has an oxidation number of 1. Reactions with specific surface oxide groups would also seem to be unlikely, since inert atmosphere heat-treatments should have resulted in greater reductions in gold loading than those presented.

The proposed mechanism can also explain the chemical effects on adsorption given in Chapter 2. Increased gold adsorption at low pH and with the presence of 'spectator' cations can be linked to the adsorption of the $M^{n+}(Au(CN)_2^-)_n$ species. Reduced adsorption at elevated temperatures has been given as evidence by other researchers of an exothermic reaction. However this reduction could also be due to the drop in solubility of gaseous oxygen. Free cyanide also causes a reduction in gold loading which could be due to dissolution of AuCN.

Thus the proposed mechanism appears to explain many of the principles of the adsorption process. One problem that cannot be answered by this study is how carbons adsorb gold. It has been shown that surface chemical oxide groups are not important, and that adsorption occurs uniformly over the total surface. Such results suggest physical rather than chemical adsorption processes. It is this point that must be investigated in the future if a complete answer to the adsorption mechanism is to be found.

7 Future Research

Although this report proposes a mechanism to explain gold adsorption by carbons their are several areas that should be investigated if a complete answer to this adsorption system is to be achieved.

This report has indicated that two species of gold cyanide are adsorbed by carbons, namely $M^{n+}(Au(CN)_2^-)_n$ and AuCN. A technique able to differentiate between these species may be X-ray Adsorption Fine Structure (XAFS). This technique enables measurement of average interatomic distances, and is also quantitative. Thus it should be possible to measure the Au:CN adsorption ratio.

More detailed research into rates of adsorption of both gold and cations is also required. From a study such as this it would be possible to see how the molar $Au:M^{n+}$ adsorption ratio changes with time. The effects of the different cations on the rate of gold adsorption may also help in understanding why cations have different effects.

Another area of interest would be complete adsorption isotherms from $M^{n+}(Au(CN)_2^-)_n$ solutions. The results from these could be compared with the structural correlations found in this study using $KAu(CN)_2$ solutions.

In conclusion it would seem that the areas needing

more thorough investigation are the analysis of the adsorbed species and the fundamental effects of cations on adsorption.

References

1 Forbes,R.J., Metallurgy in Antiquity, Netherlands: Leiden, 1950.

2 Healy,J.F., Mining and Metallurgy in the Greek and Roman World, London: Thames and Hudson, 1978.

3 Wagor,E.J., Refining of Gold and Silver Bullion, Handbook of Non-Ferous Metallurgy, Liddel,D.M., New York: McGraw Hill, 2, 1945, pp 275-288.

4 Rose,T.K., Newman,W.A.C., The Metallurgy of Gold, London: Charles Griffen, 1937.

5 Sharwood,W.J., Liddel,D.M., Hydrometallurgy of Gold and Silver, Handbook of Non-Ferous Metallurgy, Liddel,D.M., New York: McGraw Hill, 2, 1945, pp 289-344.

6 Avraamides,J., Prospects for Alternative Leaching Systems for Gold, Proc. Conf. Carbon-In-Pulp Technology for the Extraction of Gold, Kalgoorlie, AIMM, 1982, pp 358-378.

7 Puddephatt,R., The Chemistry of Gold, Topics in Inorganic and Physical Chemistry, Elsevier, 16, 1980.

8 Hassler,J.W., Activated Carbon, London: Leonard Hill, 1967.

9 Lopez-Gonzalez,J. de D., Martinez-Vilchez,F., Rodriguez-Reinoso,F., Preparation and Characterization of Active Carbons from Olive Stones, Carbon, 18(6), 1980, pp 413-418.

10 Smisek,M., Cerny,S., Active Carbon, London: Elsevier, 1970.

11 Kalback,W.M., Brown,L.F., West,R.E., The Growth of Pores in Graphitized Carbon Reacted with Carbon Dioxide, Carbon, 8(2), 1970, pp 117-124.

12 Boehm,H.P., Chemical Identification of Surface Groups, Adv. Catal., 16, 1966, pp 179-273.

13 Nelson,J.B., Riley,D.P., The Thermal Expansion of Graphite from 15°C to 800°C: Part I. Experimental, Proc. Phys. Soc., London, 57(6), 1945, pp 477-486.

14 Dubinin,M.M., A Study of the Porous Structure of Active Carbons Using a Variety of Methods, Quarterly Reviews, 9, 1955, pp 101-114.

15 Arnell,J.C., Barss,W.M., A Comparison of the X-Ray Diffraction and Nitrogen Adsorption Surface Areas of Carbon Blacks and Charcoals, Can. J. Res., 26A(4), 1948, pp 236-242.

16 Franklin,R.E., Crystallite Growth in Graphitizing and Non-Graphitizing Carbons, Proc. R. Soc., London, 209A, 1951, pp 196-218.

17 Franklin,R.E., The Interpretation of Diffuse X-Ray Diagrams of Carbon, Acta Crystallogr., 3, 1950, pp 107-121.

18 Bokros,J.C., Deposition, Structure, and Properties of Pyrolytic Carbon, Chem. Phys. Carbon, 5, 1969, pp 1-118.

19 Kipling,J.J., The Properties and Nature of Adsorbent Carbons, Quarterly Reviews, 10, 1956, pp 1-26.

20 Marsh,H., Crawford,D., Carbons of High Surface Area. A Study by Adsorption and High Resolution Electron Microscopy, Carbon, 20(5), 1982, pp 419-426.

21 Dubinin,M.M., Adsorption in Micropores, J. Colloid Interface Sci., 23, 1967, pp 487-499.

22 Annual Book of ASTM Standards, 15.01, 1985.

23 Wolff,W.F., The Structure of Gas-Adsorbent Carbons, J. Phys. Chem., 62(7), 1958, pp 829-833.

24 Davidson,R.J., Douglas,W.D., Tumilty,J.A., The Selection of Granular Activated Carbon for Use in a Carbon-In-Pulp Operation, Proc. Conf. Carbon-In-Pulp Technology for the Extraction of Gold, Kalgoorlie, AIMM, 1982, pp 193-212.

25 Dubinin,M.M., Porous Structure and Adsorption Properties of Active Carbons, Chem. Phys. Carbon, 2, 1966, pp 51-120.

26 Mattson,J.S., Mark,H.B., Activated Carbon, New York: Marcel Dekker, 1971.

27 Garten,V.A., Weiss,D.E., Willis,J.B., A New Interpretation of the Acidic and Basic Structures in Carbons I. Lactone Groups of the Ordinary and Fluorescein Types in Carbons, Aust. J. Chem., 10(3), 1957, pp 295-308.

28 Boehm,H.P., Diehl,E., Heck,W., Sappock,R., Surface Oxides of Carbon, Angew. Chem. Int. Ed. Engl., 3(10), 1964, pp 669-677.

29 Puri,B.R., Surface Oxidation of Charcoal at Ordinary Temperatures, Proc. Conf. Carbon, 5th, 1, 1962, pp 165-170.

30 Garten,V.A., Weiss,D.E., Willis,J.B., A New Interpretation of the Acidic and Basic Structures in Carbons. II : The Chromene - Carbonium Ion Couple in Carbon, Aust. J. Chem., 10(3), 1957, pp 309-328.

31 Smith,W.R., Carbon Black, Encycl. Chem. Technol., New York: Interscience, 2nd Edition, 4, 1964, pp 243-278.

32 Lahaye,J., Prado,G., Mechanism of Carbon Black Formation, Chem. Phys. Carbon, 14, 1978, pp 167-294.

33 Medalia,A.I., Heckman,F.A., Morphology of Aggregates - II: Size and Shape Factors of Carbon Black Aggregates from Electron Microscopy, Carbon, 7(5), 1969, pp 567-582.

34 Kaye,G., Structural Changes in Heat Treated Carbon Blacks, Carbon, 2(4), 1965, pp 413-419.

35 Donnet,J.B., Schultz,J., Eckhardt,A., A Study of the Microstructure of a Thermal Carbon Black, Carbon, 6(6), 1968, pp 781-788.

36 Marsh,P.A., Voet,A., Mullens,T.J., Price,L.D., Quantitative Micrography of Carbon Black Microstructure, Carbon, 9(6), 1971, pp 797-805.

37 Dollimore,D., The Characterization of Carbon Black Surfaces, J. Oil Colour Chem. Assoc., 54, 1971, pp 616-641.

38 Donnet,J.B., The Chemical Reactivity of Carbon, Carbon, 6(2), 1968, pp 161-176.

39 Heckman,F.A., Harling,D.F., Progressive Oxidation of Selected Particles of Carbon Black: Further Evidence for a New Microstructural Model, Rubber Chem. Technol., 39(1), 1966, pp 1-13.

40 Gmelins Handbuch der Anorganischen, Gold, 62, 1954.

41 Rivera-Utrilla,J., Ferro-Garcia,M.A., Mata-Arjona,A., Gonzalez-Gomez,C., Studies on the Adsorption of Caesium, Thallium, Strontium and Cobalt Radionuclides on Activated Carbons from Aqueous Solutions, J. Chem. Technol. Biotechnol., 34A(5), 1984, pp 243-250.

42 Farkas,J., A Techno-Economic Assessment for the Recovery of Several Chemical Elements from Seawater and Brines, Precious Metals: Proc. Int. Symp., AIME, Los Angeles, 1984, pp 31-45.

43 Henry,W., An Epitome of Chemistry, London, 2nd Edition, 1801.

44 Davis,W.M., Depositing Gold from its Solutions, U.S. Patent 227963, 1880.

45 Forrest,W., Forrest,R.W., MacArthur,J.S., Improvements in Extracting Gold and Silver from Ores and Other Compounds, British Patent 14174, 1887.

46 Forrest,W., Forrest,R.W., MacArthur,J.S., Improvements in Extracting Gold from Ores and Other Compounds, British Patent 10223, 1888.

47 Johnston,W.D., Method of Abstracting Gold and Silver from their Solutions in Potassium Cyanides, U.S. Patent 522260, 1894.

48 Edmands,H.R., The Application of Charcoal to the Precipitation of Gold from its Solution in Cyanide, Trans. Inst. Min. Metall., 27, 1917-1918, pp 277-301.

49 Allen,A.W., The Moore - Edmands Process of Precipitating Gold with Charcoal, Eng. Min. J., 18(12), 1918, pp 642-644.

50 Zadra,J.B., A Process for the Recovery of Gold from Activated Carbon by Leaching and Electrolysis, USBM, RI 4672, 1950.

51 Zadra,J.B., Engel,A.L., Heinen,H.J., Process for Recovering Gold and Silver from Activated Carbon by Leaching and Elecrolysis, USBM, RI 4843, 1952.

52 Lewis,A., Leaching and Precipitation Technology for Gold and Silver Ores, Eng. Min. J., 184(6), 1983, pp 48-56.

53 McDougall,G.J., Hancock,R.D., Nicol,M.J., Wellington,O.L., Copperthwaite,R.G., The Mechanism of the Adsorption of Gold Cyanide on Activated Carbon, J. S. Afr. Inst. Min. Metall., 80(9), 1980, pp 344-356.

54 Davidson,R.J., The Mechanism of Gold Adsorption on Activated Charcoal, J. S. Afr. Inst. Min. Metall., 75(4), 1974, pp 67-76.

55 Fleming,C.A., Nicol,M.J., The Absorption of Gold Cyanide onto Activated Carbon. III : Factors Influencing the Rate of Loading and the Equilibrium Capacity, J. S. Afr. Inst. Min. Metall., 84(4), 1984, pp 85-93.

56 Davidson,R.J., Veronese,V., Nkosi,M.V., The Use of Activated Carbon for the Recovery of Gold and Silver from Gold-Plant Solutions, J. S. Afr. Inst. Min. Metall., 79(10), 1979, pp 281-297.

57 Tsuchida,N., Studies on the Mechanism of Gold Adsorption and Elution in the Carbon-In-Pulp Process, Ph.D. Thesis, Murdoch University, Australia, 1984.

58 Kuz'minykh,V.M., Tyurin,N.G., Effect of the Acidity of a Cyanide Solution on Adsorption of Gold on Charcoal, Izv. Vyssh. Uchebn. Zaved., Tsvetn. Metall., 11(4), 1968, pp 65-70.

59 Dixon,S., Cho,E.H., Pitt,C.H., The Interaction Between Gold Cyanide, Silver Cyanide, and High Surface Area Charcoal, AIChE Symp. Ser. 173, 74, 1978, pp 75-83.

60 Duncan,D.M., Smolik,T.J., How Cortez Heap-Leached Low Grade Gold Ores at two Nevada Properties, Eng. Min. J., 178(7), 1977, pp 65-69.

61 Chisholm,E.O., Canadians Operating Gold Leaching Operation in New Mexico, The Northern Miner, 18th September, 1975, pp 59-60.

62 Nicol,D.I., The Adsorption of Dissolved Gold on Activated Carbon in a NIMCIX Contactor, J. S. Afr. Inst. Min. Metall., 79(17), 1979, pp 497-502.

63 Hall,K.B., Homestake Uses Carbon-In-Pulp to Recover Gold from Slimes, World Min., 27(12), 1974, pp 44-49.

64 Potter,G.M., Salisbury,H.P., Innovations in Gold Metallurgy, Min. Congr. J., 60(7), 1974, pp 54-57.

65 Fleming,C.A., Nicol,M.J., Alternative Processes to Filtration: Carbon-In-Pulp and Resin-In-Pulp in the Metallurgical Industry, Hydrometallurgy 81, C2, 1981, pp 1-16.

66 White,L., Heap Leaching Will Produce 85,000 Oz/Year of Dore Bullion for Smokey Valley Mining, Eng. Min. J., 178(7), 1977, pp 70-72.

67 Newrick,G.M., Woodhouse,G., Dods,D.G.M., A Comparison of Carbon-In-Pulp with Carbon-In-Leach, IMM meeting 'Use of Activated Carbon in Extraction of Gold and Other Metals', London, January, 1983.

68 Davidson,R.J., Duncanson,D., The Elution of Gold from Activated Carbon Using Deionized Water, J. S. Afr. Inst. Min. Metall., 77(12), 1977, pp 254-261.

69 Davidson,R.J., Veronese,V., Further Studies on the Elution of Gold from Activated Carbon Using Water as the Eluant, J. S. Afr. Inst. Min. Metall., 79(15), 1979, pp 437-445.

70 Heinen,H.J., Peterson,D.G., Lindstrom,R.E., Gold Desorption from Activated Carbon with Alkaline Alcohol Solutions, World Min. Met. Technol., 1, AIME, New York, 1976, pp 551-564.

71 Ruane,M., A Comparison of the Zadra, Anglo American and Organic Stripping Techniques, Proc. Conf. Carbon-In-Pulp Technology for the Extraction of Gold, Kalgoorlie, AIMM , 1982, pp 379-398.

72 Laxen,P.A., Carbon-In-Pulp in South Africa, Proc. Conf. Carbon-In-Pulp Technology for the Extraction of Gold, Kalgoorlie, AIMM, 1982, pp 17-41.

73 Scerensini,B., The Design, Construction and Operation of a 500,000 Tonnes Per Annum Carbon-In-Pulp Plant at Kambalda, Western Australia, Proc. Conf. Carbon-In-Pulp Technology for the Extraction of Gold, Kalgoorlie, AIMM, 1982, pp 230-270.

74 Green,M., The Effect of Charcoal in Gold-Bearing Cyanide Solutions with Reference to the Precipitation of Gold, Trans. Inst. Min. Metall., 23, 1913-1914, pp 65-78.

75 Feldtmann,W.R., The Precipitating Action of Carbon in Contact with Auriferous Cyanide Solution, Trans. Inst. Min. Metall., 24, 1914-1915, pp 329-343.

76 Rhead,T.F.E., Wheeler,R.V., The Mode of Combustion of Charcoal, J. Chem. Soc., Trans., 103(1), 1913, pp 461-489.

77 Williams,L.B., Precipitation of Gold from Cyanide Solutions by Means of Charcoal, Min. Mag., 28(3), 1923, pp 139-147.

78 McKee,R.H., Horton,P.M., Activated Char for Gold Adsorption, Chem. Metall. Eng., 32(4), 1925, pp 164-167.

79 Gross,J., Scott,J.W., Precipitation of Gold and Silver from Cyanide Solution on Charcoal, USBM, TP 378, 1927.

80 Garten,V.A., Weiss,D.E., The Ion- and Electron Exchange Properties of Activated Carbon in Relation to its Behaviour as a Catalyst and Adsorbent, Rev. Pure Appl. Chem., 7(2), 1957, pp 69-121.

81 Cho,E.H., Pitt,C.H., The Adsorption of Silver Cyanide on Activated Charcoal, Metall. Trans., 10B(2), 1979, pp 159-164.

82 Tsuchida,N., Parker,J., Muir,D.M., Competitive Adsorption Studies of Cations, Cyanide and Organics on Carbon, Proc. Conf. Chemistry of Gold and Activated Carbon, 1982.

83 Tsuchida,N., Ruane,M., Muir,D.M., Studies on the Mechanism of Gold Adsorption on Carbon, Int. Mintek 50 Conf., 1984.

84 Gallagher,P., Personal Communication, Cabot Carbon Limited, Ellesmere Port.

85 Cranston,R.W., Inkley,F.A., The Determination of Pore Structures from Nitrogen Adsorption Isotherms, Adv. Catal., 9, 1957, pp 143-154.

86 Lippens,B.C., Linsen,B.G., De Boer,J.H., Studies on Pore Systems in Catalysts I : The Adsorption of Nitrogen; Apparatus and Calculation, J. Catal., 3(1), 1964, pp 32-37.

87 Groszek,A.J., Selective Adsorption at Graphite/Hydrocarbon Interfaces, Proc. R. Soc., London, 314A, 1970, pp 473-498.

88 Adsorption of Gold From Cyanide Solution on Norit Granular Activated Carbon, Technical Bulletin, Norit N.V., The Netherlands.

89 Schaeffer,W.D., Smith,W.R., Polley,M.H., Structure and Properties of Carbon Black, Ind. Eng. Chem., 45(8), 1953, pp 1721-1725.

90 Steenberg,B., Adsorption and Exchange of Ions on Activated Charcoal, Uppsala: Almquist and Wiksells, 1944.

91 Cabot - Special Blacks Produced for Ink, Paint, Plastics and Paper, Cabot Carbon Limited, Ellesmere Port.

92 McBain,J.W., The Sorption of Gases and Vapours by Solids, London: George Routledge, 1932.

93 Joyce,R.S., Evaluation of the National Institute of Metallurgy Isotherm Test Procedure, Calgon Corporation, Pittsburg, 1981.

94 Langmuir,I., Adsorption of Gases on Glass, Mica and Platinum, J. Am. Chem. Soc., 40, 1918, pp 1361-1403.

95 Rubin,A.J., Mercer,D.L., Adsorption of Free and Complexed Metals from Solution by Activated Carbon, Adsorption of Inorganics at Solid-Liquid Interfaces, Anderson,M.A., Rubin,A.J., Ann Arbor Science, pp 295-325.

96 Dowd,J.E., Riggs,D.S., A Comparison of Estimates of Michaelis-Menten Kinetic Constants from Various Linear Transformations, J. Biol. Chem., 240(2), 1965, pp 863-869.

97 Kennedy,J.B., Neville, A.M., Basic Statistical Methods for Engineers and Scientists, London: Harper and Row, 1976.

98 Rosenzweig,A., Cromer,D.T., The Crystal Structure of $KAu(CN)_2$, Acta Crystallogr., 12(10), 1959, pp 709-712.

99 Davidson,R.J., Douglas,W.D., Tumilty,J.A., Aspects of Laboratory and Pilot Plant Evaluation of Carbon-In-Pulp with Relation to Gold Recovery, XIV Int. Min. Proc. Congr., CIM, Toronto, II(6), 1982, pp 1-19.

100 Lynch,T.P., Determination of Free Cyanide in Mineral Leachates, Analyst (London), 1984, 109, 1984, pp 421-423.

101 Straughan,B.P., Walker,S., Spectroscopy, London: Chapman and Hall, 3, 1976.

102 Kuz'minykh,V.M., Tyurin,N.G., Solubility Product of Simple Gold Cyanide, Tr. Ural. Politekh. Inst., 155. 1967, pp 123-125.

103 Anthony,M.T., Seah,M.P., XPS: Energy Calibration of Electron Spectrometers, Surf. Int. Anal., 6(3), 1984, pp 95-106.